

Analysis of a second *Drosophila*
Cornichon Protein

In a u g u r a l - D i s s e r t a t i o n
zur Erlangung des Doktorgrades
der Mathematisch-Naturwissenschaftlichen Fakultät
der Universität zu Köln

vorgelegt von
Waldemar Wojciech
aus Laurahütte

Köln, 2014

Berichterstatter/in: **Prof. Dr. Siegfried Roth**

Berichterstatter/in: **Prof. Dr. Henrike Scholz**

Tag der letzten mündlichen Prüfung: 02.07.2014

Contents

Contents	I
List of abbreviations	IV
1 Introduction	1
1.1 The model organism <i>Drosophila melanogaster</i>	1
1.2 The early secretory pathway	2
1.3 COPII vesicle formation and cargo selection	4
1.4 COPII dependent cargo concentration	6
1.5 Transmembrane cargo receptors	6
1.6 The Cornichon protein family: Conserved cargo receptors	8
1.7 Human Cornichon homolog 4: Protein interactions and specificity for secretory cargo	10
1.8 Cornichon function: Evidence for diverse roles in neurotransmission	11
1.9 Objective	13
2 Materials and methods	14
2.1 Materials	14
2.1.1 General laboratory equipment	14
2.1.2 Chemicals	14
2.1.3 Reaction kits	14
2.1.4 Restriction enzymes and buffers	15
2.1.5 Solutions and media	15
2.1.6 Fly stocks	17
2.1.7 Oligonucleotides and primers	18
2.1.8 Vectors and plasmids	20
2.1.9 Antibodies and fluorescent dyes	21
2.1.10 Microscopy	21
2.1.11 Computer software	22
2.2 Methods	22
2.2.1 Fly stock keeping and breeding	22
2.2.2 Fly stock keeping and breeding for behavioural experiments	23
2.2.3 Evaluation of mendelian crosses	23

2.2.4	Negative gravitaxis assay	23
2.2.5	Adult survivorship assay	24
2.2.6	Developmental survivorship assay	25
2.2.7	Alcohol sensitivity assay	25
2.2.8	Generation of transgenic flies	26
2.2.9	Generation of <i>cnir</i> knock-out flies	27
2.2.10	Generation of a $\Delta cnir/cni^{AR55}$ double mutant	28
2.2.11	Generation of clones	28
2.2.12	Extraction of genomic DNA	29
2.2.13	RNA extraction and cDNA synthesis	29
2.2.14	Quantification of DNA	30
2.2.15	Polymerase chain reaction (PCR)	30
2.2.16	Gel electrophoresis	31
2.2.17	Sequencing of DNA	31
2.2.18	Cloning and ligation	32
2.2.19	Transformation of bacteria	33
2.2.20	Isolation of plasmid DNA	33
2.2.21	Cloning of <i>cnir</i> donor construct	33
2.2.22	Preparation of egg shells	34
2.2.23	Dissection, fixation and antibody staining in ovaries	34
2.2.24	Dissection, fixation and antibody staining in imaginal discs	34
2.2.25	Phylogenetic analysis of Cornichon proteins and protein membrane topology	35
3	Results	36
3.1	Phylogenetic analysis of Cni proteins and the Cnir membrane topology	36
3.2	Generation of a <i>cnir</i> knock-out line	36
3.3	Survivorship of $\Delta cnir$ throughout development	42
3.4	Survivorship of adult $\Delta cnir$ flies	45
3.5	Locomotion defects of $\Delta cnir$ flies	45
3.6	Ethanol sensitivity of $\Delta cnir$ flies	48
3.7	Muscular rescue of locomotion defects	50
3.8	Neuronal rescue of locomotion defects	53
3.9	Cnir protein localization and neuronal rescue with GFP:Cnir	56
3.10	Analysis of a <i>cnir/cni</i> double mutant	61

4	Discussion	67
4.1	Generation of a mutant for <i>cnir</i> : A putative ortholog of human <i>CNIH4</i> .	67
4.2	$\Delta cnir$ is not lethal but has an impact on mortality throughout development and adult life	68
4.3	Locomotor behaviour depends on Cnir function in neurons but not in muscles	69
4.4	Loss of Cnir leads to decreased ethanol sensitivity	71
4.5	GFP tagged Cnir potentially localizes to the ER but is not functional . .	72
4.6	<i>Drosophila</i> Cni and Cnir do not show strong functional redundancy in the soma	73
4.7	Perspectives	75
References		78
Supplement		89
List of figures		91
List of tables		92
Zusammenfassung		93
Abstract		94
Danksagungen		95
Erklärung		96
Lebenslauf		97

List of abbreviations

AC	adenylyl cyclase
<i>act</i>	<i>actin</i>
AMPA	α -amino-3-hydroxy-5-methyl-4-isoxazolepropionic acid
AMPA	α -amino-3-hydroxy-5-methyl-4-isoxazolepropionic acid receptor
AR	adrenergic receptor
<i>At</i>	<i>Arabidopsis thaliana</i>
ATP	adenosine triphosphate
<i>b</i>	<i>black</i>
bp	base pair
BSA	bovine serum albumin
°C	degree Celsius
cAMP	3'-5'-cyclic adenosine monophosphate
cDNA	complementary
cds	coding sequence
CA	countercurrent apparatus
Cf	partition coefficient
CFP	cyan fluorescent protein
<i>cn</i>	<i>cinnabar</i>
Cni	Cornichon
CNIH	Cornichon homolog
Cnir	Cornichon related
COPI/II	coat protein complex I/II
CyO	Curly of Oster
DAPI	4',6-diamidino-2-phenylindole
DD2R	Dopamine D2-like receptor
DNA	deoxyribonucleic acid
Dnc	Dunce
dNTP	deoxynucleotide triphosphate
<i>Dm</i>	<i>Drosophila melanogaster</i>
EGFR	epidermal growth factor receptor
ER	endoplasmic reticulum
ERAD	ER associated degradation

List of abbreviations

<i>eye</i>	<i>eyeless</i>
ERES	ER exit sites
fig.	figure
FLP	flipase
<i>FRT</i>	<i>flipase recombination target</i>
g	gram
GAP	GTPase activating protein
GEF	guanine exchange factor
GFP	green fluorescent protein
Gg	<i>Gallus gallus</i>
Gla	glazed
GluR	glutamate receptor
GPCR	G protein coupled receptor
Grk	Gurken
h	hour
<i>Hs</i>	<i>Homo sapiens</i>
hs	heat shock promoter
IF	irregular facit
kb	kilo base pairs
kDa	kilodalton
l	liter
M	mole
MCP	bacteriophage MS2 coat protein
MET	mean elution time
mg	milligram
<i>mhc</i>	<i>myosin heavy chain</i>
min	minute
ml	milliliter
<i>Mm</i>	<i>Mus musculus</i>
mRNA	messenger ribonucleic acid
NGS	normal goat serum
NMJ	neuromuscular junction
no.	number
<i>nos</i>	<i>nanos</i>

List of abbreviations

<i>Nv</i>	<i>Nasonia vitripennis</i>
OD	optical density
PBS	phosphate buffered saline
PBT	phosphate buffered saline with Triton X-100
PCR	polymerase chain reaction
<i>pr</i>	<i>purple</i>
<i>Rn</i>	<i>Rattus norvegicus</i>
rpm	round per minute
<i>ry</i>	<i>rosy</i>
s	second
<i>Sc</i>	<i>Saccharomyces cerevisiae</i>
<i>Sco</i>	<i>Scutoid</i>
SM	second multiple
SOC	super optimal broth with catabolite repression
<i>Sp</i>	<i>Sternopleural</i>
SSC	saline-sodium citrate
tab.	table
<i>Taq</i>	<i>Thermus aquaticus</i>
TARP	transmembrane AMPAR regulatory protein
<i>Tc</i>	<i>Tribolium castaneum</i>
TGF α	transforming growth factor α
TMD	transmembrane domain
TM ₂	third multiple 2
TM _{6B}	third multiple 6B
Tris	tris(hydroxymethyl)aminomethane
<i>tub</i>	<i>tubulin</i>
U	unit
UAS	<i>upstream activating sequence</i>
UTR	untranslated region
UV	ultra violet
V	volt
<i>w</i>	<i>white</i>
wt	wild type
YFP	yellow fluorescent protein

List of abbreviations

X-Gal	bromo-chloro-indolyl-galactopyranoside
β -Gal	β -Galactosidase
μ g	microgram
μ l	microliter
μ M	micromolar

1 Introduction

1.1 The model organism *Drosophila melanogaster*

The fruit fly *Drosophila melanogaster* is one of the best studied model organisms in biology. Besides the classical advantages like the short generation time of only ten days and the high number of progeny, the *Drosophila* genome is also completely sequenced since the year 2000 [Adams *et al.*, 2000]. Furthermore, it is estimated that approximately 75 % of human disease genes have an obvious ortholog in flies, which makes *Drosophila* a valuable model for human disease [Chien *et al.*, 2002].

The advantages of *Drosophila* as a model are augmented by the availability of diverse techniques for genetic manipulation that allow the precise study of genes and their roles in cellular processes. For example, transgenesis via the P element-mediated [Rubin and Spradling, 1983] and ϕ C31 integrase transformation [Bischof *et al.*, 2007] systems offer the opportunity for expression studies of tagged proteins to monitor their cellular and subcellular localization. Furthermore, the UAS/Gal4 system [Brand and Perrimon, 1993] enables misexpression of genes to investigate their temporal and spatial requirement. In addition, the FLP/FRT system [Chou *et al.*, 1993; Xu and Rubin, 1993; Chou and Perrimon, 1996] for generation of mitotic clones can be used to analyze labeled mutant cells in direct comparison to wild type cells in the same tissue. Finally, genetic tools to create gene knock-outs via homologous recombination allow the generation of mutants for any gene of interest [Gong and Golic, 2003; Huang *et al.*, 2008].

Overall, *Drosophila* holds many tissues that are accessible for extensive manipulation and are models for many cellular and developmental events. Oogenesis, for example, requires almost all cellular processes for the development of a stem cell into a mature egg, such as cell cycle control, fate specification, cell polarization and epithelial morphogenesis [Bastock and St Johnston, 2008]. In addition, *Drosophila* imaginal discs are a common epithelial model for investigation of pattern formation and cell proliferation [McClure and Schubiger, 2005]. Furthermore, the larval neuromuscular junction (NMJ) poses a comparatively simple system to investigate developmental and functional plasticity at synapses that possess glutamate receptors homologous to those in the mammalian brain [Menon *et al.*, 2013].

Moreover, *Drosophila* is a complex organism with a rich behavioral repertoire that has been established as a model for larval and adult locomotion [Gargano *et al.*, 2005; Inagaki *et al.*, 2010; Sinadinos *et al.*, 2012], alcohol research [Devineni and Heberlein, 2013], as well as aging [Partridge *et al.*, 2011].

In this thesis, all of these advantages of *Drosophila* as a model are applied to investigate the function of Cornichon-related (Cnir). *Drosophila* Cnir belongs to a highly conserved protein family of cargo receptors, but its function has not been investigated. In the early secretory pathway of all eukaryotic cells, Cornichon proteins facilitate efficient endoplasmic reticulum (ER) export of numerous secretory proteins. Therefore, the mechanisms of early protein secretion are introduced below.

1.2 The early secretory pathway

In eukaryotic cells many proteins enter the secretory pathway in order to be accurately delivered with the correct temporal and spatial localization, such as to the plasma membrane or extracellular space. Therefore, this process is crucial for cell function and development of all eukaryotic organisms [Dancourt and Barlowe, 2010; D’Arcangelo *et al.*, 2013].

Secretory proteins have sorting elements that are recognized by the intracellular transport machinery at multiple stages of the transport process to guide the protein cargo to its proper location. The organization of the secretory pathway, which consists of membrane bound compartments, strongly depends on coat protein complexes. Those complexes recognize sorting signals at the surface of single compartments and selectively sort proteins into transport vesicles. The best studied coat complexes are clathrin and coat protein complexes I and II (COPI and COPII). Each of those complexes is a multi subunit structure, and direct binding of a subunit to a cargo protein is required for uptake into a forming carrier vesicle. However, in some cases the efficient incorporation of a cargo into a transport vesicle requires adaptor proteins or transmembrane receptors [Dancourt and Barlowe, 2010].

Translation and folding of nascent secretory proteins take place at the ER. An efficient quality control system ensures that unfolded proteins are retained or not recognized for uptake into COPII vesicles and subsequent transport to pre Golgi or Golgi compartments until proper folding occurs [Vembar and Brodsky, 2008; Dancourt and Barlowe, 2010]. The transport between ER and Golgi is highly dynamic [Sciaky *et al.*,

1997; Ward *et al.*, 2001; Losev *et al.*, 2006]. The anterograde transport of secretory proteins in COPII vesicles is equilibrated by a retrograde transport in COPI vesicles in order to recycle vesicle components and ER resident escaped proteins (fig. 1.1). However, secretory cargo advances steadily forward, while resident proteins of the early secretory pathway are dynamically transported back into the proper compartments [Dancourt and Barlowe, 2010].

To understand cargo selection for anterograde transport from the ER, it is important to elucidate the composition of COPII vesicles and mechanisms of their formation. Hence, these processes are considered next.

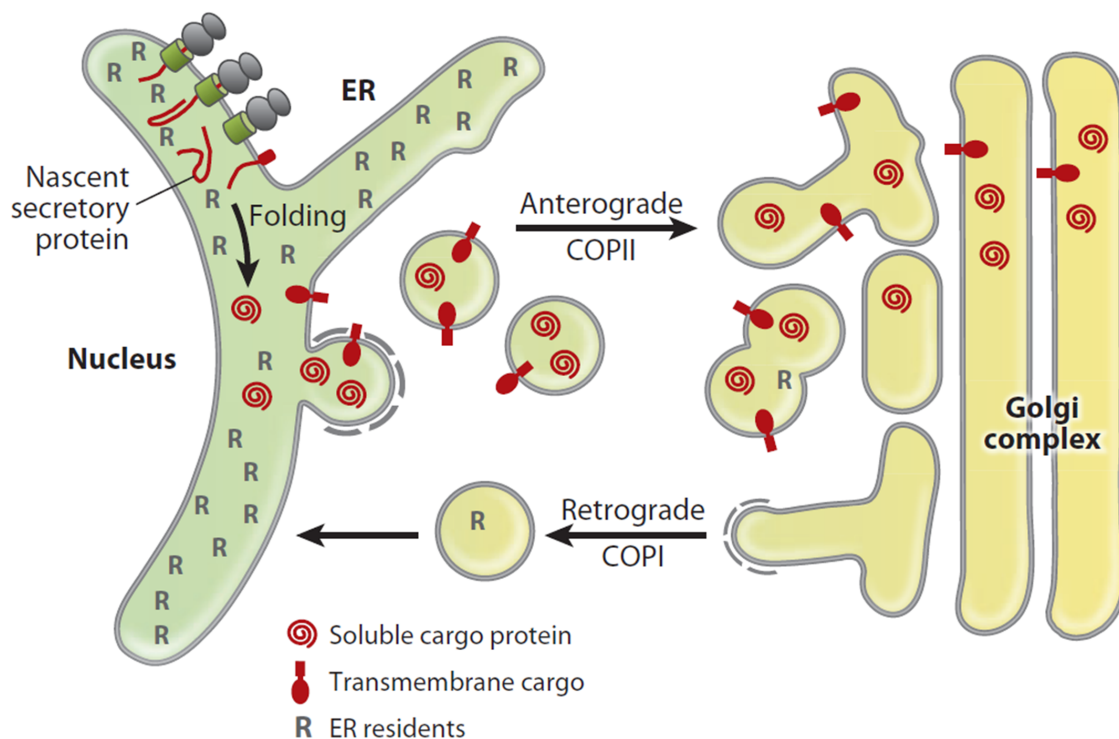


Figure 1.1 | Bidirectional transport between ER and Golgi

Scheme of the bidirectional transport between ER and Golgi. Nascent secretory proteins are translated and folded in the ER. Completely folded transmembrane and soluble cargo proteins are subsequently incorporated into COPII vesicles for anterograde transport to the pre-Golgi and Golgi compartments. The anterograde transport is balanced by a retrograde transport in COPI vesicles in order to recycle vesicle components and retrieve escaped ER resident proteins (R). As a consequence of those processes, secretory cargo moves steadily anterograde, while resident proteins localize dynamically to early secretory compartments (figure from Dancourt and Barlowe [2010]).

1.3 COPII vesicle formation and cargo selection

The machinery responsible for budding of COPII vesicles is localized to regions known as ER exit sites (ERES) [Orci *et al.*, 1991; Bannykh *et al.*, 1996; Rossanese *et al.*, 1999; Dancourt and Barlowe, 2010]. The different steps in COPII vesicle assembly are depicted in fig. 1.2.

The first event in COPII vesicle formation is the activation of the small GTPase Sar1p by its guanine exchange factor (GEF) Sec12p. As a consequence of Sar1p activation through the exchange of GDP to GTP, its hydrophobic N-terminal amphipathic α -helix is exposed and inserted into the ER membrane. That process leads to the bending of the membrane and recruitment of the Sec23-Sec24 complex. This complex serves as a cargo adaptor and furthermore as a specific GTPase activating protein (GAP) complex for Sar1p. Lastly the outer layer, consisting of Sec13-Sec31 heterotrimeres, forms around the Sar1-Sec23-Sec24 pre budding complex. This leads to formation of a cage like structure that bends the lipid bilayer of the ER and finally buds vesicles [Lee *et al.*, 2004, 2005; Budnik and Stephens, 2009; Dancourt and Barlowe, 2010; D'Arcangelo *et al.*, 2013]. *In vitro* studies have shown that cage like structures [Stagg *et al.*, 2006], as well as COPII vesicles [Matsuoka *et al.*, 1998], can be formed with merely the corepurified proteins (Sar1p, Sec23-Sec24, Sec13-Sec31) and synthetic liposomes [Dancourt and Barlowe, 2010; D'Arcangelo *et al.*, 2013].

In addition to the primary feature of forming vesicles, the COPII recognizes and selects cargo proteins for uptake into vesicles, while separating them from ER resident proteins [Salama *et al.*, 1993; Barlowe *et al.*, 1994]. Typically, cargoes can be subdivided into integral membrane proteins and soluble luminal proteins. Transmembrane proteins can have one or multiple membrane spanning segments and a type I topology with the N-terminus facing the inside, or a type II topology with the N-terminus facing the outside of the ER lumen [Dancourt and Barlowe, 2010]. Transmembrane cargoes have sorting signals presented on their cytoplasmic surfaces that direct their uptake into COPII [Bonifacino and Glick, 2004]. Biochemical approaches show that transmembrane cargo proteins bind to the Sec23-Sec24 complex. Furthermore, this interaction is sorting signal dependent [Aridor *et al.*, 1998; Kuehn *et al.*, 1998]. The presence of a non hydrolyzable GTP is able to stabilize the formation of the cargo complex consisting of Sec23-Sec24, Sar1p-GTP and cargo. In contrast, the controlled hydrolysis of GTP by Sar1p enables the complex to dissociate. Thus, the cargo can be released from its sorting subunits and COPII components can be recycled at ERES

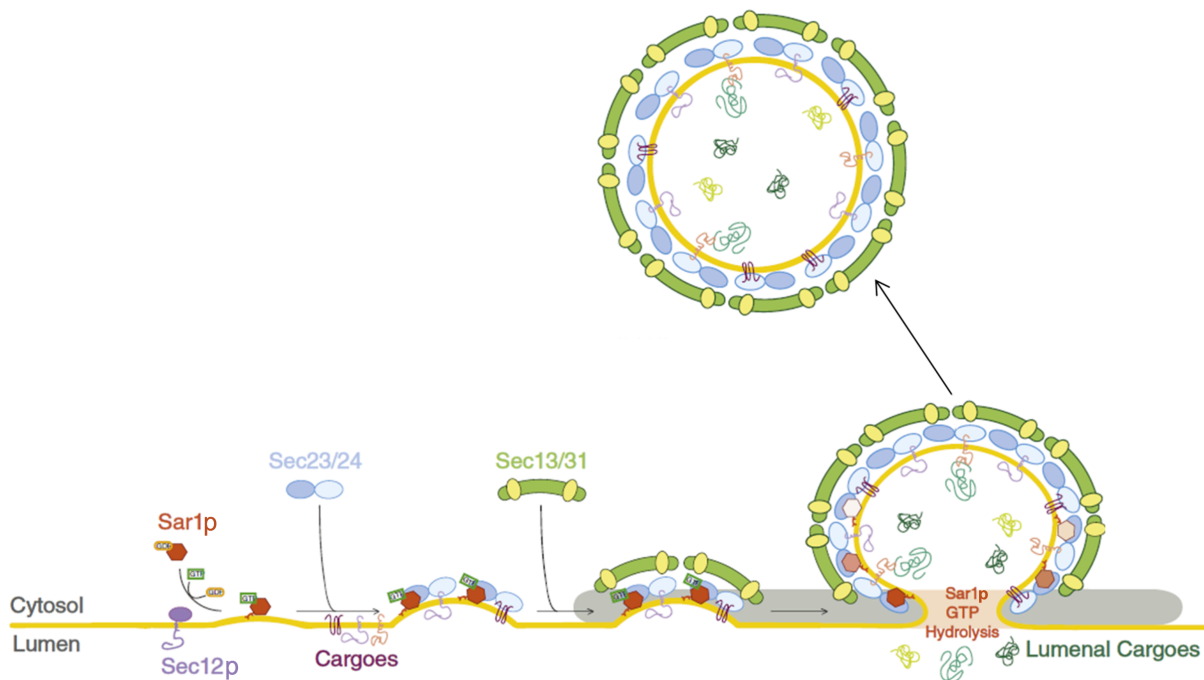


Figure 1.2 | COPII vesicle formation and cargo selection

Scheme of the COPII vesicle formation and cargo selection process. The GEF Sec12p activates Sar1p. Subsequently, Sec23-Sec24 binds to the activated membrane-bound Sar1p-GTP and form pre budding complexes. In those complexes Sec24p is responsible for binding to sorting signals present on cargo proteins. As indicated, the binding of cargo proteins to Sec24p can be direct or mediated by transmembrane sorting receptors. Ultimately, the Sec13-Sec31 complex is recruited to the pre budding cargo complexes, forming the outer layer. This leads to curvature of the ER membrane and finally budding of the vesicle (figure modified from D'Arcangelo *et al.* [2013]).

[Dancourt and Barlowe, 2010]. The binding of Sec24p to well defined sorting signals is possible due to various cargo recognition sites within this protein [Miller *et al.*, 2003; Mossessova *et al.*, 2003]. In addition, the diversity of potentially recognized sorting signals is increased by the presence of several Sec24p isoforms [Miller *et al.*, 2002; Wendeler *et al.*, 2007].

Many soluble cargo proteins do not span the ER membrane and thus cannot be recognized by COPII subunits. Furthermore, not all secretory proteins possess noticeable COPII sorting signals. Hence, transmembrane cargo receptors may be necessary to facilitate efficient export of many types of secretory cargoes from the ER by linking them to the COPII budding complex [Dancourt and Barlowe, 2010].

The cargo recognition is often associated with cargo concentration. Therefore, the mechanisms of cargo concentration will be addressed in the following section.

1.4 COPII dependent cargo concentration

Early studies already suggested that viral transmembrane proteins can be concentrated during transport from the ER to the Golgi [Quinn *et al.*, 1984] and that some viral glycoproteins can be concentrated up to tenfold during vesicle budding from the ER [Balch *et al.*, 1994]. Those results were supported by *in vitro* data [Salama *et al.*, 1993; Rexach *et al.*, 1994; Aridor *et al.*, 1998; Kuehn *et al.*, 1998] and genetic experiments [Kappeler *et al.*, 1997; Nishimura and Balch, 1997] indicating a COPII dependent concentrative ER export of integral membrane cargo [Dancourt and Barlowe, 2010]. As previously mentioned, the recognition of signals in transmembrane cargo strongly relies on Sec24p [Miller *et al.*, 2003; Mossessova *et al.*, 2003].

Although transmembrane cargoes are concentrated during transport, soluble secretory proteins show both, concentrative [Mizuno and Singer, 1993; Malkus *et al.*, 2002] or bulk flow mechanisms [Martínez-Menárguez *et al.*, 1999]. Which mechanism is used depends mainly on the cargo investigated [Barlowe, 2003; Dancourt and Barlowe, 2010]. Therefore, bulk flow and concentrative ER export mechanisms cannot be seen as mutually exclusive [Dancourt and Barlowe, 2010]. Importantly, there is evidence that secretory cargo requires cargo receptors for concentration into COPII during budding from the ER [Barlowe *et al.*, 1994; Kuehn *et al.*, 1998; Dancourt and Barlowe, 2010].

As previously discussed, cargo receptors are crucial for recognition and concentration of cargo. How cargo receptor binding to its cargoes is regulated, the impact of cargo receptors on ER quality control and the consequences of mutation of a specific cargo receptor are described below.

1.5 Transmembrane cargo receptors

Many abundant membrane proteins that localize to early secretory compartments and transport intermediates act in cargo sorting and transport between the ER and Golgi. Cells lacking specific cargo receptors show particular sorting defects characterized by an inefficient export of a subset of secretory proteins from the ER, while other secretory proteins traffic at normal rates. Cargo sorting receptors are believed to cycle between ER and Golgi compartments in COPII and COPI vesicles due to cytoplasmically exposed coat recognition signals. Thus, anterograde transport of a specific cargo through binding in the ER is followed by dissociation in the pre Golgi and

Golgi compartments. The dissociation is induced by a lower pH and potentially by Ca^{2+} gradients. This in turn leads to conformational changes in cargo receptors to decrease their affinity for cargo. In addition, every characterized cargo receptor forms oligomeric complexes, allowing major conformational shifts in slightly different pH conditions, which is a widely used mechanism for regulation of binding affinity [Dancourt and Barlowe, 2010].

Cargo receptors can be subdivided into canonical and non canonical. The first link luminal cargo to the COPII coat while the latter facilitate transport of integral membrane proteins, which could exhibit their own ER export motifs [D'Arcangelo *et al.*, 2013].

While cargo receptors appear not to be involved in cargo folding, the binding of cargo to a receptor is directly connected to the ER quality control. For instance, yeast strains lacking certain cargo receptors show activation of the unfolded protein response pathway [Belden and Barlowe, 2001a; Bue *et al.*, 2006; Jonikas *et al.*, 2009; Dancourt and Barlowe, 2010]. Furthermore, a terminally misfolded ER associated degradation (ERAD) substrate in yeast has a reduced turnover rate when its cargo receptor is lacking. It could be that in this case susceptibility of the misfolded cargo for ERAD depends on prior binding to its receptor for ER exit and subsequent retrieval from post ER compartments [Kincaid and Cooper, 2007]. Yet, an affinity of a cargo receptor for its misfolded cargo can also be reduced, which might help to guide the misfolded cargo away from the ER folding chaperones, making it more prone to ERAD [Dancourt and Barlowe, 2009, 2010]. Furthermore, some data demonstrate that several cargo receptors recognize preferentially completely folded and assembled cargo [Otte and Barlowe, 2004; Appenzeller-Herzog *et al.*, 2005; Dancourt and Barlowe, 2009, 2010]. Thus many different mechanisms possibly couple cargo binding to its receptor to the ER quality control.

Although cargo receptors share most of the common features described in the previous sections, each of them has specific activities. The following section will address the function of the Cornichon protein family of cargo receptors in more detail.

1.6 The Cornichon protein family: Conserved cargo receptors

Drosophila Cornichon (Cni) is the founding member of a conserved protein family of cargo receptors [Roth *et al.*, 1995]. At least two Cni paralogs can be found in almost all eukaryotes analyzed so far, ranging from plants to vertebrates. In *Drosophila*, the *cni* mutation is characterized by a ventralized embryo due to a failure in ER export of the TGF α ligand Gurken (Grk). For proper signaling, Grk must be processed and transported to the oocyte surface [Roth *et al.*, 1995; Herpers and Rabouille, 2004; Bökel *et al.*, 2006; Dancourt and Barlowe, 2010]. It has been shown molecularly that the first 30 membrane proximal residues of Grk are necessary for interaction with the N-terminal half of Cni. The *Drosophila* genome encodes a second Cni paralog known as *Cni-related* (Cnir). Although very little is known about *cnir*, there are hints that the two *Drosophila cni* genes have partially overlapping functions. For example, the lack of one *cnir* copy in a *cni* amorphic mutant background leads to synthetic lethality. Furthermore, it has been shown that expression of *cnir* under the control of a *cni* promoter rescues the synthetic lethality, as well as some somatic phenotypes of *cni* mutant flies [Bökel *et al.*, 2006]. Mechanistically, the recognition of cargo by Cni proteins, as well as its role as a cargo receptor, seem to be conserved, since studies of the mammalian Cornichon homolog 1 (CNIH1) shows that the protein colocalizes with makers of the early secretory pathway and that it affects secretion of mammalian TGF α [Castro *et al.*, 2007; Dancourt and Barlowe, 2010].

One of the molecularly best studied Cni proteins is the yeast Erv14p, a small hydrophobic protein, which spans the ER membrane three times and is a non canonical cargo receptor (fig. 1.3). Hence, it has one cytoplasmic loop and one that faces the ER lumen. Erv14p is a component of COPII vesicles that mediate cargo export of the transmembrane secretory protein, Axl2p, to the cell surface. The delivery of Axl2p is important for budding site selection [Powers and Barlowe, 1998, 2002]. It has been demonstrated that Erv14p physically interacts with Axl2p, as well as the COPII pre budding Sec23-Sec24-Sar1-GTP complex. Binding of Erv14p to subunits of the COPII coat is believed to depend on conserved residues in its cytoplasmic second loop domain [Powers and Barlowe, 2002].

Furthermore, Erv14p is involved in the transport of Sma2p which is important for prospore membrane formation during yeast sporulation. Prospore membrane defects

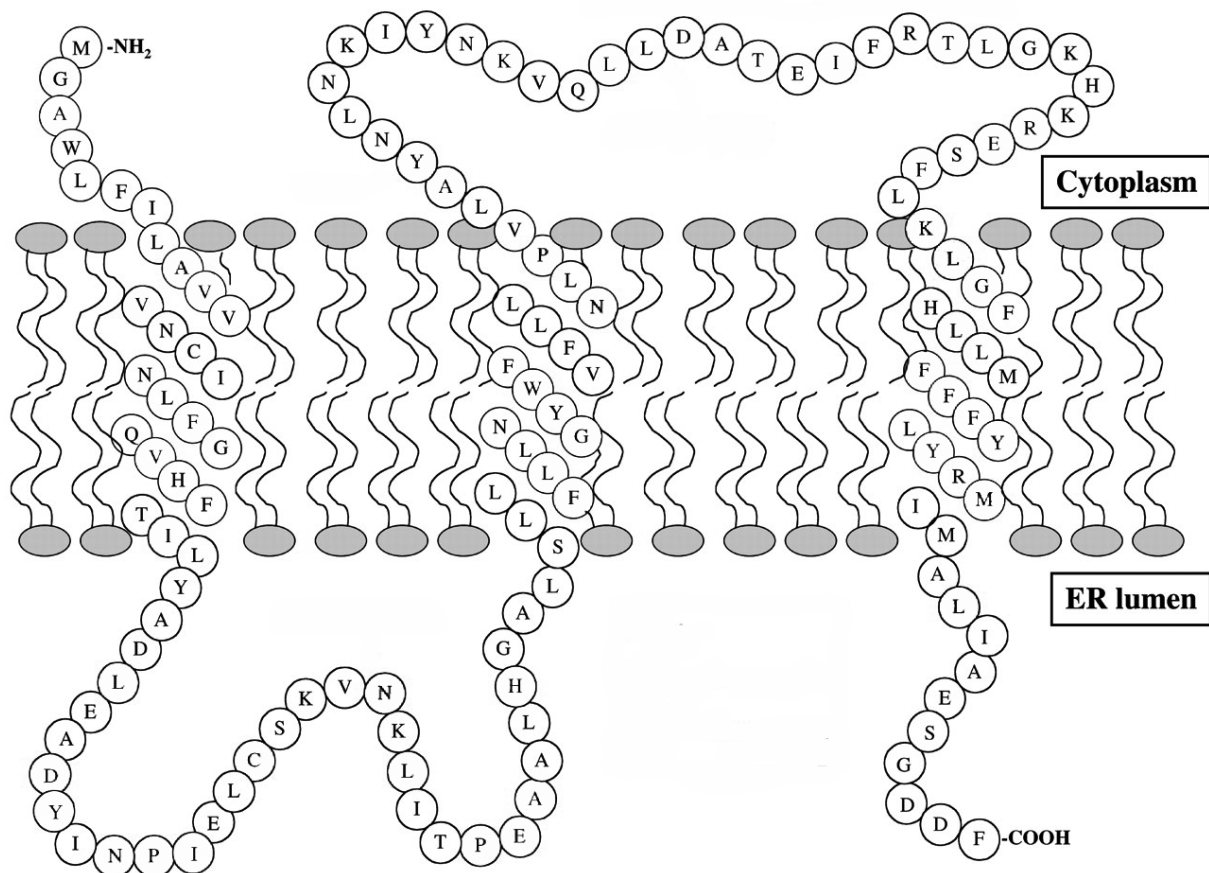


Figure 1.3 | Model of Erv14p

Model of the Erv14p protein structure with its N-terminus being cytoplasmically localized, while its C-terminus resides in the ER lumen. The cytoplasmic second loop is believed to be crucial for Erv14p binding to the COPII coat (figure modified from Powers and Barlowe [2002]).

in *erv14* mutants can be partially rescued by overexpression of its paralog Erv15p and can be enhanced in the double mutant. This indicates functional redundancy of both yeast Cni paralogs [Nakanishi *et al.*, 2007]. Moreover, it has been demonstrated that a large group of transmembrane bitopic and polytopic proteins requires Erv14p as a cargo receptor [Castillon *et al.*, 2009; Herzig *et al.*, 2012]. Strikingly, those proteins do not share a known functional or structural similarity, nor a sequence motif. However, all of them reside in late secretory pathway membranes that are populated with proteins of longer transmembrane domains (TMDs) compared to TMDs of ER resident proteins [Sharpe *et al.*, 2010; Herzig *et al.*, 2012]. Indeed, it was shown that cargo specificity of Erv14p depends on a TMD length of at least 22 amino acids to accelerate cargo export from the ER. Thus, recognition of cargo occurs through physical

properties, rather than sequence motifs [Herzig *et al.*, 2012]. It could be that Erv14p functions as a chaperone to protect cargo TMDs from degradation, which is possibly triggered by hydrophobic mismatches between the thin lipid bilayer of the ER and the long TMDs of those cargoes [D'Arcangelo *et al.*, 2013].

Although TMD length of cargo proteins is also crucial for their Golgi exit and localization to the plasma membrane, Erv14p does not play a role in this later sorting process. It has been speculated that in this case Golgi exit of cargo requires another cargo receptor, or depends on a different vesicle composition [Herzig *et al.*, 2012].

1.7 Human Cornichon homolog 4: Protein interactions and specificity for secretory cargo

Novel investigations identify the human CNIH4 as an interaction partner of members from the three major families of G protein coupled receptors (GPCRs). GPCRs represent the largest superfamily of cell surface receptors and although they do not possess a high sequence homology they share a seven TMD topology, with each TMD being 20-30 amino acids long. GPCRs are categorized into six families (A-F), with A-C representing the main families [Caers *et al.*, 2012; Sauvageau *et al.*, 2014]. GPCRs regulate an immense number of physiological and cellular processes like proliferation, development, sensory perception, metabolism, nerve transmission, neuromodulation and locomotion [Bendena *et al.*, 2012]. Thus, they are activated by a broad range of ligands. For example, family A GPCRs are activated by odorants, biogenic amines, neuropeptides, peptidergic hormones, lipids, nucleotides, proteases, and even photons. Family B GPCRs bind to hormones and peptides, while family C (metabotropic glutamate) binds to amino acids, ions, and tastants [Allen and Roth, 2011]. Yet, all known neuropeptide GPCRs belong to family A (rhodopsin-like) or family B (secretin-like) [Caers *et al.*, 2012]

After synthesis, folding and assembly, GPCRs are packed into COPII vesicles at ERES [Dupré *et al.*, 2006; Dong *et al.*, 2008; Sauvageau *et al.*, 2014] and transported through the pre Golgi and Golgi compartments to the plasma membrane. During the trafficking process, many GPCRs undergo consecutive post translational modifications like N- and O-glycosylation, which can be used as readouts for their maturation state [Dong *et al.*, 2007; Sauvageau *et al.*, 2014]. Strikingly, the ER exit has been shown

to be the bottleneck in maturation and cell surface transport of GPCRs [Petaja-Repo *et al.*, 2000; Sauvageau *et al.*, 2014].

Human CNIH4 interacts selectively with members from the three major families of GPCRs (A-C) and the COPII components Sec23 and Sec24. Furthermore, it does not bind single TMD proteins like EGFR, the T-cell receptors CD4 and CD8, or the 12 TMD adenylyl cyclase, which implies CNIH4 specificity in cargo selection. CNIH4 localizes to the early secretory pathway and overexpression, as well as knock down of CNIH4, causes retention of GPCRs in the ER. However, low levels of CNIH4 are crucial for maturation and cell surface expression of the G protein coupled β_2 -adrenergic receptor (family A). In contrast to the knock-down of CNIH4, the overexpression leads to proteasome mediated degradation of receptors. This indicates an active function of CNIH4 in degradation of ER retained cargo. CNIH4 does not colocalize with GPCRs at the plasma membrane and selectively binds to the immature ER form of β_2 -adrenergic receptor, indicating no permanent interaction. Taken together, the data suggest an important function of CNIH4 in regulation of GPCR export levels [Sauvageau *et al.*, 2014].

Interestingly, many *Drosophila* GPCRs, neuropeptides and GPCR signaling pathways elements are important models for their vertebrate homologs due to high functional conservation. Even minor changes in GPCRs, or their regulatory proteins can result in behavioral plasticity because of changes in GPCR controlled pathways [Bendena *et al.*, 2012]. However, there is no evidence for involvement of *Drosophila* Cni proteins in the control of GPCR trafficking and the potentially resulting behavioral alterations.

Although Cni proteins represent a conserved family of cargo receptors, there is evidence that they also possess a role beyond trafficking of transmembrane cargo. New studies show that some Cni paralogs are involved in regulation of neurotransmission through Glutamate receptors. Therefore, the Cni function in neurons is highlighted next.

1.8 Cornichon function: Evidence for diverse roles in neurotransmission

Several recent studies identify Cni proteins as a functional subunit of ionotropic glutamate receptors (GluRs) of the AMPA (α -amino-3-hydroxy-5-methyl-4-isoxazolepropio-

nic acid) subtype [Schwenk *et al.*, 2009; Kato *et al.*, 2010; Shi *et al.*, 2010; Coombs *et al.*, 2012]. The tetrameric AMPA receptors (AMPA receptors) consist of the pore-lining α -subunits GluA1-4 and auxiliary β -subunits that regulate their gating properties and trafficking. Thereby, the β -subunits mediate swift excitatory synaptic transmission in the mammalian brain [Harmel *et al.*, 2012]. The transmembrane AMPAR regulatory proteins (TARPs) have six isoforms and are β -subunits of most AMPARs [Gill *et al.*, 2011]. Nevertheless, it has been shown that the majority of AMPARs in the rat brain are co-assembled with Cornichon homolog 2 and 3 (CNIH2 and CNIH3), rather than TARPs. In heterologous cells, CNIH proteins increase surface expression of AMPARs and furthermore alter channel gating by slowing deactivation and desensitization kinetics [Schwenk *et al.*, 2009; Kato *et al.*, 2010; Shi *et al.*, 2010; Coombs *et al.*, 2012]. The picture is complicated further by a diverse localization of CNIH2 in different neuron types depending on the expressed TARP isoform. For instance, CNIH2 can be found in the surface of hippocampal neurons, while it is absent at the surface of Purkinje neurons of stargazer mice expressing a different TARP isoform [Gill *et al.*, 2011]. In addition, CNIH2 differentially modulates AMPAR kinetics depending on the TARP isoform composition in the receptor complex [Gill *et al.*, 2012].

The first *in vivo* analysis of Cni proteins was performed in *CNIH2/CNIH3* conditional knock-out mice. Glutamate gated currents are strongly reduced in *CNIH2/CNIH3* mutant hippocampal neurons due to the selective binding of CNIH2 and CNIH3 to GluA1 [Herring *et al.*, 2013]. Thus only GluA1 containing AMPARs, which are predominant in hippocampal neurons and deactivate slowly, can be localized to the plasma membrane [Lu *et al.*, 2009; Herring *et al.*, 2013]. It is reasoned that interaction of CNIH2 and CNIH3 with other GluA α -subunits is prevented depending on the TARP isoform expressed in hippocampal neurons. Therefore, transport and gating of different AMPARs seems to be regulated by the interaction of its α -subunits, CNIHs and TARPs [Herring *et al.*, 2013]. In keeping with the importance of CNIH2 in regulation of AMPARs, its deletion has been reported to be involved in mild intellectual disorders in human disease [Floor *et al.*, 2012]. Furthermore, elevation of the *CNIH1-3*, but not *CNIH4*, mRNA levels have been reported in the prefrontal cortex of schizophrenia patients [Drummond *et al.*, 2012].

Other studies indicate that CNIH2 still possesses its conserved function as a cargo receptor continuously cycling between ER and Golgi in a COPII dependent manner. In the ER, CNIH2 is believed to alter the glycosylation pattern of GluA2, thus regulating

AMPA maturation and thereby possibly influencing AMPAR function at synapses [Harmel *et al.*, 2012; Brockie *et al.*, 2013].

A study of the sole Cni homolog (CNI-1) in *Caenorhabditis elegans* shows that it colocalizes with the AMPAR subunit GLR-1 and the Sec24 COPII component, indicating a role in regulation of GLR-1 trafficking. Furthermore, CNI-1 colocalizes with synaptic GLR-1. In contrast to the reports on CNIH2 and CNIH3 function in hippocampal neurons of knock-out mice [Herring *et al.*, 2013], nematode mutants for *cni-1* possess elevated synaptic transmission through AMPARs. Consistently, worms lacking CNI-1 function display a higher number of GluRs at synapses [Brockie *et al.*, 2013]. In addition, reconstitution experiments with the vertebrate CNIH1 and CNIH2 show similar results. Therefore, although Cni proteins seem to have an evolutionarily conserved function in the regulation of AMPARs there might be additional regulatory effects on AMPAR transport in vertebrate neurons [Brockie *et al.*, 2013].

Although the primary neurotransmitter in excitatory synapses in the fly brain is acetylcholine [Yasuyama and Salvaterra, 1999], the *Drosophila* larval neuro muscular junction (NMJ) synapses use ionotropic GluRs homologous to AMPARs in the mammalian brain. Moreover, many synaptic components are conserved between *Drosophila* and vertebrates [Chen *et al.*, 1986; Davis *et al.*, 1989; Lahey *et al.*, 1994; Tabuchi and Südhof, 2002; Banovic *et al.*, 2010; Sun *et al.*, 2011; Menon *et al.*, 2013]. However, no connection between Cni proteins and Glutamate receptors has been described in the fly.

1.9 Objective

The aim of this thesis was to investigate the loss of function phenotype of the *Drosophila cni* gene and its impact on the viability and behavior of the fly. Furthermore, the goal was to analyze potential functional overlaps with its paralog *cni*.

2 Materials and methods

2.1 Materials

2.1.1 General laboratory equipment

All plastic laboratory equipment used was ordered from the companies Eppendorf (Wesseling-Berzdorf), Sarstedt (Nümbrecht), Simport Plastics Ltd. (Beloeil, QC Canada), Regina Industries Ltd. (Newcastle, England), Sorenson BioScience (West Salt Lake City, USA) and Ratiolab (Dreieich).

2.1.2 Chemicals

All chemicals used during this thesis were ordered from the companies Roth (Karlsruhe), Sigma Aldrich (Steinheim), Invitrogen (Karlsruhe), VWR International GmbH (Darmstadt) and Polysciences Europe GmbH (Eppelheim).

2.1.3 Reaction kits

Table 2.1 shows all used reaction kits and the company they were manufactured by. The kits were all used according to the supplied manuals.

Table 2.1 | Reaction Kits

Reaction Kit	Company
GenElute Plasmid Midiprep Kit	Sigma Aldrich, Steinheim
HiSpeed Plasmid Midi Kit	Qiagen, Hilden
Zymoclean Gel DNA Recovery Kit	Zymo Research, Orange, USA
ZR Plasmid Miniprep Classic	Zymo Research, Orange, USA
TOPO TA Cloning Kit Dual Promoter	Invitrogen, Karlsruhe
pENTR Directional TOPO Cloning Kit	Invitrogen, Karlsruhe
SuperScript II Reverse Transcriptase	Invitrogen, Karlsruhe

2.1.4 Restriction enzymes and buffers

Table 2.2 shows all restriction enzymes that were used, as well as the company they ordered from and the buffers they were used in. Each enzyme was used according to suggestions of the manufacturer.

Table 2.2 | Restriction enzymes

Enzyme	Company	Buffer
NotI	Thermo Scientific, Schwerte	Buffer O
NdeI	Thermo Scientific, Schwerte	Buffer O
BglII	Thermo Scientific, Schwerte	Buffer BamHI
AscI	NEB, Ipswich, England	Buffer BamHI

2.1.5 Solutions and media

All solutions and media used for this thesis are listed in table 2.3 in alphabetical order and were made with distilled H₂O (Milli-Q Water Purification System, Millipore, Eschborn) or labeled individually if not.

Table 2.3 | Solutions and media

Solution/Medium	Components
Ampicillin:	100 mg/ml stock solution in 50 % ethanol
Apple juice agar:	40 g agar 1 l H ₂ O 333.4 ml commercial apple juice 6.4 g commercial sugar 2.66 g liquid nipagin
BSA (10 %):	BSA in PBS
Fly food 1:	85 g agar-agar 766 g maize groats (Küper, Oberhausen) 180 g dry yeast (Biospringer, Maisons Alford, France) 100 g soy flour (Edelsoja, Hamburg) 816 g malt extract (Leyh-Pharma GmbH, Trusetal) 408 g beet treacle (Grafschafter Krautfabrik, Meckenheim)

Fly food 2 (20 l):	150 ml nipagin solution 45 ml propionic acid 160 g agar-agar 1200 g polenta 300 g dry yeast 1600 ml beet treacle 57 ml propionic acid 160 ml nipagin filled with H ₂ O to 20 l
Homogenization buffer:	160 mM sucrose 80 mM EDTA pH 8 100 mM Tris pH 8 0.5 % SDS 0.1 mg/ml Proteinase K
Injection buffer:	0.1 mM phosphate buffer pH 7.4 5 mM KCl
LB-medium:	0.5 % NaCl 1 % peptone 140 0.5 % Bacto yeast adjusted to pH 7 with 2 M NaOH
LB-agar:	LB-medium with 15 g/l agar
NGS 100 %:	normal goat serum in H ₂ O
PBS 10 x:	80 g NaCl 2 g KCl 14.4 g of Na ₂ HPO ₄ 2.4 g of KH ₂ PO ₄ dissolved in 800 ml H ₂ O, adjusted pH 7.4, filled up to 1 l with H ₂ O and autoclaved
PBT:	PBS with Triton-X 100
Proteinase K:	50 mg/ml diluted in PBT
SOC medium (1 l):	20 g bacto-tryptone 5 g bacto-yeast extract 0.5 g NaCl 10 ml 250 mM KCl pH 7

	5 ml 2 M MgCl ₂
	autoclaved and 20 ml of sterile 1 M glucose added
TAE buffer 50 x (1 l):	242 g Tris
	57.1 ml acetic acid
	100 ml 0.5 M EDTA pH 8
TE buffer 10 x:	100 mM Tris pH 8
	10 mM EDTA
X-Gal:	100 mg/ml stock solution in DMF (dimethylformamide)

2.1.6 Fly stocks

Table 2.4 shows all fly stock used during this thesis, as well as their source. The fly stocks from the collection of Prof. Dr. Siegfried Roth (Institute for Developmental Biology, University of Cologne) are labeled by SCR (stock collection Roth). Stocks received from other groups from the university of cologne are labeled as: SCS (Stock collection Scholz), SCU (Stock collection Uhlirova), SCL (Stock collection Leptin). $\Delta cnir [w^+]$ stocks without specific labeling derive from line no. 5.

Table 2.4 | Fly stocks

Fly stock	Source
w^{1118}	SCR
w^{1118}	SCS
$w^- ; IF/CyO ; MKRS/TM6B$	SCR
$w^- ; Gla/CyO ; MKRS/TM2$	SCR
$w^{1118} ; Sp/CyO ; TM2/TM6B$	SCS
$w^{1118} ;; appl::Gal4$	SCS
$w^- ; IF/CyO ; appl::Gal4/TM6B$	this thesis
$w^- ;; act::Gal4$	SCL
$w^- ;; mhc::Gal4$	SCL
$y^- w^- hs::FLP ; Sp/SM6 ; TM6$	SCR
$hs::Cre ; Sco/CyO$	SCL
$y^- w^- ; Ubi::GFP Ubi::GFP FRT40A/CyO$	BL#5198
$eye::FLP ; FRT40A tub::Gal80/CyO ; act::Gal4 UAS::GFP/TM6B$	SCU

<i>y⁻ w⁻ ;; hs::FLP hs::I-SceI/TM6</i>	BL#6935
<i>y⁻ w⁻ ; Pin/CyO ; Gal4^{221[w⁻]}</i>	BL#26259
<i>w⁻ ;; P{dcnir}/TM2 (no. 14)</i>	this thesis
<i>w⁻ ; Δcnir [w⁺]/CyO (no. 5, 7, 21, 24 and 40)</i>	this thesis
<i>w⁻ ; Δcnir [w⁺]/CyO ; MKRS/TM6B (no. 5)</i>	this thesis
<i>w⁻ ; Δcnir [w⁺] (no. 5, 7, 21, 24 and 40)</i>	this thesis
<i>w¹¹¹⁸ ; Δcnir [w⁺] (no. 5 in Scholz <i>w¹¹¹⁸</i> background)</i>	this thesis
<i>w⁻ ; Δcnir/CyO ; MRKS/TM6B (no. A1, B1 and C6)</i>	this thesis
<i>w⁻ ; Δcnir/CyO (no. B2 and C2)</i>	this thesis
<i>b cni^{AR55} pr cn/CyO</i>	SCR
<i>b cni^{AR55}/CyO</i>	SCR
<i>b cni^{AR55} FRT40A/CyO ; ry/ry</i>	SCR
<i>b cni^{AA12}/CyO</i>	SCR
<i>w⁻ ; b Df(2L)III18/CyO b</i>	SCR
<i>b cni^{AR55}/CyO ; UAS::Tc-Star:3xHA/TM6B</i>	this thesis
<i>b cni^{AR55} pr cn/CyO ; nos Gal4 UAS::MCP:GFP/TM6B</i>	this thesis
<i>Δcnir [w⁺] b cni^{AR55} FRT40A/CyO (no. 2 and 9)</i>	this thesis
<i>Df(2l)JS7/SM6a</i>	SCR
<i>Df(2l)JS7 b cni^{AR55} pr cn/CyO</i>	SCR
<i>IF/CyO ; UAS::cnir/TM6B (no. 11-5)</i>	this thesis
<i>IF/CyO ; UAS::GFP:cnir/TM6B (no. 12-1)</i>	this thesis
<i>IF/CyO ; UAS::cnir:GFP/TM6B (no. 10-2)</i>	this thesis
<i>w⁻ ; Δcnir [w⁺] ; UAS::cnir</i>	this thesis
<i>w⁻ ; Δcnir [w⁺] ; UAS::GFP:cnir</i>	this thesis
<i>w⁻ ; Δcnir [w⁺] ; UAS::cnir:GFP</i>	this thesis
<i>w⁻ ; Δcnir [w⁺] ; appl::Gal4</i>	this thesis
<i>w⁻ ; Δcnir [w⁺] ; mhc::Gal4</i>	this thesis

2.1.7 Oligonucleotides and primers

Table 2.5 contains all used oligonucleotides and primers, as well as their sequence from 5' to 3'. All oligonucleotides were synthesized by Sigma-Aldrich (Steinheim).

The primers were prediluted to a 100 μ M stock and a 1/10 dilution of this stock was used for final application.

Table 2.5 | Oligonucleotides

No.	Oligonucleotide	Sequence from 5' to 3'
1.	cnir5' homology arm_fw	GCGGCCGCTTGTTCGCGCAGACAGACTG
2.	cnir5' homology arm_rev	CATATGTATTGCACTATAAAATTCGCTTTTCAC
3.	cnir3' homology arm_fw	AGATCTAGTTTAGCCAAATAAGCCTGCAC
4.	cnir3' homology arm_rev	GGCGCGCCCCTGACAACGAAAACCTGCCG
5.	cnir_seq1	ACTTCGCCGGCATGTAC
6.	cnir_seq2	GGTCAGTACGAACTGCTC
7.	cnir_seq3	GTAAGAAAGTAACCACGTCC
8.	cnir_seq4	CGATCACCTTGCTGCAG
9.	cnir_seq5	AAGTTAACCCAAGAATTTTATAATG
10.	cnir_seq6	CCCGCAGAGCACCCAA
11.	cnir_seq7	AGTCAAAGGAAATAGCCCG
12.	cnir_seq8	GGACACTGTGTGCGGC
13.	cnir_seq9	GCAAATGCTCTTATCAAATTCT
14.	cnir_seq10	GTACATGCCGGCGAAGT
15.	cnir_seq11	GGCCAGCAAACCAAAAACAA
16.	cnir_seq12	TTGTTTTGGTTTGCTGGCC
17.	cnir_seq13	GGTTACGGGGCCACAG
18.	cnir_seq14	CCCACAAGCGGGTCCT
19.	cnir_seq15	ATGGGGTTTCTTTAGTCCC
20.	cnir_seq16	ATCGACGATCTGCGTGATT
21.	cnir_seq17	GGCGGCGAAAAAAGCGA
22.	cnir_seq18	GTTGCTGTTTTGATAATGGAAC
23.	cnir_seq19	ACAGGACCAACACAACAAAAT
24.	cnir_seq20	TGCCCATCAGGTACCGC
25.	cnir_seq21	CTGTCCTGCTCGTCGAC
26.	Deletion_Hsp70	GAGTGCCGTTTACTGTGCGA
27.	Deletion_v(2)K05816	GGTCCTTCTAGTTGGGTGTG
28.	Deletion_CG17258	AGTCTCCTTGCTCGGCTTC
29.	Deletion_white	TTCCGGGTGCTCGCATATC

30.	cnir_del_fw_contr	GCCATACAATCGAATCCACGA
31.	cnir_del_rev_contr	ATGGGTTCAAAGGTGACCGG
32.	cnir_RT	ATTTCGTCGTCCTCATAACCG
33.	cnir_RT2	AGTCGGGGATTGCTAAAGGT
34.	cnir_cDNA_fw	CACCATGTTTCTGCCCCGAAACAGCC
35.	cnir_cDNA_rev	CTATGTCGAGATGAGCGAATAAA
36.	cnir_cDNA_rev2	GAAATCCGTTACTATTTTCGTCGT
37.	M13 forward	GTAAAACGACGGCCAG
38.	M13 reverse	CAGGAAACAGCTATGAC

2.1.8 Vectors and plasmids

All vectors and plasmids used for this thesis and their source is given in table 2.6.

Table 2.6 | Vectors and plasmids

Vector/Plasmid	Source
<i>pCRII-TOPO</i>	Invitrogen, Karlsruhe
<i>pCRII-TOPO 5' hom. arm</i>	this thesis
<i>pCRII-TOPO 3' hom. arm</i>	this thesis
<i>pGX-attP</i>	Huang <i>et al.</i> [2008]
<i>pGX-attP-cnir 5' hom. arm</i>	this thesis
<i>pGX-attP-cnir 5' 3' hom. arms</i>	this thesis
<i>pGE-attB</i>	Huang <i>et al.</i> [2008]
<i>pENTR/D-TOPO</i>	Invitrogen, Karlsruhe
<i>pENTR/D-TOPO-cnir_cDNA_N-ter</i>	this thesis
<i>pENTR/D-TOPO-cnir_cDNA_C-ter</i>	this thesis
<i>pTGW (1075)</i>	DGRC
<i>pTGW-cnir_cDNA_N-ter</i>	this thesis
<i>pTGW (1076)</i>	DGRC
<i>pTWG-cnir_cDNA_C-ter</i>	this thesis
<i>pTW (1129)</i>	DGRC
<i>pTW-cnir_cDNA_N-ter</i>	this thesis

2.1.9 Antibodies and fluorescent dyes

Tables 2.7, 2.8 and 2.9 contain all antibodies and fluorescent dyes employed, the organism they were raised in, their source and the dilutions that were used. All antibody stocks were kept at -20 °C for long term storage, while predilutions were kept at 4 °C.

Table 2.7 | Primary antibodies

Antibody	Organism	Source	Dilution
anti-GFP	rabbit	Invitrogen, Karlsruhe	1:1000
anti-GFP	mouse	Invitrogen, Karlsruhe	1:1000
anti-DE-cadherin (DCAD2)	rat	DSHB, Iowa City, USA	1:100
anti-Sec23	rabbit	abcam, Cambridge, USA	1:100

Table 2.8 | Secondary antibodies

Antibody	Organism	Source	Dilution
anti-rabbit-Alexa Fluor 488	goat	Invitrogen, Karlsruhe	1:400
anti-mouse-Alexa Fluor 488	goat	Invitrogen, Karlsruhe	1:400
anti-rat-Alexa Fluor 568	goat	Invitrogen, Karlsruhe	1:400
anti-rabbit-Alexa Fluor 568	goat	Invitrogen, Karlsruhe	1:400

Table 2.9 | Fluorescent dyes

Dye	Source	Dilution/Concentration
DAPI	Vector Laboratories, Servion, Switzerland	1.5 µg/ml

2.1.10 Microscopy

The examination of fluorescent antibody staining was performed on an Axioplan2 light microscope (Zeiss, Göttingen). This microscope is equipped with an HBO UV lamp and an AxioCam color 412-312 digital camera, driven by Axiovision (Release 4.6.3, Zeiss, Göttingen) software.

2.1.11 Computer software

Table 2.10 in this section shows all computer programs and the applications they were used for.

Table 2.10 | Computer software

Software	Application
Adobe Photoshop CS4	image processing
CLUSTL 2.0.12	sequence alignment
DFM 28	automated fly counting and calculation of the MET
Gene Codes Corporation Sequencher 4.9	sequence analysis
GraphPad Software QuickCalcs	calculation of p values from χ^2
JabRef 2.9.2	reference management
Microsoft Office 2010	figure assembly and statistical analysis
Oligo Calculator version 3.26	oligonucleotide analysis
pDRAW32 revision 1.1.104	DNA sequence analysis
Phylogeny.fr [Dereeper <i>et al.</i> , 2008]	phylogenetic analysis
Statsoft, Inc. STATISTIKA 9.1	statistical analysis
TeX Live 2013	writing
TeXstudio 2.3	writing
TMpred	protein membrane topology prediction
TMHMM v. 2.0	protein membrane topology prediction
Zeiss Axio Vision Release 4.6.3	image capturing

2.2 Methods

2.2.1 Fly stock keeping and breeding

All *Drosophila* fly stocks were kept as described in Ashburner [1989] on fly food 1 at room temperature in plastic vials (Regina Industries Ltd, Newcastle, England). To reduce the generation time, crosses were kept at 25 °C. For each cross unfertilized female flies were used to grant virginity and thus the genetic purity of the crosses. Therefore, female flies were collected that were younger than 8 h at 25 °C and younger than 20 h at 18 °C.

2.2.2 Fly stock keeping and breeding for behavioural experiments

To ensure stringent parameters for all behavioral experiments, all flies were kept on fly food 2 at 25 °C, stable humidity levels of 60 % and in 12 h light/dark cycle during crosses and waiting periods. Each cross was set up in big plastic vials with 30 virgin female flies and 15 male flies. The flies were allowed to lay eggs for 4 days and then transferred to new vials up to 4 times. The male progeny from each cross were collected 14 days after the cross was set up and used for experiments 2-4 days later, to allow the flies to recover from CO₂ treatment.

2.2.3 Evaluation of mendelian crosses

For the evaluation of Mendelian crosses a χ^2 test was applied in Microsoft Excel 2010 and p values were calculated via GraphPad Software QuickCalcs with one degree of freedom. The formula used to calculate χ^2 was $(O_1-E_1)^2/E_1+(O_2-E_2)^2/E_2$ with O being the counted number flies and E the expected number flies of a genotype.

2.2.4 Negative gravitaxis assay

A negative gravitaxis assay was used to identify motor function defects in *Drosophila* [Inagaki *et al.*, 2010]. The setup of the countercurrent apparatus enables testing of two experimental groups in parallel under exactly identical conditions (fig. 2.1).

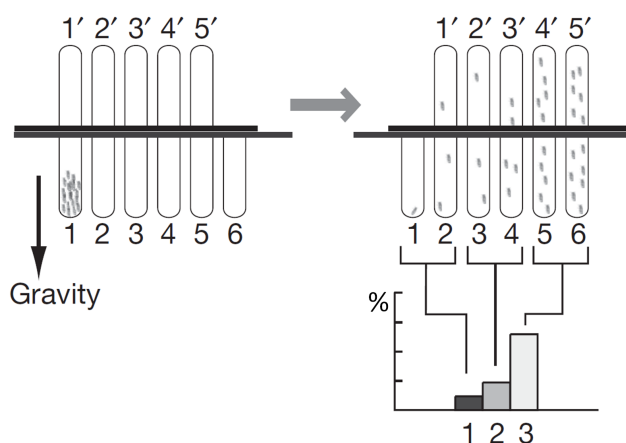


Figure 2.1 | Scheme of the countercurrent apparatus

The countercurrent apparatus used for the negative gravitaxis assay. Numbers 1' to 5' and 1 to 6 represent the upper and lower tubes, respectively, from left to right. Upon application of gravity flies walk up against the earth's gravitational field and progress through the apparatus. Subsequently, the distribution of flies in the apparatus is subdivided into 3 groups for graphical presentation. Figure from Kamikouchi *et al.* [2009].

The assay was performed with 35-42 male flies per experimental group. The flies were transferred to the first tube and permitted to settle for 5 min. In step 1 the apparatus was knocked on a surface to shake down all flies. In step 2 the position of

the apparatus was shifted to the left and the flies were allowed to climb for 30 s. In step 3 the position of the apparatus was shifted to the right, transferring all flies that managed to climb at least 50 % of the distance to the next vial. The steps 1-3 were repeated 5 times. To immobilize flies during counting, the apparatus was incubated on -20 °C for 2 min 3 times, knocking the flies down between the repeats. Flies remaining in vials 1-2 were scored as group 1, those remaining in vials 2-4 as group 2 and those remaining in vials 5-6 as group 3. Before each experimental repeat the apparatus was incubated at room temperature for 30 min. The statistical evaluation was performed in Microsoft Excel 2010. The partition coefficient (Cf) was calculated using the formula $Cf = (N_2 + 2N_3 + 3N_4 + 4N_5 + 5N_6) / (5(N_1 + N_2 + N_3 + N_4 + N_5 + N_6))$ with N_k being the number of flies in the k^{th} tube. The comparison between Cf values was made using a t-test with the setting tails=2 and test type=2.

2.2.5 Adult survivorship assay

The assay was used to determine the lifespan of adult *Drosophila*.

Each test group consisted of approximately 100 male flies kept in medium fly vials. The flies were kept as described in 2.2.2 and transferred to fresh food vials two times per week. The first transfer was made on day 4 and the second on day 7. After each transfer dead flies remaining in the old food vial were scored. Each death is considered an event. The statistical evaluation of survivorship data was made in Microsoft Excel 2010 using the log rank test [Bland and Altman, 2004; Ziegler *et al.*, 2007] with the formula $LR = (O_1 - E_1)^2 / E_1 + (O_2 - E_2)^2 / E_2$. $O_G = \sum$ of observed events in a group over all time points and $E_G = \sum$ of all E_{Gi} . $E_{Gi} = d_i \times r_{Gi} / r_i$ with E_{Gi} being the expected number of events in a group at a time point, d_i the number of events (both groups) at the time point, r_{Gi} the number of individuals under risk in a group before the event and r_i the total number of individuals (both groups) under risk before the event. The calculation of p values from χ^2 was made via GraphPad Software QuickCalcs with one degree of freedom. To compensate for the error of cross comparisons between experimental groups, the Bonferroni correction was applied, dividing the significance level (e.g. $p \leq 0.001$) by the total number of comparisons made.

2.2.6 Developmental survivorship assay

The developmental survivorship assay was used to determine mortality in single steps of the *Drosophila* life cycle. First, flies were allowed to lay eggs on an apple juice agar plate with a drop of yeast paste over night. Subsequently, eggs were collected and 100 eggs per genotype were transferred to fresh apple juice agar plates. Each single egg had at least 2 egg diameters distance to the next one to prevent hypoxic effects. Every petri dish was surrounded by liquid yeast to prevent larvae from escaping. After two days all eggs were checked for fertilization and the hatched larvae were transferred into big food vials. This was done via transfer of the outer ring of the apple juice agar. 14 days after egg lay the eclosed adult flies were removed from the food vial. Ultimately, all pupae and adults were scored. The statistical comparison of survival rates from one developmental stage into the next was made with an ANOVA test that was performed via Statsoft, Inc. STATISTIKA 9.1. The parameters used were post-hoc analysis and Tukey's HSD (honestly significant difference). The statistical evaluation of survivorship data was made in Microsoft Excel 2010 as described in section 2.2.5 using the log rank test [Bland and Altman, 2004; Ziegler *et al.*, 2007]. The calculation of p values from χ^2 was made via GraphPad Software QuickCalcs with one degree of freedom. To compensate for the error of cross comparisons among experimental groups, the Bonferroni correction was applied as described in section 2.2.5.

2.2.7 Alcohol sensitivity assay

The alcohol sensitivity assay was used to identify a potential influence of ethanol on motor function in *Drosophila*. The experiments were performed in an inebriometer (fig. 2.2 described in Cohan and Graf [1985] and Bellen [1998]). The apparatus is filled with ethanol fumes and enables to score for alcohol induced loss of motor function. Intoxicated flies fall through the column and are counted automatically by passing through a laser barrier installed at the exit of the apparatus.

Each test group consisted of approximately 100 male flies which were inserted into the inebriometer. The settings for ethanol pressure were 2.5 and for H₂O pressure 2.2. For each experimental group the mean elution time (MET) was determined via DFM 28. The statistical evaluation of the alcohol sensitivity assay was performed using an ANOVA test in Statsoft, Inc. STATISTIKA 9.1. The parameters used were post-hoc analysis and Tukey's HSD (honestly significant difference).

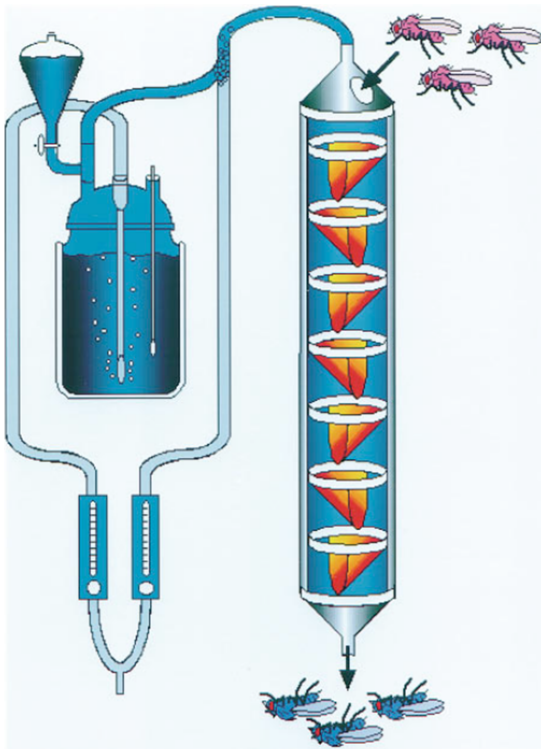


Figure 2.2 | Scheme of the inebriometer
Inebriometer for measurement of alcohol sensitivity of *Drosophila*. Flies are inserted into the column filled with ethanol fumes and gradually fall through as their postural control decreases due to alcohol influence. Flies that fall through the column are automatically counted by passing through a laser barrier installed at the exit of the apparatus. Figure from Bellen [1998].

2.2.8 Generation of transgenic flies

The generation of transgenic flies was performed via P element-mediated transgenesis [Rubin and Spradling, 1983]. The system integrates a transgene into a random position in the fly genome.

For the injection procedure flies were allowed to lay eggs on an apple juice agar plate for 30 min. Then, the embryos were dechorionated with bleach and stuck onto an apple juice agar stripe. Subsequently, they were transferred to a cover slip, which was covered with heptane glue on one edge in order to attach the embryos. After the transfer the embryos were dried for 16 min in a desiccator and then covered with 10S voltalef oil. The injections were made with an Eppendorf FemtoJet micro injector and for each construct 400 μ g transformation vector carrying the transgene of choice was injected. Phenol red was added to the injection mixture to facilitate visualization of the injected liquid. Subsequently, the cover slip with the injected embryos was transferred into a petri dish filled with apple juice agar and surrounded by liquid yeast to avoid the escape of hatched larvae. Larvae that hatched about 24 h after injection, were then transferred to food vials and allowed to develop till adulthood.

Freshly eclosed injected flies were then crossed to $w^- ; IF/CyO ; MKRS/TM6B$ or $w^- ; Gla/CyO ; MKRS/TM2$ flies and their progeny were screened for the appearance of red eyes. Afterwards, red eyed flies were backcrossed with the previously mentioned stocks to map the insertion to a chromosome and balance the stock.

2.2.9 Generation of *cnir* knock-out flies

The generation of *cnir* knock-out flies was performed via the ends out gene targeting sytem [Gong and Golic, 2003; Huang *et al.*, 2008]. This system uses a transgenic donor construct containing homology arms flanking the gene of interest. Upon enzymatic excision and linearization, the donor mimics a DNA double strand break. Then, the endogenous DNA repair machinery of *Drosophila* uses this donor for homologous recombination, replacing the targeted gene locus with a marker gene provided by the donor.

In the first cross $w^- ; p\{dcnir\}/TM2$ female flies were crossed with $y^- w^- ; hs::FLP$ $hs::I-SceI/TM6$ male flies. Females were allowed to lay eggs for approximately 72 h. Subsequently, larvae were given a 1 h heat shock in a circulating water bath at 38 °C on 4 consecutive days to activate the donor construct via FLP mediated excision and I-SceI mediated linearization (mosaic eyes indicated by *). $w^- ; hs::FLP$ $hs::I-SceI/p\{dcnir\}^*$ females were collected and crossed to $y^- w^- ; Pin/CyO ; Gal4^{221[w^-]}$ males to test for the presence of the *UAS-reaper* construct, which is part of the donor but lays outside of the homology arms. Thus, it should be lost in the progeny in case of targeted homologous recombination at the designated genomic locus. Potential $w^- ; \Delta cnir/Pin$ or CyO flies were crossed to $y^- w^- ; Pin/CyO ; Gal4^{221[w^-]}$ flies for an additional selection against the presence of the *UAS-reaper* construct and for chromosome mapping. Stocks were established in case of the insertion of the *white* marker on the second chromosome. The insertion site of the *P\{dcnir\}* construct and the successful replacement of the *cnir* locus (*cnir* start codon till stop codon) was tested via PCR. The position of the 5' homology arm was confirmed using the primer pair no. 26/27 and the position of the 3' homology arm using the primer pair no. 28/29. Furthermore, the primers no. 32-33 were used to test for the presence of the *cnir* locus as they lay within the cds of the *cnir* gene and span the second intron. The control primer pair for this PCR was no. 30/31 inside of the *V(2)k05816* gene upstream of the 5' homology arm.

To eliminate the w^+ marker from $w^- ; \Delta cnir [w^+]$ flies (stock no. 5), females from this stock were crossed to $hs::Cre ; Sco/CyO$ males. The flies were allowed to lay eggs for approximately 72 h. Afterwards, larvae were heat shocked in a circulating water bath for 10 min at 37 °C. Eclosed females were crossed to $w^- ; IF/CyO ; MKRS/TM6B$ males. Progeny from this cross with white eyes was then crossed to the same marker stock and finally used to establish $w^- ; \Delta cnir$ stocks. The successful removal of the w^+ marker was tested using the primer pair no. 13/16.

2.2.10 Generation of a $\Delta cnir/cni^{AR55}$ double mutant

To generate a $\Delta cnir/cni^{AR55}$ double mutant $w^- ; \Delta cnir [w^+]$ female flies were crossed to $b cni^{AR55} FRT_{40A}/CyO ; ry/ry$ male flies. Then, $\Delta cnir [w^+]/b cni^{AR55} FRT_{40A}$ females were crossed to $w^- ; b Df(2L)III18/CyO b$ males for recombination. To preselect flies likely carrying the cni mutation (putative $\Delta cnir [w^+] b cni^{AR55} FRT_{40A}/CyO b$), flies were selected based on the presence of the black marker gene in close proximity to cni^{AR55} . Those flies were then crossed to $b cni^{AA12}/CyO$ flies. This was done to check for the presence of cni^{AR55} based on the cni mutant egg phenotype of putative $\Delta cnir [w^+] b cni^{AR55} FRT_{40A}/b cni^{AA12}$ mothers. To check for the presence of $\Delta cnir$ in putative $\Delta cnir [w^+] b cni^{AR55} FRT_{40A}/CyO$ lines, males from those stocks were crossed to w^{1118} females. The male progeny from this cross were screened for the presence of the w^+ marker.

2.2.11 Generation of clones

The generation of mitotic clones was done via the FLP/FRT system [Xu and Rubin, 1993]. For the induction of mutant clones in the *Drosophila* female germ line $y^- w^- hs::FLP ; Sp/SM6 ; TM6$ female flies were crossed to $y^- w^- ; Ubi::GFP Ubi::GFP FRT_{40A}/CyO$ male flies. $y^- w^- hs::FLP ; Ubi::GFP Ubi::GFP FRT_{40A}/SM6 ; TM6$ males were collected in the next generation and crossed to $\Delta cnir [w^+] b cni^{AR55} FRT_{40A}/CyO$ females. The flies were allowed to lay eggs for approximately 72 h. Afterwards, larvae were heat shocked in a circulating water bath for 1 h at 37 °C on four consecutive days for clone induction. Eclosed $y^- w^- hs::FLP ; Ubi::GFP Ubi::GFP FRT_{40A}/\Delta cnir [w^+] b cni^{AR55} FRT_{40A}$ female flies were then collected for dissection of ovaries.

For induction of mutant clones in larval imaginal discs $eye::FLP ; FRT_{40A} tub::Gal80/CyO ; act::Gal4 UAS::GFP/TM6B$ females were crossed to $\Delta cnir [w^+] b cni^{AR55} FRT_{40A}/$

CyO males. *eye::FLP ; FRT40A tub::Gal80/Δcnir [w⁺] b cni^{AR55} FRT40A ; act::Gal4 UAS::GFP/+* third instar larvae were collected for dissection of eye imaginal discs.

2.2.12 Extraction of genomic DNA

During the DNA extraction all centrifugation steps were carried out at 14000 rpm in a microcentrifuge 5417R (Eppendorf, Wesseling-Berzdorf) at 4 °C.

For the extraction of genomic DNA 1 to 5 young and healthy adult flies were transferred to a 1.5 ml reaction tube and frozen at -80 °C for 5 min. After this, 200 μl of homogenization buffer containing 50 μg/ml proteinase K were added and the flies were crushed with a tissue grinder. Subsequently, the mixture was incubated at 58 °C overnight. Then, 100 μl of 4.5 M NaCl were added and the reaction tube agitated. Then, 225 μl of chloroform were added and the mixture agitated for 10 min on a wheel. Afterwards, the tube was centrifuged for 10 min and the upper phase of the mixture was transferred to a new reaction tube. To precipitate DNA 1 volume of 100 % isopropanol was added to the transferred upper phase and the tube was agitated. Afterwards, the tube was centrifuged for 10 min. Subsequently, the isopropanol was decanted, the pellet washed with 0.5 ml of 70 % ethanol and incubated at room temperature for 15 min. After another centrifugation step for 10 min, the ethanol was decanted, the pellet dried for 5 min at room temperature and ultimately redissolved in 20-30 μl of H₂O.

2.2.13 RNA extraction and cDNA synthesis

During RNA extraction all centrifugation steps were carried out in a microcentrifuge 5417R (Eppendorf, Wesseling-Berzdorf) at 4 °C.

5 ovaries were dissected in cold PBS and transferred into a tube with 250 μl of Trizol. Afterwards, 250 μl of Trizol and 2 μl of glycogen were added. Then, the mixture was incubated at room temperature for 5 min. Subsequently, 100 μl of chloroform were added, the tube vortexed and incubated at room temperature for 2-3 min. Afterwards, the tube was centrifuged at 12000 rpm for 15 min. Then, the aqueous phase was transferred to a new tube, 250 μl of 100 % isopropanol were added and the mixture was incubated at room temperature for 10 min. After this, the sample was centrifuged at 12000 rpm for 10 min, the RNA pellet washed with 5000 μl of 100 % ethanol and vortexed. After centrifugation at 9500 rpm for 5 min, the RNA pellet was dried at

room temperature for 5-10 min. Then, the RNA was redissolved in 20 μ l of RNase free H₂O, vortexed and centrifuged briefly. Ultimately, the RNA was incubated at 55-60 °C for 10 min, centrifuged shortly and kept at -80 °C for further application.

For the synthesis of cDNA the SuperScript II Reverse Transcriptase (Invitrogen, Karlsruhe) was used according to the supplied manual. The priming method of choice was Oligo(dT) that hybridize to 3' poly(A) tails. This method is recommended for new mRNA targets in the user manual.

2.2.14 Quantification of DNA

The DNA was quantified via spectral photometry on a NanoDrop 2000c Spectrophotometer (Thermo scientific, Schwerte) NanoPhotometer (Implen, München). The quality of the DNA was determined by the OD₂₆₀/OD₂₈₀ ratio.

2.2.15 Polymerase chain reaction (PCR)

All PCRs [Mullis *et al.*, 1986; Mullis and Faloona, 1987; Saiki *et al.*, 1988] were carried out in a C1000 and S1000 Thermal Cycler (Bio Rad, München). The method was used to amplify DNA fragments of interest by running through a sequence of cyclically repeated reaction steps shown in the list below.

All fragments that were used for cloning were amplified with the Expand High Fidelity PCR System (Roche, Mannheim). All other PCRs that did not require the proofreading activity of the previously mentioned system were run using the RED-Taq DNA Polymerase (Sigma Aldrich, Steinheim) ready-to-use mixture or my-Budget 5x PCR-Mastermix "Ready-to-Load" (Bio-Budget, Krefeld). All PCRs with amplicons larger than 3 kb were run at an extension temperature of 68 °C to preserve the DNA polymerase. For smaller amplicons the extension temperature was raised to 72 °C. The extension time depended on the expected product size and was adapted from the Expand High Fidelity PCR System manual. Furthermore, the annealing temperature of the primers was determined with the Oligo Calculator version 3.26 and thus varies.

Reaction mixture for standard PCR (50 μ l):

0.75 μ l Expand High Fidelity enzyme mix (2.6 U)

5 μ l Expand High Fidelity buffer (10 x)

1 μ l dNTP (10 mM)

1 μ l DNA template (50-500 ng/ μ l)

2 μ l primer forward (10 μ M)

2 μ l primer reverse (10 μ M)

filled with H₂O to final volume

Reaction Step	Temperature	Time
1. Initial denaturation of DNA	94 °C	2 min
2. Denaturation of DNA	94 °C	15 s
3. Annealing of the primer	50-62 °C	30 s
4. Extension	68 or 72 °C	1-8 min
5. Final Extension	68 or 72 °C	4-8 min

reaction steps 2-4 cycled 30-35 x

2.2.16 Gel electrophoresis

DNA fragments were separated and analyzed on 0.8%-1% agarose gels containing ethidium bromide in a final concentration of 0.5 μ g/ml. All gels were made with 0.5 x TAE buffer. The electrophoresis was performed in a Mupid-One (Eurogentec, Köln) gel chamber in 0.5 x TAE buffer. Samples in 1 x loading buffer were loaded into gel slots. As a reference marker for fragment sizes 3-5 μ l of SmartLadder, 1 kb DNA ladder, or 1 kb plus DNA ladder (Eurogentec, Köln; Invitrogen, Karlsruhe) were loaded on the gel. The separation of the fragments was carried out at 50-100 V. For visualization of the DNA fragments, the gel was excited with UV light of a wavelength of 366 nm on a transilluminator (Molecular Imager Gel Doc XR, Bio Rad, München) and photographed.

2.2.17 Sequencing of DNA

For sequencing of DNA samples were send to GATC Biotech (Konstanz). Alternatively, the Big Dye Terminator v3.1 Cycle Sequencing Kit (Applied Biosystems, Darm-

stadt) was used. The method is a modified PCR-based version of the original Sanger sequencing protocol [Sanger *et al.*, 1977]. During this PCR the nucleotides are fluorescently labeled.

Reaction mixture (10 μ l):

0.25 μ l Big dye v3.1
2.5 μ l Big dye buffer
DNA (approximately 50 ng/ μ l plasmid or PCR product)
0.25 μ l primer 10 mM
filled with H₂O to final volume

Reaction step	Temperature	Time
1. Denaturation of DNA	96 °C	10 s
2. Annealing of the primer	55 °C	5 s
3. Extension	60 °C	4 min

reaction steps 1-3 cycled 32 x

2.2.18 Cloning and ligation

The cloning into the pCRII-TOPO and pENTR/D-TOPO vectors, as well as Gateway cloning into a Destination Vector was performed according to the user manuals from Invitrogen (Karlsruhe).

For conventional ligation of an insert into a vector, the protocol from Invitrogen was used with slight modifications. The reaction conditions are given in the list below.

Reaction mixture (20 μ l):

30 fmol vector
90 fmol insert
4 μ l T₄ DNA ligase buffer 5 x
1 μ l T₄ DNA ligase 1 U
filled with H₂O to final volume

incubated at room temperature for 3 h

2.2.19 Transformation of bacteria

For amplification of plasmid DNA electro competent DH5 α *E.coli* were used. The bacteria were stored in 50 μ l aliquots at -80 °C, thawed on ice and 1 μ l of isolated plasmid or 2 μ l of ligation were added. Afterwards, the bacteria were incubated on ice for 1 min and accordingly transferred into an electroporation cuvette (PEQLAB Biotechnologie GMBH, Erlangen). Subsequently, they were given an electronic pulse of 1800 V in an EasyjecT Prima electroporator (Equibio, Ashford, England) and transferred into 250 μ l of SOC medium. Then, the bacteria were incubated at 37 °C with agitation for 1 h. Afterwards, they were plated onto LB-agar with ampicillin and optionally also with X-gal.

2.2.20 Isolation of plasmid DNA

For the isolation of low concentrations of plasmid DNA the ZR Plasmid Miniprep Classic (Zymo Research, Orange, USA) was used. If higher concentrations of plasmid DNA were desired, either the GenElute Plasmid Midiprep Kit (Sigma Aldrich, Steinheim) or HiSpeed Plasmid Midi Kit (Qiagen, Hilden) were used. The bacteria were grown as described in the user manuals.

2.2.21 Cloning of *cnir* donor construct

The *cnir* 5' and 3' homology arms were amplified via standard PCR with the forward and reverse primers matching their names (tab. 2.6 no. 1-4). Both homology arms were cloned into the *pCRII-TOPO* vector and fully sequenced using the primers 5-25 in table 2.6. The 5' homology arm was cut from the *pCRII-TOPO* 5' *hom. arm* vector by a double digestion with the restriction enzymes NotI and NdeI in the buffer O. Then, the vector was purified via gel extraction. In parallel, the *pGX-attP* underwent the same restriction and purification procedure. Then, the 5' homology arm was cloned into the *pGX-attP* vector. Subsequently, the *pGX-attP-cnir* 5' *hom. arm* vector and the *pCRII-TOPO* 3' *hom. arm* vector were double digested with BglII and AscI in the buffer BamHI respectively. Ultimately, the 3' homology arm was cloned into the *pGX-attP-cnir* 5' *hom. arm* vector. The *pGX-attP-cnir* 5' 3' *hom. arms* plasmid was used as transformation vector to generate w^- ;; *P{dcnir}/TM2* flies.

2.2.22 Preparation of egg shells

Flies of the desired genotype were allowed to lay eggs on an apple juice agar plate with a drop of yeast paste over night. Then, eggs were collected with a brush, washed with H₂O and transferred to a microscopy slide with Hoyer's medium/lactic acid (1:1). The preparations were kept at 60 °C for at least 24 h before microscopy.

2.2.23 Dissection, fixation and antibody staining in ovaries

For detection of protein localization in ovarian tissues fluorescent antibody staining was performed. For detection, a primary antibody against the protein of choice is used for specific binding. Finally, a fluorescently labeled secondary antibody against the primary is used for final detection of protein localization.

All steps during dissection and fixation, washing, blocking reactions and incubations during the procedure were made with PBT (PBS 0.1 % Triton X-100), at room temperature with a volume of 1 ml and if not, labeled individually. Each washing step, blocking reaction and incubation were carried out with agitation.

Three to four days before dissection freshly hatched female flies were put into fly vials with dry yeast to stimulate production of big ovaries. Afterwards, they were dissected in cold PBT.

The ovaries were fixed in 4 % formaldehyde diluted in PBT and shook for 10 min on a wheel. Afterwards, they were used directly for the following staining procedure. First, the fixed ovaries were washed twice with PBT for 5 min and then blocked in PBT (PBS 1 % Triton X-100) with 1 % BSA for 1 h. Afterwards, the incubation with the primary antibody was made in PBT (PBS 1 % Triton X-100) with 1 % BSA at 4 °C over night. On the next day the ovaries were washed again twice with PBT for 5 min and then blocked in PBT with 10 % NGS for 1 h. Subsequently, the ovaries were incubated with the secondary antibody in PBT for 2-3 h. Finally, they were washed twice with PBT and mounted in Vectashield, or alternatively Vectashield with DAPI.

2.2.24 Dissection, fixation and antibody staining in imaginal discs

For detection of protein localization in imaginal discs fluorescent antibody staining was performed. The detection procedure is described in 2.2.23

All steps during dissection and fixation, washing, blocking reactions and incubations during the procedure were made with PBT (PBS 0.1 % Triton X-100), at room

temperature with a volume of 1 ml and if not, labeled individually. Each washing step, blocking reaction and incubation were carried out with agitation.

Third instar larvae were dissected on ice and fixed in 4% paraformaldehyde for 20 min. Afterwards, the larval carcasses containing imaginal discs were washed 3 times with PBT for 5 min and then blocked in PBT with 5% NGS for 1 h. Then, the incubation with the primary antibody was made in PBT at 4 °C over night. Subsequently, the carcasses were washed three times with PBT for at least 20 min. Then, secondary antibody was added to the imaginal discs and they were incubated for 2-3 h in the dark. Finally, the imaginal discs were washed three times with PBT for 20 min and then mounted on microscopy slides in Vectashield, or alternatively Vectashield with DAPI.

2.2.25 Phylogenetic analysis of Cornichon proteins and protein membrane topology

The *Drosophila* Cornichon protein sequences were downloaded from flybase.org in FASTA format and then blasted in ncbi.nlm.nih.gov to obtain homologous protein sequences from other species. The phylogenetic analysis was made via Phylogeny.fr [Dereeper *et al.*, 2008] using the "one click" settings. The prediction of the transmembrane topology of Cornichon proteins was made via TMHMM v2.0 and TMPred.

3 Results

3.1 Phylogenetic analysis of Cni proteins and the Cnir membrane topology

To obtain a more comprehensive view on the phylogeny of Cni proteins, a phylogenetic analysis was performed (fig. 3.1). Although almost all eukaryotes possess at least two Cni paralogs it is not always possible to see direct orthology of Cni proteins across species. Cni paralogs from *Arabidopsis thaliana* (*At*), for example, rather group together and do not show specific homology to Cni proteins from yeast, invertebrates or vertebrates. Strikingly, the *At* Cni-like₁ protein has four transmembrane domains (TMDs) (topology predicted by TMHMM v2.0 and TMpred), which is in contrast to the three TMDs of most Cni proteins as depicted for *Drosophila* Cnir in fig 3.2.

Furthermore, the *At* putative CNI protein has only two TMDs (topology predicted by TMHMM v2.0 and TMpred). However, human CNIH₄ splice variants with only two TMDs have also been reported [Sauvageau *et al.*, 2014]. Both Cni paralogs from *Saccharomyces cerevisiae* (*Sc*) also group together, without showing a clear sequence homology with any Cni protein from other species. However, amongst invertebrates and vertebrates the relationship between individual Cni proteins becomes more obvious. The only Cni present in *Caenorhabditis elegans* (*Ce*), and the Cni proteins from insects, including *Drosophila melanogaster* (*Dm*) Cni, are most closely related to the vertebrate paralogs CNIH₁, CNIH₂ and CNIH₃, where CNIH₂ and CNIH₃ may have arisen from CNIH₁ by two consecutive gene duplications.

Interestingly, the vertebrate CNIH₄ proteins show higher sequence homology to the insect Cnir proteins than to their paralogs CNIH₁-CNIH₃, suggesting an ancient original duplication within the animal lineage.

3.2 Generation of a *cnir* knock-out line

There is no published *cnir* mutant *Drosophila* stock. Therefore, a *cnir* knock-out line was generated via ends out gene targeting in the *Drosophila* germ line [Gong and Golic, 2003; Huang *et al.*, 2008]. This system makes use of a transgenic donor construct containing homology arms flanking the gene of interest. Upon enzymatic excision and linearization, the donor mimics a DNA double strand break. Then, the endogenous

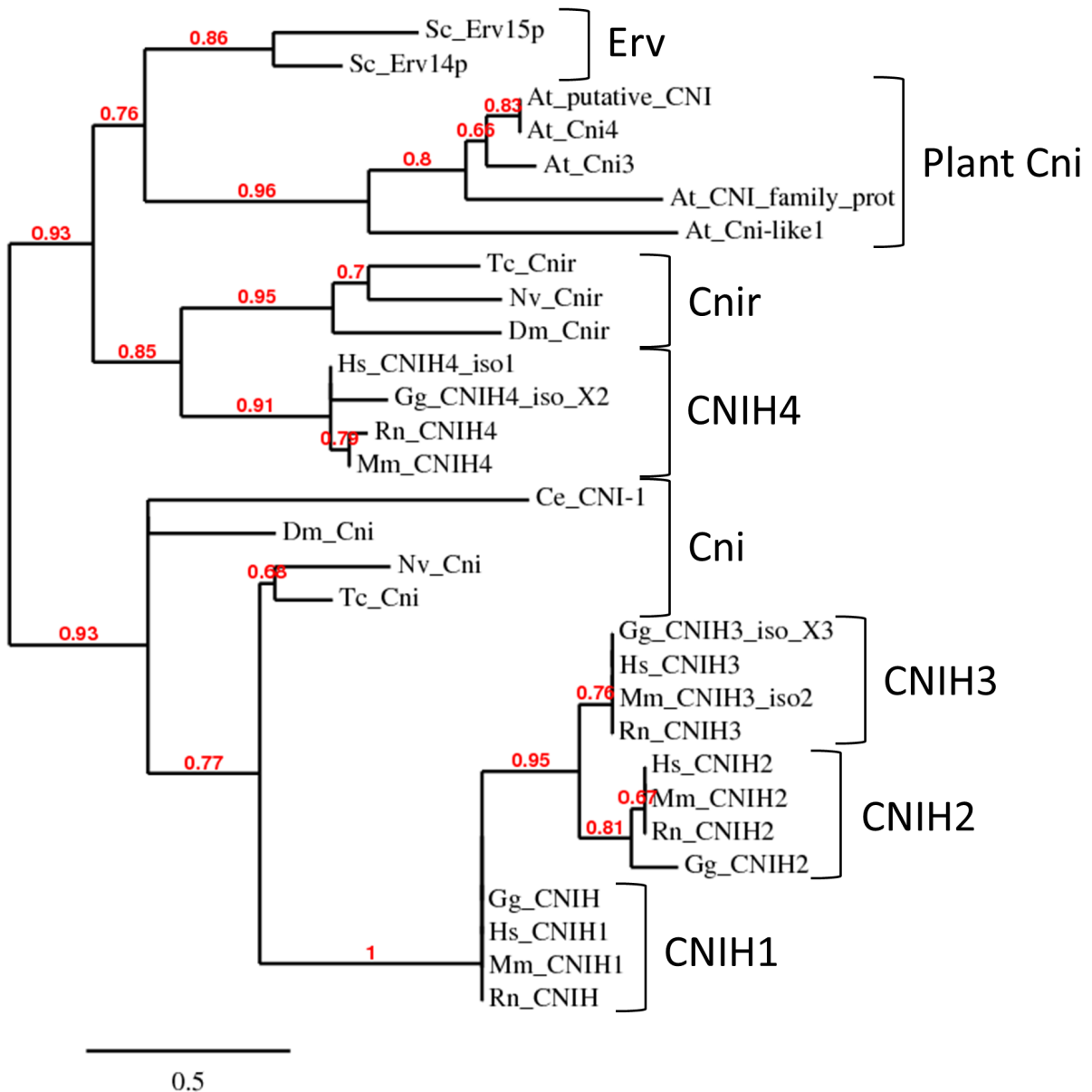


Figure 3.1 | Phylogenetic Analysis of Cni Proteins

Phylogenetic analysis of Cni proteins from *Arabidopsis thaliana* (At), *Saccharomyces cerevisiae* (Sc), *Drosophila melanogaster* (Dm), *Nasonia vitripennis* (Nv), *Tribolium castaneum* (Tc), *Mus musculus* (Mm), *Gallus gallus* (Gg), *Rattus norvegicus* (Rn) and *Homo sapiens* (Hs). Red numbers show branch support values. PhyML phylogenetic analysis using aLRT statistical test for branch support [Dereeper *et al.*, 2008].

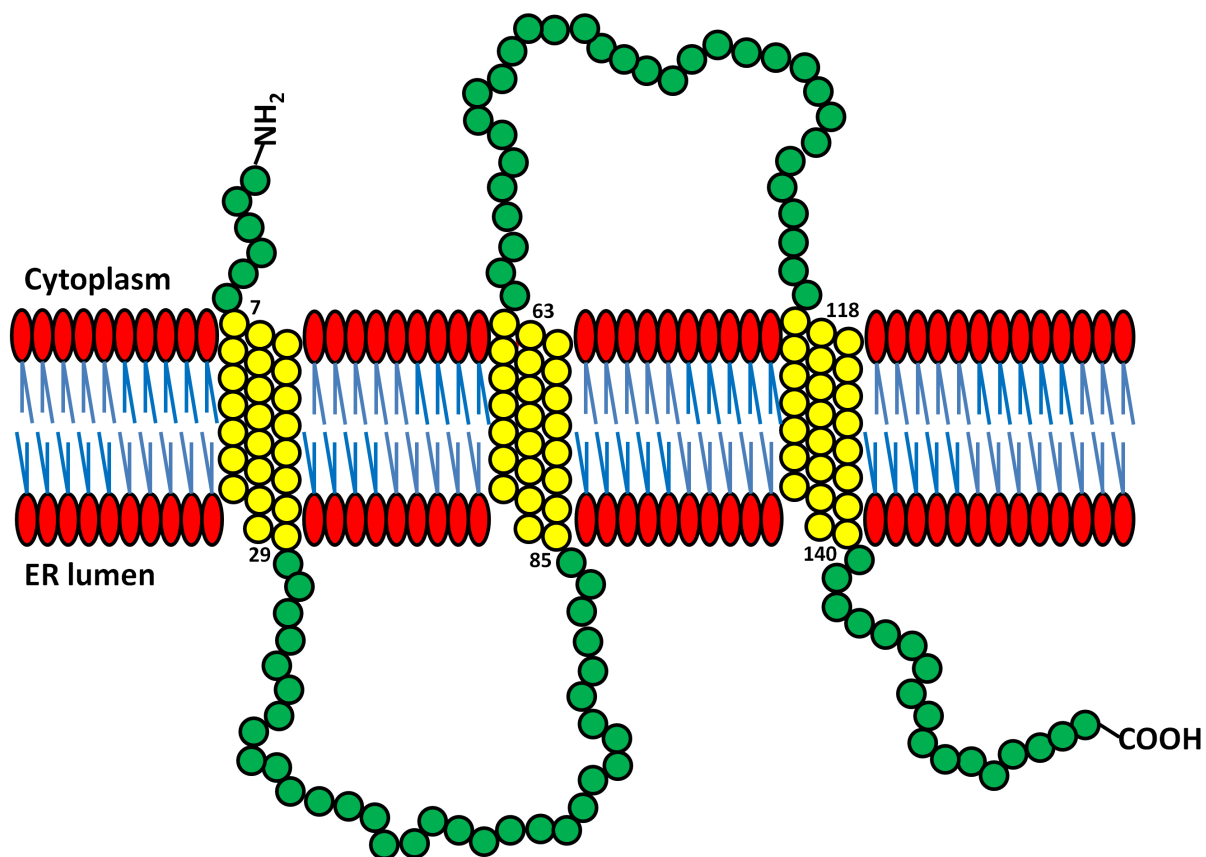


Figure 3.2 | Predicted Cnir membrane topology

Model for the predicted membrane topology of Cnir using TMHMM v2.0 and TMPred. The N-terminus is facing the cytoplasm, while the C-terminus lays in the ER lumen. All 157 amino acids of Cnir are displayed. The residues of the three transmembrane helices are labeled yellow and all other amino green. The lipids of the ER membrane are indicated by red ovals with blue tails.

DNA repair machinery of *Drosophila* uses this donor for homologous recombination, replacing the targeted gene locus with a marker gene provided by the donor. The *cnir* gene is located on the left arm of chromosome 2 and has only one transcript of 871 bp length (fig. 3.3; flybase.org). It encodes a small protein of 157 amino acids and a molecular weight of 18.43 kDa (fig. 3.2; <http://www.uniprot.org>). The genomic locus of *cnir* is flanked by multiple genes within a region of only ~10 kb. The aim was to remove the *cnir* coding sequence (cds) and the introns (590 bp), but leave the untranslated regions (UTRs) intact. The deletion locus can be targeted via site-specific transgenesis [Bischof *et al.*, 2007]. Therefore, intact UTRs simplify the generation a N- or C-terminally epitope tagged Cnir driven from its endogenous promoter with only small alterations of the transcript. The *cnir* genomic locus and gene structure, as well

as the position of the homology arms used for targeting of *cnir* are depicted in fig. 3.3.

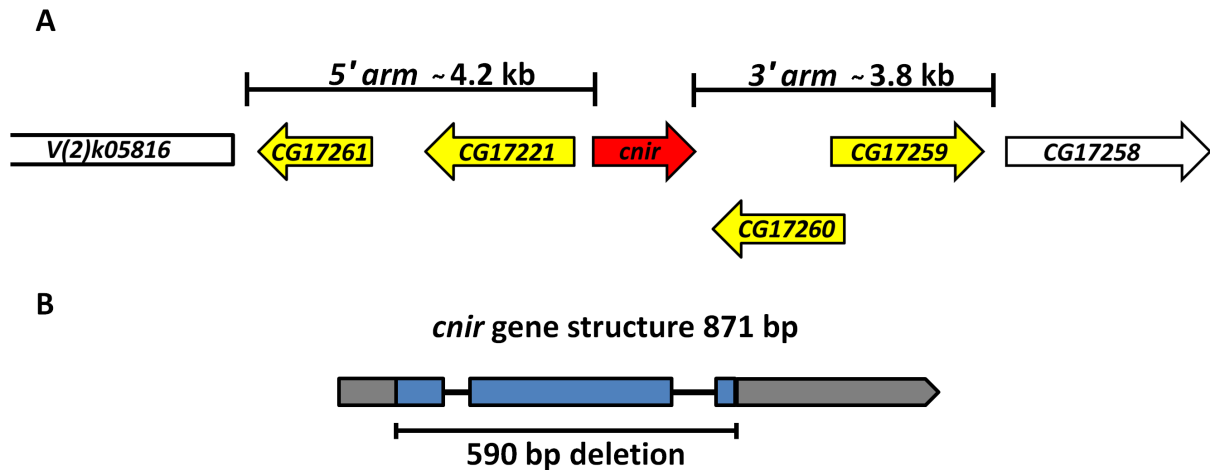


Figure 3.3 | The *cnir* genomic locus

A. Scheme of the *cnir* genomic locus and the positions of the 5' and 3' homology arms used for cloning of the $P\{dcnir\}$ donor construct. The *cnir* gene is highlighted in red and genes included in the homology arms are marked in yellow. B. *cnir* gene structure from 5' to 3' with 3 exons (blue), 2 introns (black lines) and UTRs (grey). The planned deletion of 590 bp for a *cnir* knock-out is indicated below the scheme.

A scheme of the targeting strategy employed for the knock-out of the *cnir* locus is depicted in figure 3.4. The transgenic $P\{dcnir\}$ donor consists of the previously mentioned homology arms (5' and 3') flanking an *attP* site, a *white* (w^+) marker gene, and two *loxP* sites, which in turn flank the *white* gene. Furthermore, $P\{dcnir\}$ has a $UAS::Reaper$ construct downstream of the 3' homology arm, which causes lethality upon GAL_4 mediated neuronal activation. In the event of a specific recombination, $P\{dcnir\}$ integrates into the target genomic locus and $UAS::Reaper$ will be lost as a consequence, while it is likely to be maintained in the case of non targeted integrations. Thus, $UAS::Reaper$ helps to select against false positive targeting events. The $P\{dcnir\}$ is activated by FLP mediated excision from its insertion site on the third chromosome and subsequent I-Sce-I mediated linearization (indicated by *), which mimics a DNA double strand break. In a subsequent process, the donor is used by the endogenous DNA double strand break repair machinery to replace the *cnir* gene with the *white* marker gene. The *loxP* sites were used for subsequent Cre mediated excision of *white*. This allows *attP* site-specific transgenic targeting of the knock-out locus as described by Bischof *et al.* [2007].

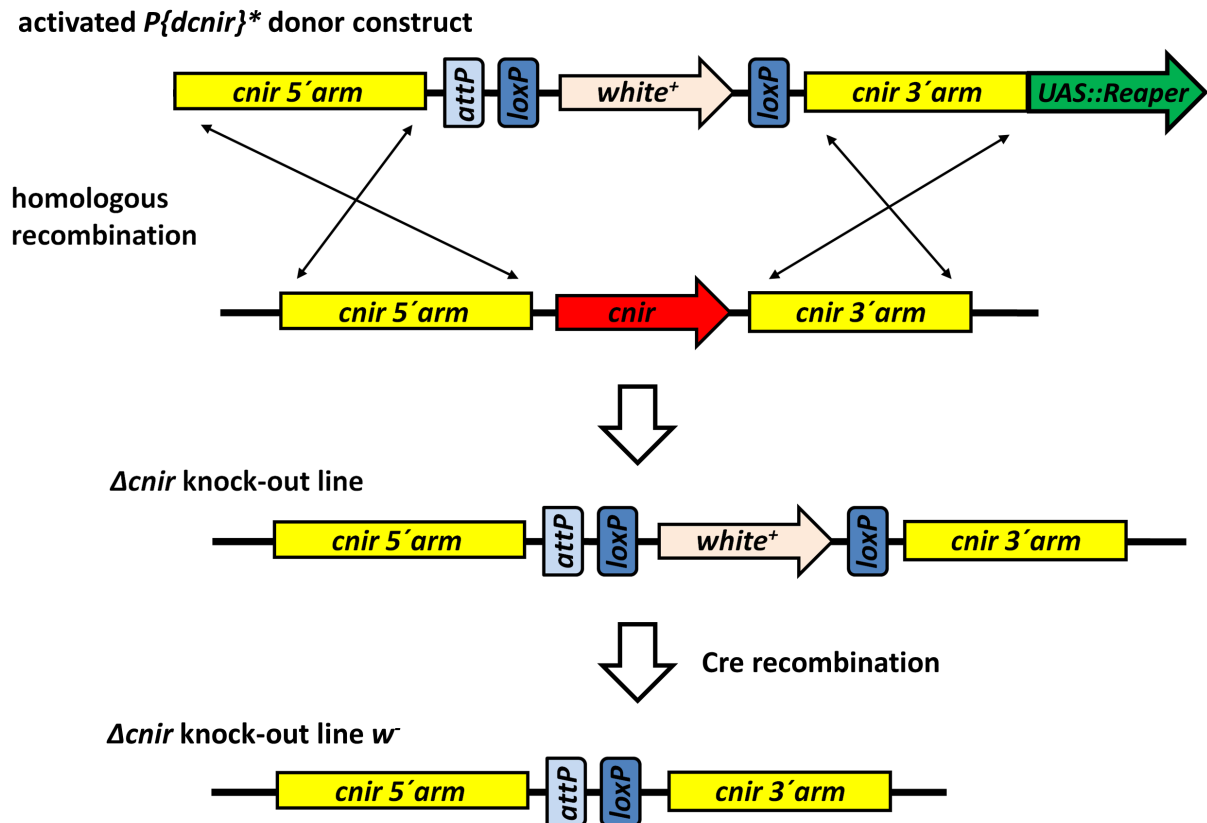


Figure 3.4 | Targeting of *cnir*

A scheme of the targeting strategy for the *cnir* locus. First, the linearized and thus activated $P\{dcnir\}^*$ construct is used as a template for homologous recombination. The donor is engineered such that two homology arms flank the sequence designated to replace the targeted locus. Through successful homologous recombination the endogenous *cnir* region is replaced from start to stop codon by the sequence between both homology arms. Furthermore, a specific integration leads to a loss of the *UAS::Reaper* construct downstream of the 3' homology arm, which can be used for selection against false positive targeting. Ultimately, Cre mediated recombination is utilized for excision of the *white* marker gene, allowing *attP* site-specific transgenic targeting of the knock-out locus.

Out of 380 targeting crosses, 47 putative Δ *cnir* flies were obtained, of which 23 contained an insertion on the second chromosome, indicating successful *cnir* targeting. Five of the subsequently established potential *w*⁻; Δ *cnir* [*w*⁺] stocks (no. 5, 7, 21, 24 and 40) were tested via PCR for the position of the appropriate $P\{dcnir\}$ insertion. A scheme illustrating the locations of all test PCR fragments and documentation of the actually obtained PCR amplicons is depicted in fig. 3.5.

First, the insertion of $P\{dcnir\}$ was tested using the position of the homology arms as a reference. The first primer pair was positioned inside of the *white* marker gene

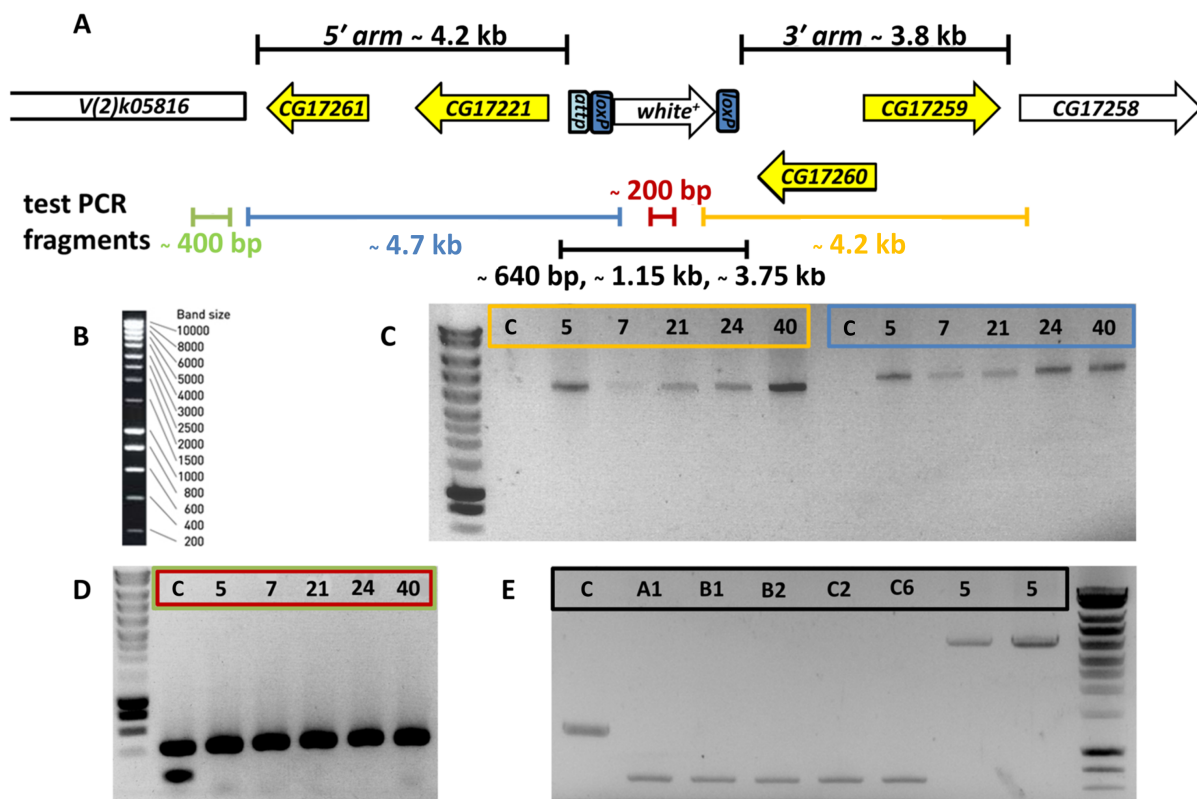


Figure 3.5 | Test for *cnir* knock-out and removal of the *white* marker

A. Scheme of the $\Delta cnir$ founder line with the *white* marker gene still present. The position of each test PCR fragment used for validation of a successful knock-out with the expected product size indicated (colored lines). B. SmartLadder (Eurogentec, Köln) as a size reference for the test PCR fragments. C. Test PCR products for the insertion of the *white* marker and replacement of the *cnir* sequence from start to stop codon, as well as the position of the 3' (orange) and 5' (blue) homology arms. D. Obtained amplicons for the *cnir* gene (red) and a control fragment upstream of the 5' homology arm (green). E. PCR fragments for the sequence between both homology arms before and after Cre mediated excision of the *white* marker gene (black). $w^- ; \Delta cnir [w^+]$: 5, 7, 21, 24 and 40; $w^- ; \Delta cnir$: A1, B1, B2, C2 and C6; $w^- ; P\{d cnir\}/TM2$: C in gels C and D; wt: C in gel E.

and downstream of the 3' homology arm (fig. 3.5 C; orange). The second primer pair lay upstream of the 5' homology arm and again inside of the *white* marker (fig. 3.5 C; blue). Thus, only an insertion in the accurate genomic locus can yield PCR products. The control PCR was made using genomic DNA from $w^- ; P\{d cnir\}/TM2$ flies, which possess the endogenous *cnir* locus, as well as the $P\{d cnir\}$ insertion on the third chromosome. A fragment of the expected 4.2 kb size was obtained for the position of the 3' homology arm. Furthermore, a 4.7 kb product was obtained for

the position of the 5' homology arm. The genomic DNA from $w^- ; P\{dcnir\}/TM2$ flies did not yield any PCR products, confirming that an amplification of the expected fragments is only possible with $P\{dcnir\}$ insertion in the designated genomic locus.

To confirm whether the *cnir* gene was successfully removed from its endogenous genomic locus, a test PCR was made using a primer pair spanning the second intron of the *cnir* gene with an expected amplicon of 200 bp (fig. 3.5 D; red). A control PCR was made on the same genomic DNA, aiming to amplify a 400 bp product inside of the *V(2)k05816* gene upstream of the 5' homology arm (fig. 3.5 D; green). It was possible to obtain both products from $w^- ; P\{dcnir\}/TM2$ genomic DNA. This result also reconfirms that the lack of product in the previously described experiment is not due to poor quality of genomic DNA. However, all $\Delta cnir$ stocks lack the smaller product, while the larger could be obtained. Those results indicate a successful deletion of the *cnir* gene in the tested stocks.

After removal of the *white* marker gene via Cre mediated recombination, the $w^- ; \Delta cnir$ stocks (no. A1, B1, B2, C2 and C6) were tested with a primer pair spanning the sequence between both homology arms (fig. 3.5 E; black). Therefore, in case of a successful removal of w^+ a 640 bp product is expected, while a 3.75 kb product is expected in case of the presence of the full $P\{dcnir\}$ sequence between the homology arms in the $w^- ; \Delta cnir [w^+]$ stock (no. 5). A control PCR was made on wt genomic DNA, which should yield a 1.25 kb product because of the presence of the endogenous *cnir* locus. Amplicons of the expected size were obtained from genomic DNA of all tested $w^- ; \Delta cnir$ stocks and both controls, indicating a successful Cre mediated excision of the *white* marker gene.

3.3 Survivorship of $\Delta cnir$ throughout development

Since $w^- ; \Delta cnir [w^+]$ mutant flies turned out to be viable, they were first analyzed for survival rates throughout development. Lethality rates were determined after fertilization, hatching, pupation and eclosion. To see if the loss of *cnir* causes increased mortality in any of those stages, each stage was considered independently (fig. 3.6).

For this and all following experiments the $w^- ; \Delta cnir [w^+]$ line no. 5 was used. For reasons of simplification, the stock will be referred to thereafter as $\Delta cnir$ only. As a control for $\Delta cnir$ mutants (n= 498), w^{1118} (n= 500) and $\Delta cnir/+$ (n= 500) flies were used. The heterozygous flies were used to identify putative dominant or dosage effects of the *cnir* mutation.

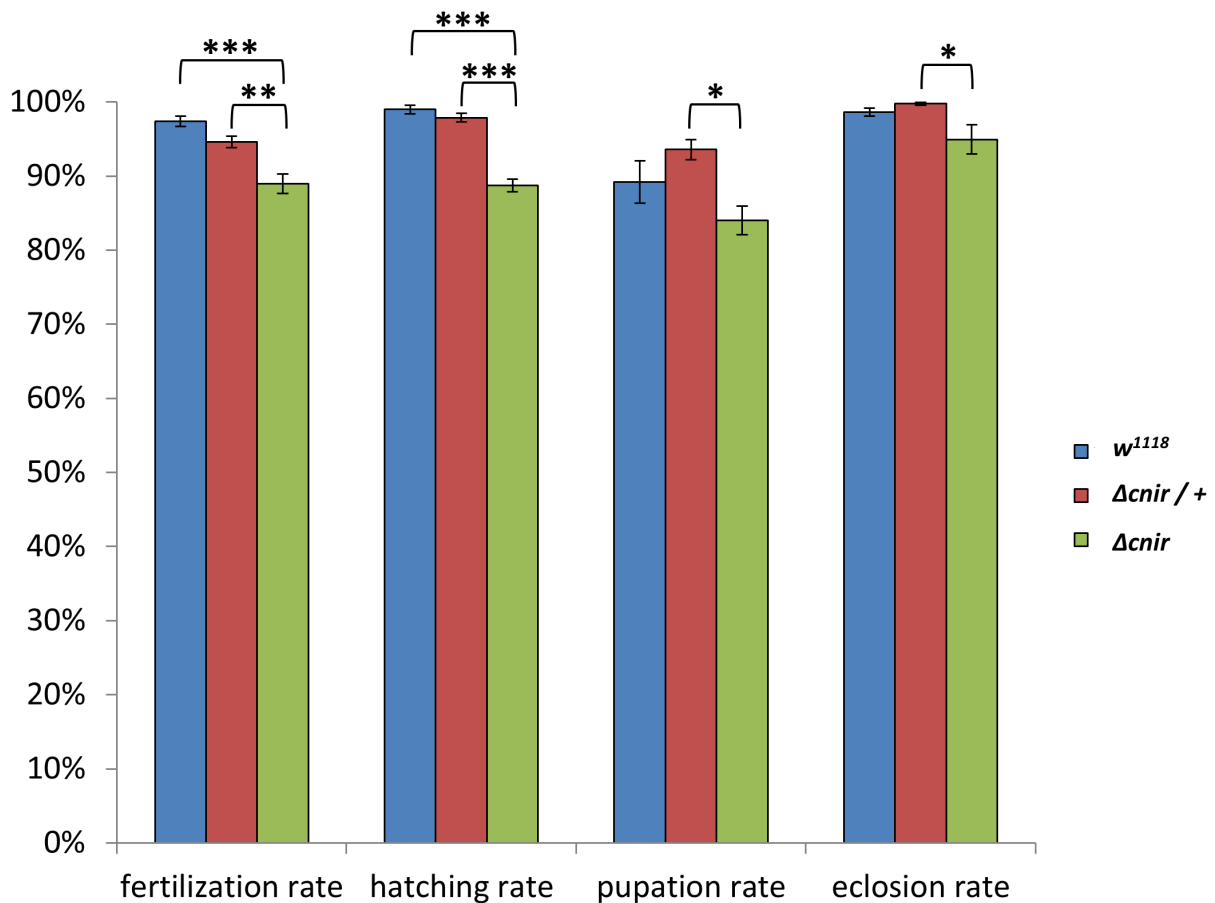


Figure 3.6 | Analysis of survival rates throughout development

The *Δcnir* flies have a reduced fertilization and hatching rate in comparison to both control genotypes. However, *Δcnir* flies show a lower pupation and eclosion rate only in comparison to the heterozygous control. Bars= mean ± sem; *Δcnir* (green) n= 498; *w*¹¹¹⁸ (blue) n= 500; *Δcnir*/+ (red) n= 500; *p ≤ 0.05; **p ≤ 0.01; ***p ≤ 0.001

The fertilization rate of eggs from *w*¹¹¹⁸ flies (97.4 ± 0.7%) does not differ significantly from that of *Δcnir*/+ flies (94.6 ± 0.8%). However, the fertilization rates from both genotypes are significantly higher compared to that of *Δcnir* (p ≤ 0.01; p ≤ 0.001)

The hatching rates of *w*¹¹¹⁸ larvae (98.0 ± 0.6%) and that of *Δcnir*/+ larvae (97.9 ± 0.6%) again do not differ significantly. Compared to the hatching rate of *Δcnir* larvae (88.7 ± 0.8%), that of both *w*¹¹¹⁸ and *Δcnir*/+ larvae is higher (p ≤ 0.001 for both comparisons).

However, the rate of pupation in *Δcnir* (84.0 ± 1.9%) is not significantly lower than that of *w*¹¹¹⁸ (89.2 ± 2.8%), while it is significantly lower (p ≤ 0.05) than that of *Δcnir*/+ (93.6 ± 1.4%).

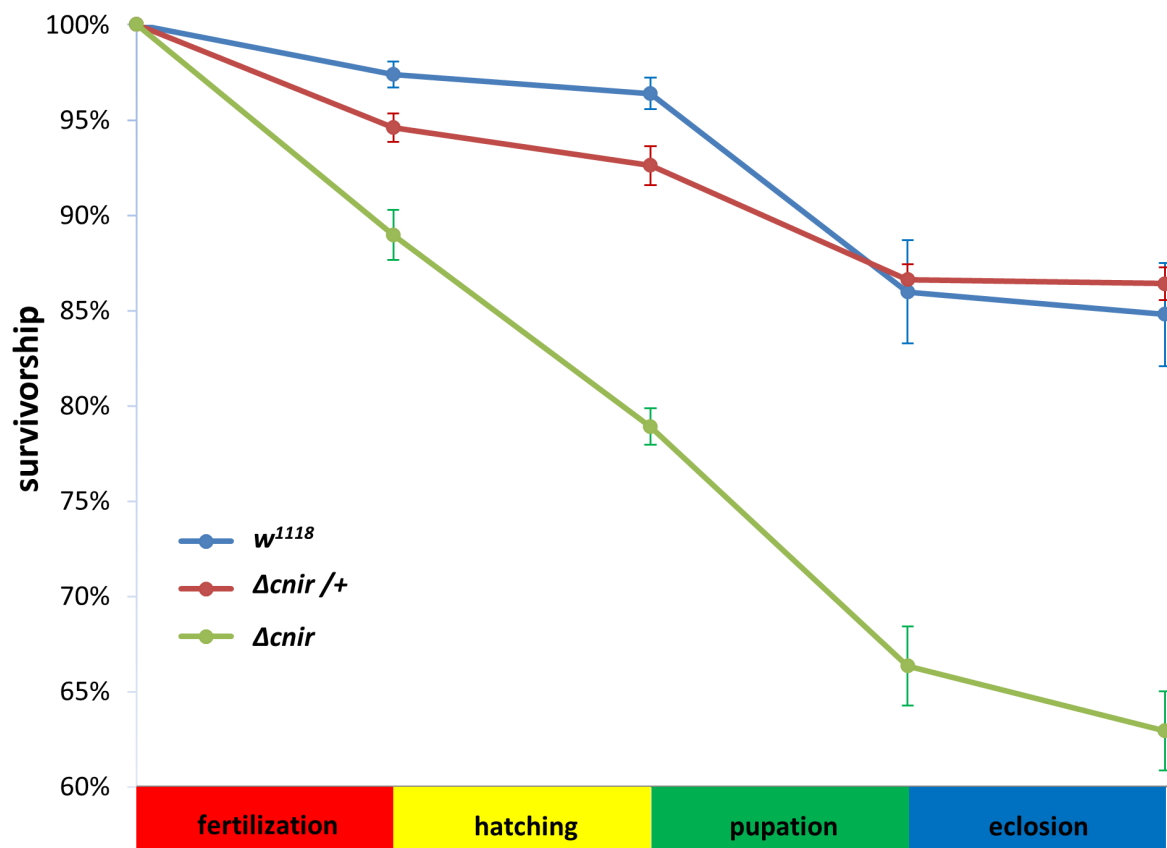


Figure 3.7 | Survivorship until adulthood

Survival curves for the experimental genotypes. $\Delta cnir$ survival till adulthood is lower ($p \leq 0.0001$) than $\Delta cnir/+$ and also lower ($p \leq 0.0001$) than w^{1118} survival. Both control genotypes do not differ in their survivorship till adulthood. Thus the lack of both *cnir* copies has an influence on survivorship till adulthood, while the lack of just one copy does not exhibit any effect. Bars = mean \pm sem; $\Delta cnir$ (green) $n = 498$; w^{1118} (blue) $n = 500$; $\Delta cnir/+$ (red) $n = 500$.

The same can be observed for the eclosion rate, which is not significantly different between $\Delta cnir$ ($94.9 \pm 2.0\%$) and w^{1118} ($98.6 \pm 0.6\%$), whereas it is significantly lower in $\Delta cnir$ ($p \leq 0.05$) compared to $\Delta cnir/+$ ($99.8 \pm 0.2\%$).

Analogous to adult lifespan experiments, the generated data was used to investigate the cumulative survivorship of each experimental genotype across all developmental stages until adulthood (fig. 3.7). The evaluation of the data also shows that $\Delta cnir$ mutant survivorship into adulthood is lower ($p \leq 0.0001$) than that of w^{1118} and also lower ($p \leq 0.0001$) than that of the $\Delta cnir/+$ genotype. Thus, *cnir* mutants have a higher risk of mortality passing through the investigated developmental stages in comparison to both control genotypes, which do not differ significantly in

their survivorship until adulthood. Hence, the lack of one *cnir* copy also does not lead to an increased mortality. In total, only $62.9 \pm 2.1\%$ $\Delta cnir$ flies reach adulthood, while $84.8 \pm 2.7\%$ w^{1118} and $86.4 \pm 0.9\%$ $\Delta cnir/+$ flies emerge as adults. Most notably, a strikingly high proportion of the eclosed $\Delta cnir$ flies sticks to the food inside of the vial, which cannot be observed for the control genotypes.

3.4 Survivorship of adult $\Delta cnir$ flies

Beyond the previously described increased mortality throughout development, $\Delta cnir$ mutant flies held under stock keeping conditions have a shorter lifespan than other common laboratory fly stocks. To evaluate the lifespan of the mutants, a survival experiment was performed comparing the mutant stock with $\Delta cnir/+$ heterozygous and w^{1118} control flies. The survival curves for the three experimental genotypes are depicted in fig. 3.8.

The median lifespan of $\Delta cnir$ flies is 37 days and their maximum lifespan is 74 days. The evaluation of the survival curves shows that mutant flies have a shorter lifespan ($p \leq 0.0001$) than w^{1118} flies, which have a median lifespan of 40.5 days and a maximum lifespan of 81 days. Furthermore, mutant flies have a shorter lifespan ($p \leq 0.0001$) than $\Delta cnir/+$ flies, which display a median lifespan of 47.5 days and a maximum lifespan of 95 days. However, w^{1118} flies also have a shorter lifespan ($p \leq 0.0001$) than $\Delta cnir/+$ heterozygous flies. This result indicates putative stress in w^{1118} flies, rather than a positive influence of the lack of one *cnir* copy in the heterozygous flies. Importantly, $\Delta cnir$ have a reduced lifespan in comparison to both control genotypes.

3.5 Locomotion defects of $\Delta cnir$ flies

A major trait of $\Delta cnir$ flies is that they preferentially remain at the bottom of the food vial. This is surprising, as normally flies tend to walk up against the earth's gravitational field when they are exposed to a gravity stimulus, which is a robust behavior known as negative gravitaxis [Beckingham *et al.*, 2005]. Therefore, this behavior can be used to quantify potential locomotion defects by monitoring the distribution of flies in the countercurrent apparatus (CA) after execution of the climbing assay [Inagaki *et al.*, 2010]. The CA consist of six tubes (see 2.2.4) and flies distribute in the CA depending on how often they chose to climb up the tube wall. In a genetically homogeneous population of independently acting flies with a constant likelihood to climb

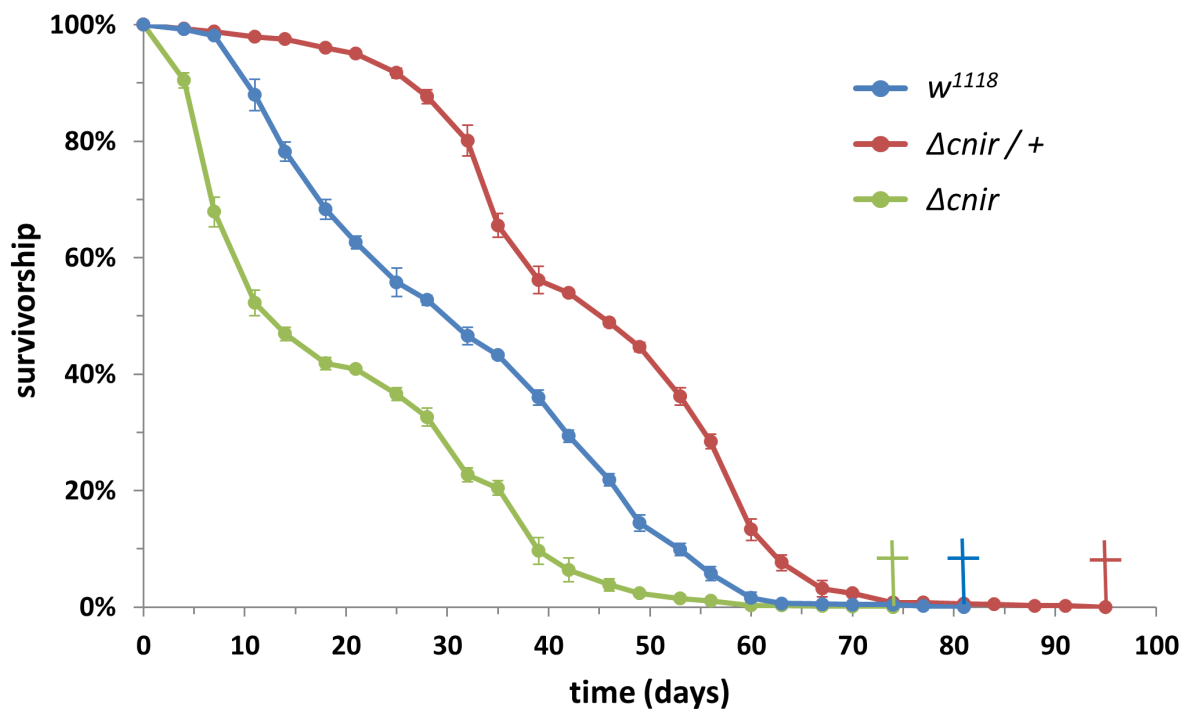


Figure 3.8 | Survivorship of adult *Drosophila*

Survival curves for the experimental genotypes. $\Delta cnir$ flies have a shorter lifespan ($p \leq 0.0001$) than $\Delta cnir/+$ and also a shorter lifespan ($p \leq 0.0001$) than w^{1118} control flies. Furthermore, w^{1118} flies have a shorter lifespan ($p \leq 0.0001$) than $\Delta cnir/+$ flies. Bars = mean \pm sem; w^{1118} : $n = 977$; $\Delta cnir/+$ $n = 943$; $\Delta cnir$ $n = 979$. Maximum lifespan is indicated by colored crosses.

up the wall in all attempts (0-5), the distribution of flies in the CA should be binomial [Benzer, 1967; Inagaki *et al.*, 2010]. The comparison of measured- to binomial distributions with the partition coefficient Cf has shown that wt and mutant flies distribute in a binomial fashion [Benzer, 1967; Kamikouchi *et al.*, 2009]. Thus, calculating the Cf can be used to quantify negative gravitaxis [Inagaki *et al.*, 2010].

The behavioral assay demonstrated that $\Delta cnir$ are able to climb up the vial wall given enough time after application of a gravity stimulus. However, the legs appear to be slightly shaky. Because the X chromosome of the $\Delta cnir$ stock did not definitely correspond to the w^{1118} control stock background, it was essential to test for a putative influence of this chromosome in the locomotion assay used. Therefore, only $\Delta cnir/+$ flies carrying this X chromosome were used in the assay. Furthermore, this genotype allowed the simultaneous testing of whether the lack of one *cnir* copy has dominant or dosage effects that alter locomotion.

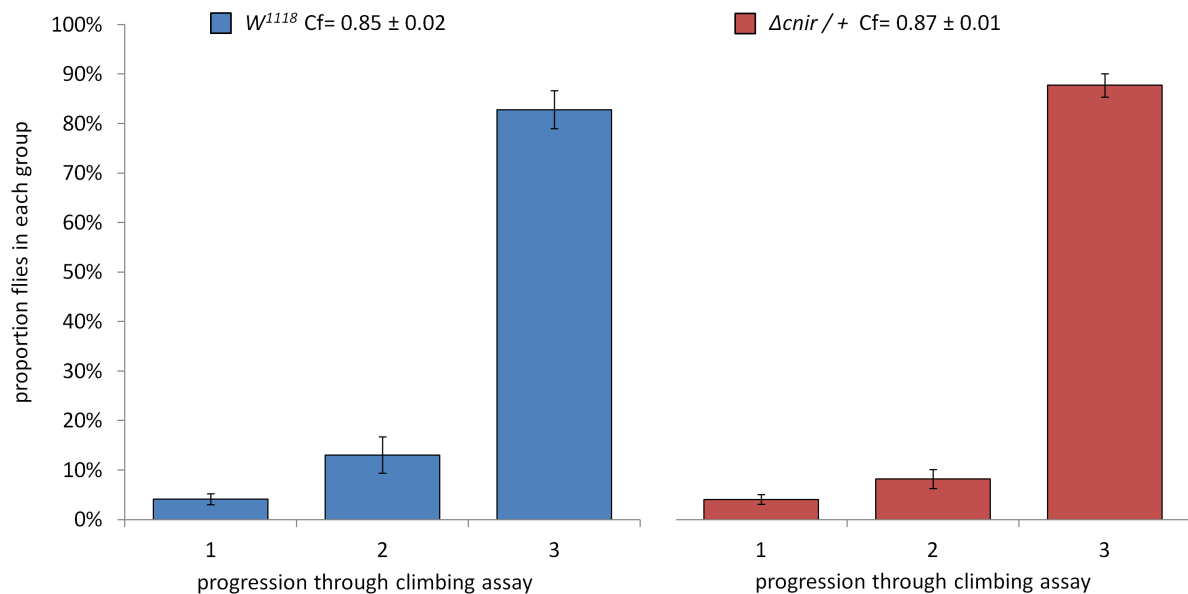


Figure 3.9 | Locomotion of w^{1118} and $\Delta cnir/+$ flies

Distribution of flies in groups of the CA after the climbing assay. Analysis of the Cf value reveals no statistically significant difference between w^{1118} (blue) and $\Delta cnir/+$ (red) flies. Furthermore, both experimental genotypes reach group 3 of the CA above the literature value for wt flies [Inagaki *et al.*, 2010]. Thus, there are no dominant or dosage influences on locomotion through the lack of one *cnir* copy. w^{1118} : 4.2 ± 1.1% group 1, 13 ± 3.7% group 2, 82.8 ± 3.8% group 3; $\Delta cnir/+$: 4.1 ± 1% group 1, 8.2 ± 1.9% group 2, 87.7 ± 2.4% group 3; bars= mean ± sem; n= 10 trials per experimental group.

The distribution of flies in the CA after the locomotion assay is depicted in fig. 3.9. Both experimental groups were tested in 10 trials. After execution of the climbing assay the vast majority (82.8 ± 3.8%) of w^{1118} flies successfully climbed through the CA in group 3. Similarly most (87.7 ± 2.4%) $\Delta cnir/+$ flies also reached group 3. It has been reported that at least 60% of wt flies progress to group 3 of the CA upon correct execution of the assay [Inagaki *et al.*, 2010]. Moreover, the statistical evaluation reveals no significant difference in the distribution of flies in the countercurrent apparatus between w^{1118} (Cf= 0.85 ± 0.02) and $\Delta cnir/+$ (Cf= 0.87 ± 0.01) flies. Thus, there is no detectable influence of the X chromosome in the $\Delta cnir$ stock on the locomotion assay used. Furthermore, there are no obvious dominant or dosage effects caused by the lack of one *cnir* copy.

Because $\Delta cnir/+$ flies showed no locomotion defects, they were used as a control for assaying the locomotion of $\Delta cnir$ flies (fig. 3.10). Both experimental groups were tested in 10 trials.

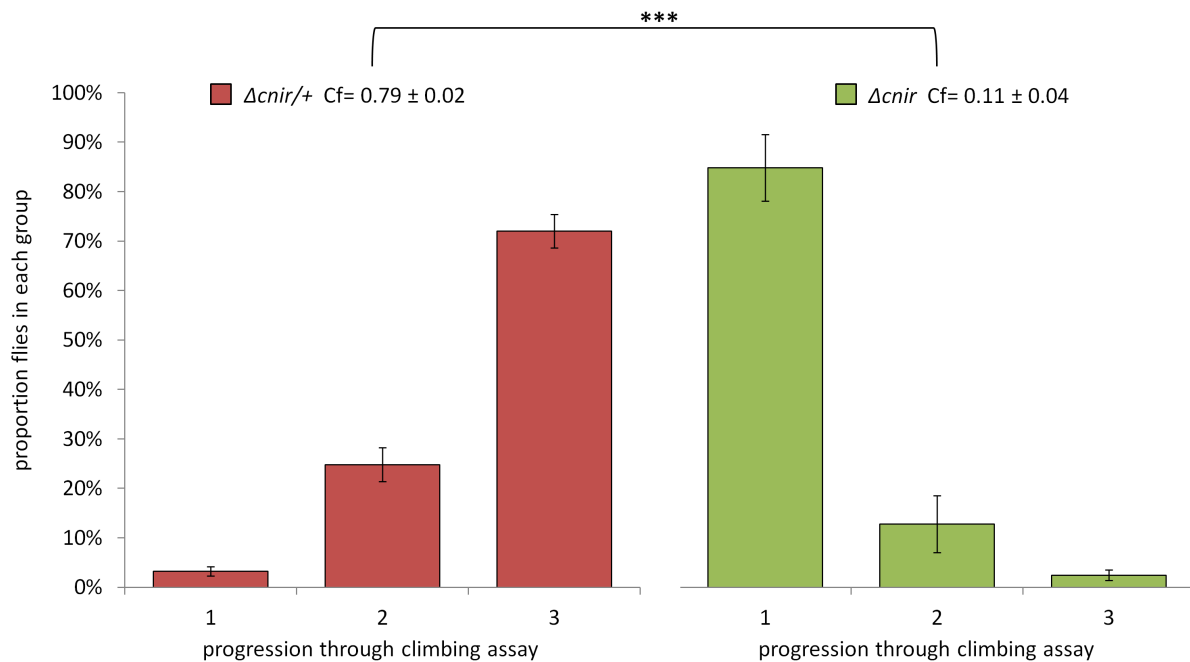


Figure 3.10 | Locomotion of $\Delta cnir/+$ and $\Delta cnir$ flies

Distribution of flies in groups of the CA after the climbing assay. Analysis of the Cf value reveals a statistically significant difference between $\Delta cnir/+$ (red) and $\Delta cnir$ (green) flies. Moreover, $\Delta cnir$ flies show impaired locomotion and do not reach group 3 of the CA above the literature value for wt flies [Inagaki *et al.*, 2010]. $\Delta cnir/+$: 3.2 ± 0.9% group 1, 24.8 ± 3.4% group 2, 72 ± 3.4% group 3; $\Delta cnir$: 84.8 ± 6.7% group 1, 12.8 ± 5.8% group 2, 2.4 ± 1.1% group 3; bars: mean ± sem; n=10 trials per experimental group; ***p ≤ 0.001.

Similar to the previous results, the majority (72 ± 3.4%) of $\Delta cnir/+$ flies progressed to group 3 of the CA. In contrast, most (84.8 ± 6.7%) $\Delta cnir$ flies remain in group 1 of the CA. The statistical evaluation shows a highly significant difference (p ≤ 0.001) in the distribution of flies between $\Delta cnir/+$ (Cf= 0.79 ± 0.02) and $\Delta cnir$ (Cf= 0.11 ± 0.04). Hence, the lack of *cnir* function leads to a strong impairment of *Drosophila* locomotion.

3.6 Ethanol sensitivity of $\Delta cnir$ flies

As previously shown, $\Delta cnir$ flies show strong locomotion defects. Since ethanol influences postural control [Bellen, 1998; Devineni and Heberlein, 2013] and thus locomotion, it was tested whether flies with an already defective locomotion show enhanced sensitivity to ethanol.

Flies naturally show a negative gravitaxis behavior when tested in the inebriometer and stay at the top of the column. However, if exposed to ethanol fumes in the column they lose postural control and fall progressively from one baffle to the next. Thus, sensitivity to ethanol can be measured as the mean elution time (MET) needed for flies to reach the bottom of the column [Devineni and Heberlein, 2013].

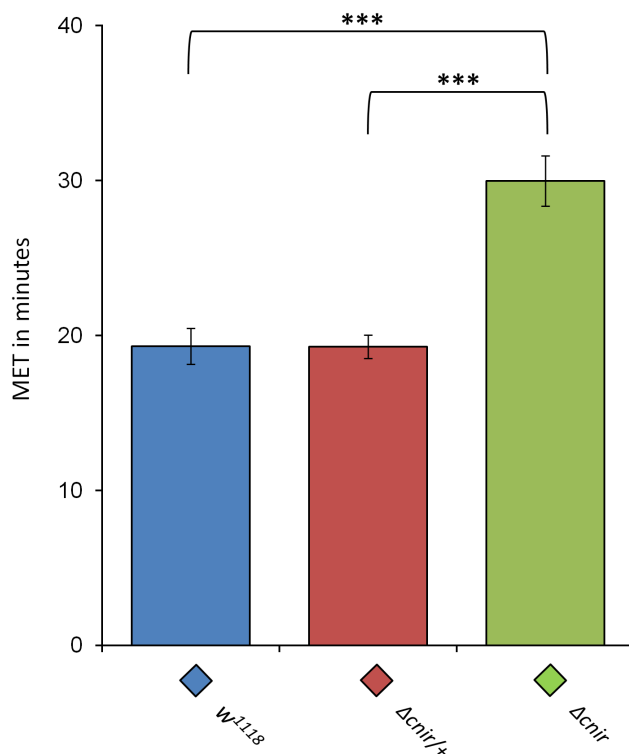


Figure 3.11 | Ethanol sensitivity of w^{1118} , $\Delta cnir/+$ and $\Delta cnir$ flies

MET values of flies after exposure to ethanol fumes. Analysis of the MET reveals no statistically significant difference in ethanol sensitivity between w^{1118} (blue) and $\Delta cnir/+$ (red) flies. However, both genotypes are significantly more sensitive to ethanol fumes than $\Delta cnir$ flies (green). Hence, the lack of one *cnir* copy does not have any effect on sensitivity towards ethanol. Although impaired in locomotion, $\Delta cnir$ flies are less sensitive for the loss of postural control caused by ethanol exposure. Bars: mean \pm sem; n=10 trials per experimental group; *** $p \leq 0.001$.

The results for ethanol sensitivity of the tested genotypes w^{1118} , $\Delta cnir/+$ and $\Delta cnir$ are depicted in fig. 3.11. Each experimental group was tested in 10 trials. There is no statistically significant difference in ethanol sensitivity between w^{1118} (MET= 19.3 ± 1.15) and $\Delta cnir/+$ (MET= 19.27 ± 0.75) flies. This indicates that the lack of one *cnir* copy does not have any effect on ethanol sensitivity in *Drosophila*. Although $\Delta cnir$ flies are strongly impaired in locomotion, surprisingly they are less sensitive to ethanol fume induced loss of postural control (MET= 29.97 ± 1.63). This MET is significantly higher than that of w^{1118} ($p \leq 0.001$) or $\Delta cnir/+$ ($p \leq 0.001$) flies.

3.7 Muscular rescue of locomotion defects

Locomotor disturbance in *Drosophila* is due to pathology of muscles, peripheral neurons, or the central nervous system [Slawson *et al.*, 2011]. To test whether the locomotion defects of $\Delta cnir$ flies are due to a lack of *cnir* function in muscle cells or neurons, rescue experiments in both tissues were conducted. A *UAS::cnir* rescue construct was expressed in muscle cells of $\Delta cnir$ flies using a *mhc::Gal4* driver line [Schuster *et al.*, 1996].

To examine potential dominant influences of the *UAS::cnir* rescue construct or the *mhc::Gal4* driver line on locomotion, both were tested heterozygously in $\Delta cnir$ flies (fig. 3.12). Furthermore, this experiment can reveal a putative leaky expression of the *UAS::cnir* construct, indicated by a rescue without Gal4 driven expression. Each experimental group was tested in 10 trials.

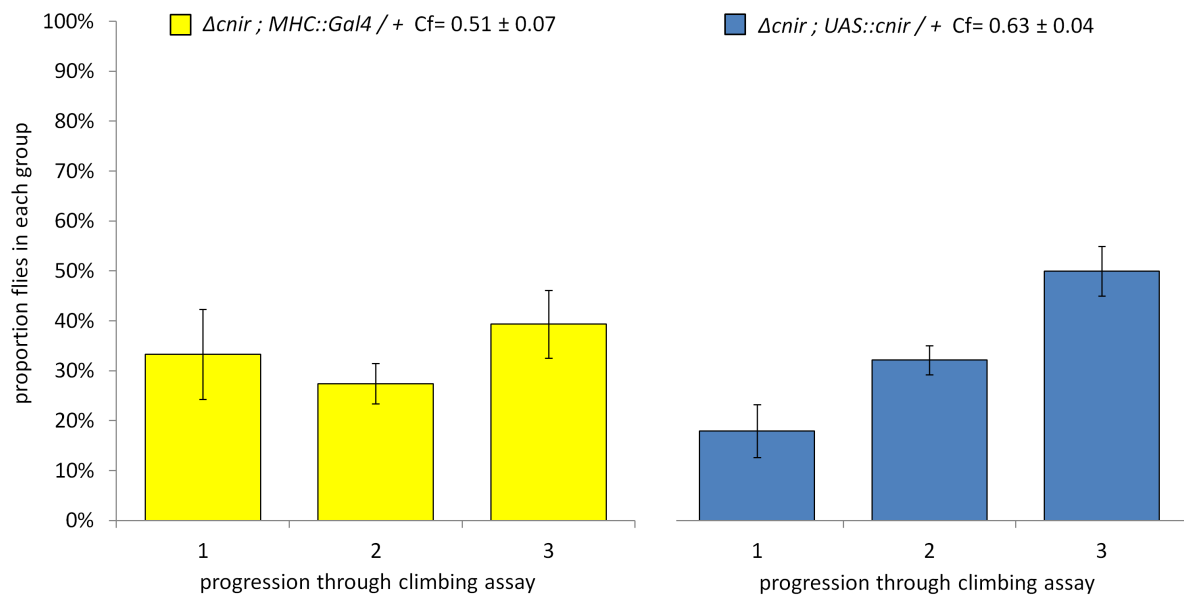


Figure 3.12 | Locomotion of $\Delta cnir ; mhc::Gal4/+$ and $\Delta cnir ; UAS::cnir/+$ flies

Distribution of flies in groups of the CA after the climbing assay. Analysis of the Cf value reveals no statistically significant difference between $\Delta cnir ; mhc::Gal4/+$ (yellow) and $\Delta cnir ; UAS::cnir/+$ (blue) flies. Furthermore, both experimental genotypes show impaired locomotion and do not reach group 3 of the CA above the literature value for wt flies [Inagaki *et al.*, 2010]. $\Delta cnir ; mhc::Gal4/+$: 33.3 ± 9.0% group 1, 27.4 ± 4.1% group 2, 39.3 ± 6.8% group 3; $\Delta cnir ; UAS::cnir/+$: 17.9 ± 5.3% group 1, 32.1 ± 2.9% group 2, 50.0 ± 5.0% group 3; bars= mean ± sem; n= 10 trials per experimental group.

In the $\Delta cnir ; mhc::Gal4/+$ genotype flies are distributed fairly evenly across all three groups of the CA. In comparison, $\Delta cnir ; UAS::cnir/+$ flies were distributed slightly more graded in the CA groups with $50.0 \pm 5.0\%$ of flies reaching group 3. However, the statistical analysis shows that there is no significant difference in the distribution of $\Delta cnir ; mhc::Gal4/+$ flies ($Cf = 0.51 \pm 0.07$) and $\Delta cnir ; UAS::cnir/+$ flies ($Cf = 0.63 \pm 0.04$). Furthermore, in both experimental groups less than 60% of flies reach group 3 of the CA, in contrast to wt expectations [Inagaki *et al.*, 2010]. Hence, both tested genotypes show impaired locomotion and either can be used as a negative control for the rescue experiment.

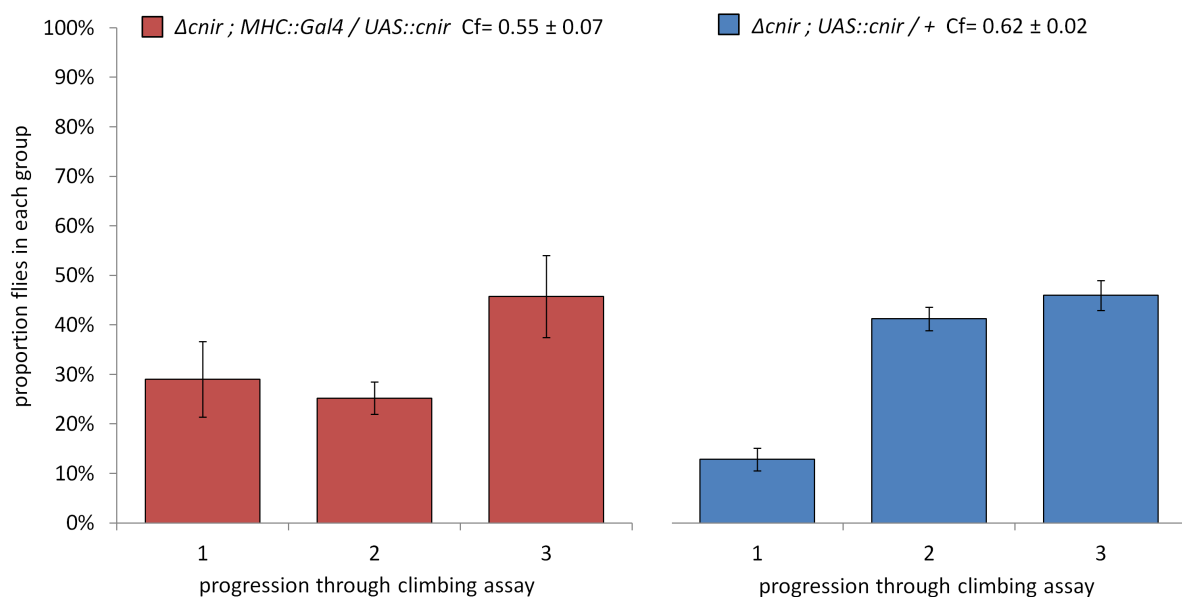


Figure 3.13 | Locomotion of $\Delta cnir ; mhc::Gal4/UAS::cnir$ and $\Delta cnir ; UAS::cnir/+$ flies

Distribution of flies in groups of the CA after the climbing assay. Analysis of the Cf value reveals no statistically significant difference between $\Delta cnir ; mhc::Gal4/UAS::cnir$ (red) and $\Delta cnir ; UAS::cnir/+$ (blue) flies. Moreover, both experimental genotypes show defective locomotion and do not reach group 3 of the CA above the literature value for wt flies [Inagaki *et al.*, 2010]. Therefore, expression of Cnir in muscle cells of $\Delta cnir$ mutants does not rescue locomotor impairment. $\Delta cnir ; mhc::Gal4/UAS::cnir$: 29.0 ± 7.6% group 1, 25.2 ± 3.3% group 2, 45.8 ± 8.3% group 3; $\Delta cnir ; UAS::cnir/+$: 12.8 ± 2.3% group 1, 41.2 ± 2.3% group 2, 46.0 ± 3.0% group 3; bars = mean ± sem; n = 10 trials per experimental group.

Next, it was tested whether muscle specific activation of the $UAS::cnir$ construct via $mhc::Gal4$ in $\Delta cnir$ flies rescues the locomotion defect (fig. 3.13). $\Delta cnir ; UAS::cnir/+$ flies served as control since they showed a slightly higher Cf value in the previous

experiment, making a potential statistically significant rescue more robust. Both experimental groups were tested in 10 trials.

Less than half ($45.8 \pm 8.3\%$) of $\Delta cnir$ flies expressing Cnir in muscle reached group 3 of the CA. In comparison, $cnir$ mutant flies carrying only the $UAS::cnir$ construct were distributed nearly evenly in the last two groups of the CA ($46.0 \pm 3.0\%$ group 3). There is no statistically significant difference in the distribution of $\Delta cnir ; mhc::Gal4/UAS::cnir$ rescue flies ($Cf = 0.55 \pm 0.07$) compared to $\Delta cnir ; UAS::cnir/+$ ($Cf = 0.62 \pm 0.02$) control flies. Moreover, neither experimental group reaches the literature value of at least 60% flies in group 3 for wt [Inagaki *et al.*, 2010]. Therefore, expression of $cnir$ in muscle cells does not rescue the locomotion defects of $\Delta cnir$ flies.

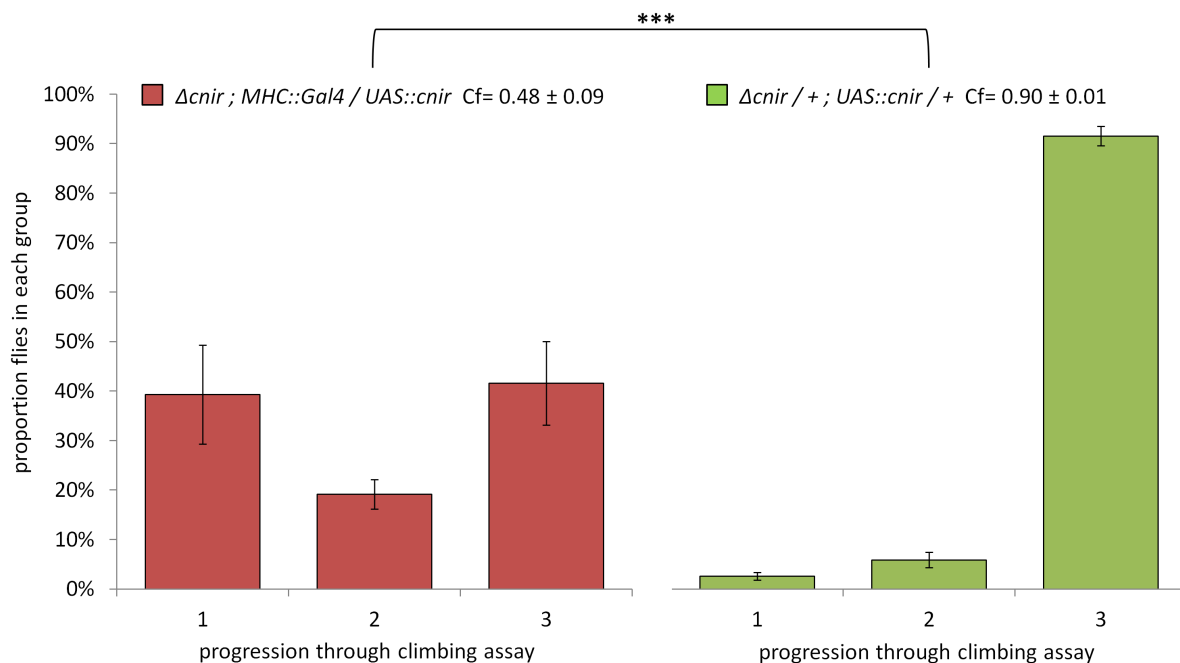


Figure 3.14 | Locomotion of $\Delta cnir ; mhc::Gal4/UAS::cnir$ and $\Delta cnir/+ ; UAS::cnir/+$ flies
 Distribution of flies in groups of the CA after the climbing assay. Analysis of the Cf value reveals a statistically significant difference between $\Delta cnir ; mhc::Gal4/UAS::cnir$ (red) and $\Delta cnir/+ ; UAS::cnir/+$ (green) flies. Thus, $\Delta cnir ; mhc::Gal4/UAS::cnir$ flies have impaired locomotion in comparison to the $\Delta cnir/+ ; UAS::cnir/+$ control, which reaches group 3 of the CA above the literature value for wt flies [Inagaki *et al.*, 2010]. This confirms that there is no rescue via muscle specific expression of Cnir in $\Delta cnir$ flies. $\Delta cnir ; mhc::Gal4/UAS::cnir$: $39.3 \pm 10.0\%$ group 1, $19.1 \pm 3.0\%$ group 2, $41.6 \pm 8.4\%$ group 3; $\Delta cnir/+ ; UAS::cnir/+$: $2.6 \pm 0.8\%$ group 1, $5.9 \pm 1.5\%$ group 2, $91.6 \pm 1.9\%$ group 3; bars: mean \pm sem; n=10 trials per experimental group; *** $p \leq 0.001$.

Since at least one copy of the third chromosome in the experimental genotypes (fig. 3.12 and 3.13) is altered in comparison to the initially characterized $\Delta cnir$ flies (fig 3.10), it was tested whether the locomotion defects are still caused solely by the $\Delta cnir$ mutation. For this purpose the rescue genotype $\Delta cnir ; mhc::Gal4/UAS::cnir$ was compared to $\Delta cnir/+ ; UAS::cnir/+$ control flies, which only lack one copy of *cnir* (fig. 3.14). Both experimental groups were tested in 10 trials.

Again, only less than half ($41.6\% \pm 8.4\%$) of the rescue flies reached group 3 of the CA. In contrast, almost all flies ($91.6\% \pm 1.9\%$) from the heterozygous control climbed into group 3 of the CA. In this case, the distribution of flies differs statistically significant ($p \leq 0.001$) between $\Delta cnir ; mhc::Gal4/UAS::cnir$ flies ($Cf = 0.48 \pm 0.09$) and $\Delta cnir/+ ; UAS::cnir/+$ flies ($Cf = 0.90 \pm 0.01$). In addition, only heterozygous control flies climb into group 3 of the CA above the literature threshold (60 %) for wt [Inagaki *et al.*, 2010]. Hence, the locomotion defects are caused by the lack of *cnir* function and are not due to heterozygous alterations of the third chromosome. Furthermore, the motor impairment cannot be rescued via muscle specific expression of *Cnir* in $\Delta cnir$ flies.

3.8 Neuronal rescue of locomotion defects

As mentioned before, locomotor impairment in *Drosophila* is due to pathology of muscles, peripheral neurons, or the central nervous system [Slawson *et al.*, 2011].

As the rescue experiments in muscle tissue were not successful, it was tested whether pan neuronal *appl::Gal4* [Torroja *et al.*, 1999] driven *cnir* expression leads to rescue of locomotion impairment of $\Delta cnir$ flies. As for the muscle rescue experiments, the *UAS::cnir* construct and the *appl::Gal4* line were tested heterozygously for putative dominant influences on locomotion in a $\Delta cnir$ mutant background (fig. 3.15). Both experimental groups were tested in 10 trials.

A vast majority ($85.9 \pm 5.4\%$) of $\Delta cnir ; appl::Gal4/+$ flies was not able to leave group 1 of the CA. In comparison, $\Delta cnir ; UAS::cnir/+$ were distributed almost evenly in the last two groups of the CA ($39.5 \pm 2.4\%$ group 3). The statistical analysis shows a significant difference ($p \leq 0.001$) in the distribution of $\Delta cnir ; appl::Gal4/+$ flies ($Cf = 0.10 \pm 0.03$) and $\Delta cnir ; UAS::cnir/+$ flies ($Cf = 0.61 \pm 0.02$).

This result might indicate a leaky expression of the *UAS::cnir* construct, leading to a minor rescue of the locomotion impairment. However, in both experimental groups less than 60 % of flies reached group 3 of the CA as reported for wt flies [Inagaki *et al.*,

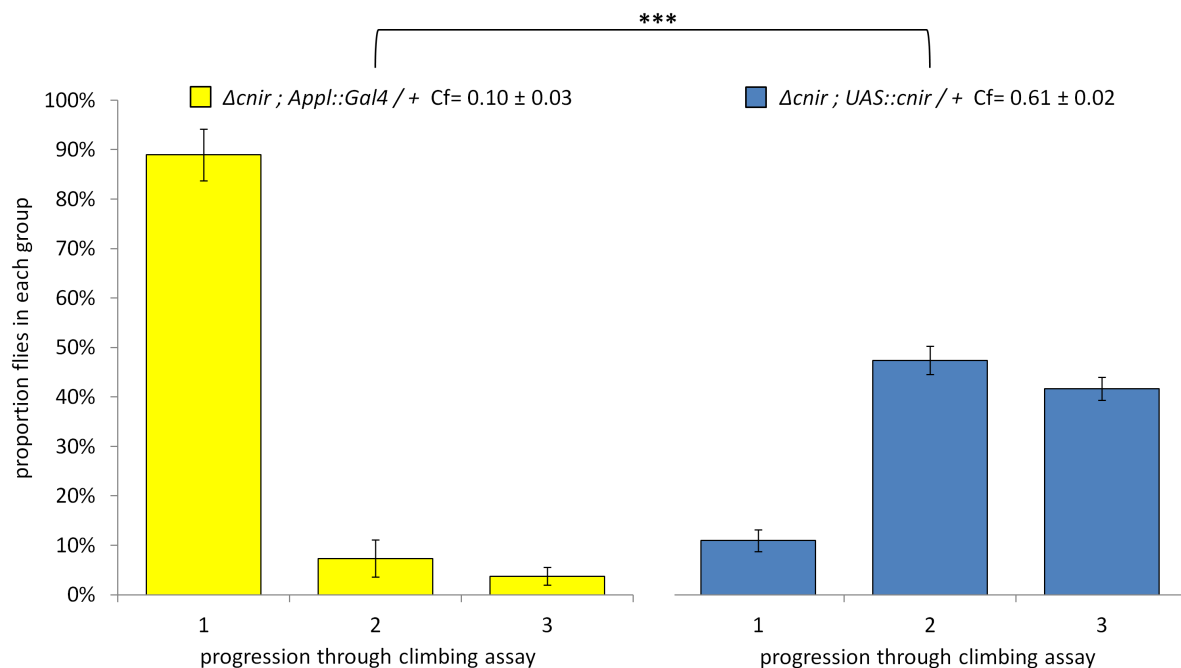


Figure 3.15 | Locomotion of $\Delta cnir ; appl::Gal4/+$ and $\Delta cnir ; UAS::cnir/+$ flies

Distribution of flies in groups of the CA after the climbing assay. Analysis of the Cf value reveals a statistically significant difference between $\Delta cnir ; appl::Gal4/+$ (yellow) and $\Delta cnir ; UAS::cnir/+$ (blue) flies. This could indicate a minor rescue of locomotor impairment via leaky expression of *UAS::cnir*. However, both genotypes show impaired locomotion and do not reach group 3 of the CA above the literature value expected for wt flies [Inagaki *et al.*, 2010]. $\Delta cnir ; appl::Gal4/+$: 85.9 ± 5.4% group 1, 9.4 ± 3.6% group 2, 4.7 ± 2.0% group 3; $\Delta cnir ; UAS::cnir/+$: 13.0 ± 2.3% group 1, 47.5 ± 2.3% group 2, 39.5 ± 2.4% group 3; bars: mean ± sem; n=10 trials per experimental group; ***p ≤ 0.001.

2010]. Thus, both tested genotypes show defective locomotion and either could be used as a negative control for the rescue experiment. Due to the higher Cf value, $\Delta cnir ; UAS::cnir/+$ flies were chosen as control in the rescue experiment, as the higher Cf value makes a potential statistically significant rescue more robust. Each experimental group was tested in 10 trials (fig. 3.16).

In the $\Delta cnir ; appl::Gal4/UAS::cnir$ rescue genotype expressing *cnir* in neuronal cells, most flies did indeed reach group 3 of the CA (75.9 ± 3.7%). In the control genotype $\Delta cnir ; UAS::cnir/+$, fewer than 60% of flies reached group 3 of the CA, similar to the previous assay (compare figs. 3.15 and 3.16). The distribution of flies differs significantly (p ≤ 0.001) between $\Delta cnir ; appl::Gal4/UAS::cnir$ (Cf = 0.81 ± 0.02) and $\Delta cnir ; UAS::cnir/+$ (Cf = 0.66 ± 0.03). Furthermore, the rescue genotype reaches group 3 of the CA above the literature threshold for wt flies [Inagaki *et al.*, 2010]. Thus,

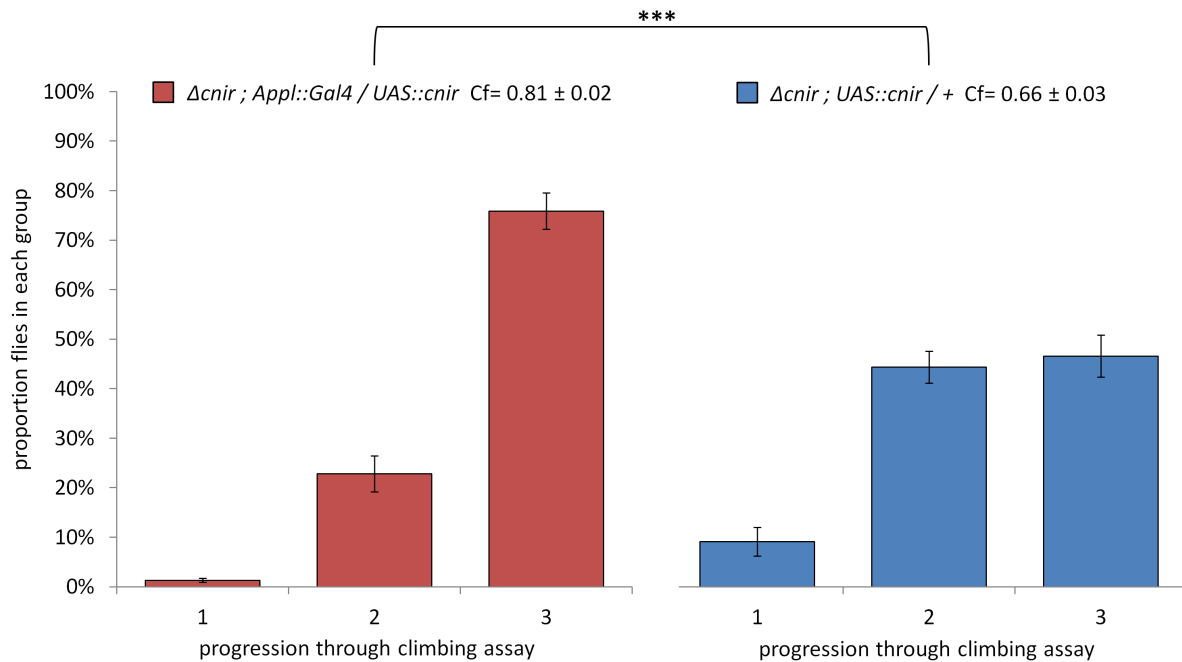


Figure 3.16 | Locomotion of $\Delta cnir ; appl::Gal4/UAS::cnir$ and $\Delta cnir ; UAS::cnir/+$ flies

Distribution of flies in groups of the CA after the climbing assay. Analysis of the Cf value reveals a statistically significant difference between $\Delta cnir ; appl::Gal4/UAS::cnir$ (red) and $\Delta cnir ; UAS::cnir/+$ (blue) flies. Furthermore, only $\Delta cnir ; appl::Gal4/UAS::cnir$ flies show wt locomotion and reach group 3 of the CA above the literature threshold [Inagaki *et al.*, 2010], indicating a successful rescue. $\Delta cnir ; appl::Gal4/UAS::cnir$: 1.3 ± 0.4% group 1, 22.8 ± 3.6% group 2 75.9 ± 3.7% group 3; $\Delta cnir ; UAS::cnir/+$: 9.1 ± 2.9% group 1, 44.4 ± 3.2% group 2, 46.6 ± 4.2% group 3; bars= mean ± sem; n= 10 trials per experimental group; ***p ≤ 0.001.

expression of *cnir* in neurons is crucial for reconstitution of functional locomotion in $\Delta cnir$ flies.

Although statistically significant, it was next tested, whether the neuronal rescue of locomotion in $\Delta cnir$ flies (fig. 3.16) is complete, or just partial. For this purpose, the rescue genotype was compared to $\Delta cnir/+ ; UAS::cnir/+$ flies, as a more rigorous and robust representative of wt climbing behavior (fig. 3.17). Each experimental group was tested in 10 trials.

As in the last assay (fig. 3.17), most (66.7 ± 4.5%) $\Delta cnir ; appl::Gal4/UAS::cnir$ flies climbed into group 3 of the CA. However, an even greater majority of $\Delta cnir/+ ; UAS::cnir/+$ flies (91.2 ± 1.4%) reached group 3 of the CA. The distribution of flies is significantly different (p ≤ 0.001) between the rescue genotype (Cf= 0.76 ± 0.0) and the heterozygous control (Cf= 0.89 ± 0.01), where the latter performed substantially

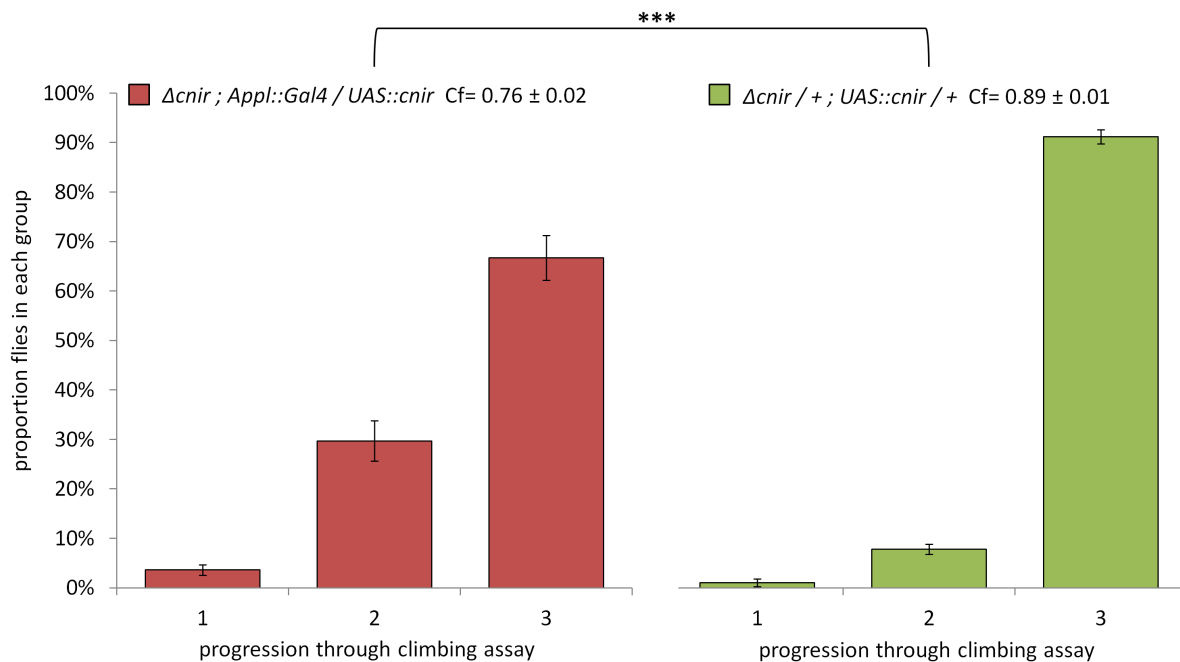


Figure 3.17 | Locomotion of $\Delta cnir ; appl::Gal4/UAS::cnir$ and $\Delta cnir/+ ; UAS::cnir/+$ flies
 Distribution of flies in groups of the CA after the climbing assay. Analysis of the Cf value reveals a statistically significant difference between $\Delta cnir ; appl::Gal4/UAS::cnir$ (red) and $\Delta cnir/+ ; UAS::cnir/+$ (green) flies. Thus, the rescue of locomotor impairment via Cnir expression in neurons could be only partial. $\Delta cnir ; appl::Gal4/UAS::cnir$: $3.6 \pm 1.1\%$ in group 1, $29.7 \pm 4.1\%$ group 2, $66.7 \pm 4.5\%$ group 3; $\Delta cnir/+ ; UAS::cnir/+$: $1.0 \pm 0.8\%$ group 1, $7.8 \pm 1.0\%$ group 2, $91.2 \pm 1.4\%$ group 3; bars= mean \pm sem; n= 10 trials per experimental group; ***p \leq 0.001.

better. Hence, the rescue through neuronal expression of Cnir in $\Delta cnir$ flies might be only partial.

3.9 Cnir protein localization and neuronal rescue with GFP:Cnir

To investigate the subcellular localization of Cnir, a N-terminally and a C-terminally tagged Cnir under the control of the UAS promoter were generated. The *act::GAL4* [Wang *et al.*, 2007] driven expression of both epitope tagged Cnir versions in the large and flat cells of the squamous follicular epithelium of stage 10 egg chambers is depicted in fig. 3.18. Both N-terminally and C-terminally GFP tagged Cnir localize to the circumference of the nucleus in densely packed puncta. However, the punctate distribution also extends far into the cytoplasm of the cell. Furthermore, the density

of the dots decreases with increasing distance to the nucleus. The Protein Disulfide Isomerase (PDI) is a ER resident protein [Ferrari and Söling, 1999]. The distribution of Cnir resembles the localization reported for PDI in the squamous follicular epithelium of *Drosophila* egg chambers [Bökel *et al.*, 2006].

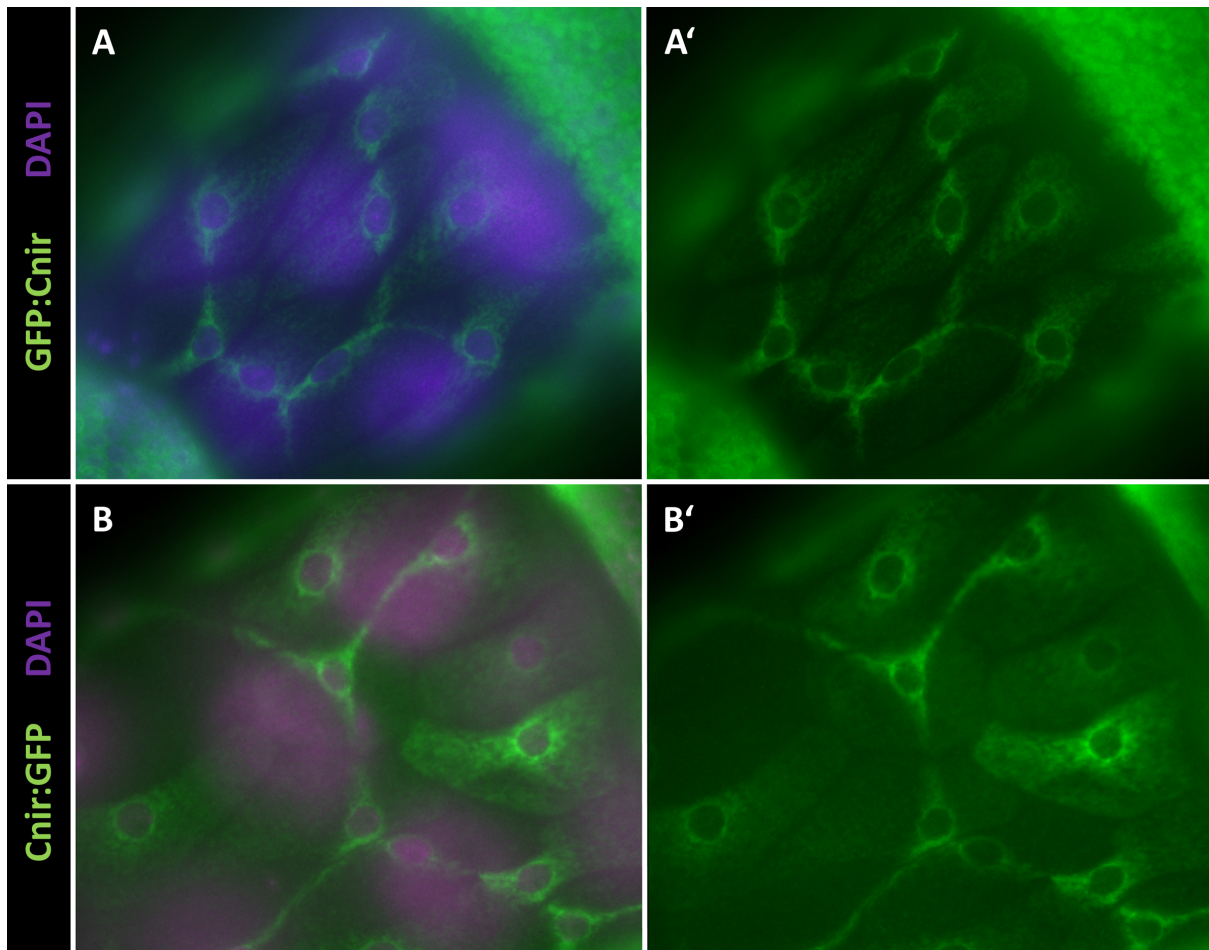


Figure 3.18 | Subcellular localization of GFP tagged Cnir

Cells of the squamous follicular epithelium of stage 10 egg chambers. Both, the N-terminally and C-terminally GFP tagged Cnir localize to a large structure, which is most dense in proximity to the nucleus but also extends far into the cytoplasm. A: Overlay of DNA stained with DAPI (blue) and GFP:Cnir labeled with an anti-GFP antibody (green); A' single channel image of GFP:Cnir from A; B Overlay of DNA stained with DAPI (blue) and Cnir:GFP labeled with an anti-GFP antibody (green); B' single channel image of Cnir:GFP from B.

It was crucial to address the question whether the GFP tagged Cnir proteins are biologically functional. For this purpose, rescue experiments were conducted driving *appl::Gal4* mediated expression [Torroja *et al.*, 1999] of N-terminally GFP tagged Cnir in neuronal cells of Δ *cnir* flies. Analogous to the neuronal rescue described

previously, $\Delta cnir ; appl::Gal4/+$ and $\Delta cnir ; UAS::GFP:cnir/+$ flies were first tested for dominant influences of the transgenic constructs on the third chromosome (fig.3.19). Furthermore, this test served as a control for leaky expression of the $UAS::GFP:cnir$ construct, which could be indicated by a rescue in the absence of the $appl::Gal4$ driver. Each experimental group was tested in 5 trials.

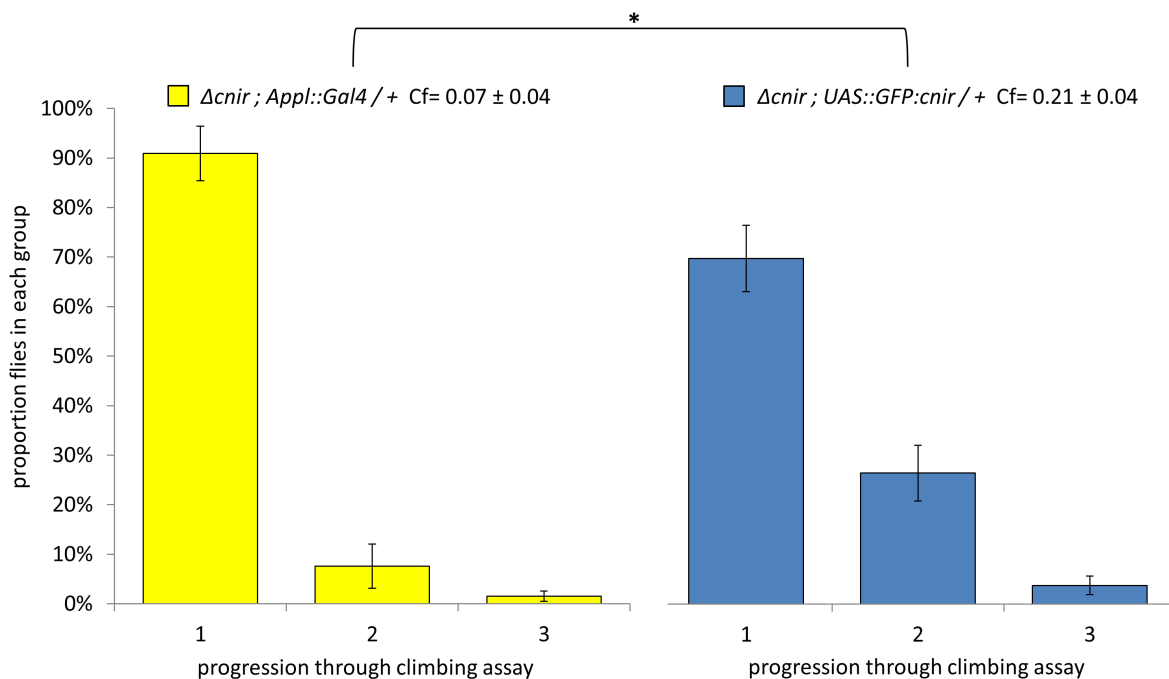


Figure 3.19 | Locomotion of $\Delta cnir ; appl::Gal4/+$ and $\Delta cnir ; UAS::GFP:cnir/+$ flies

Distribution of flies in groups of the CA after the climbing assay. Analysis of the Cf value reveals a statistically significant difference between $\Delta cnir ; appl::Gal4/+$ (yellow) and $\Delta cnir ; UAS::GFP:cnir/+$ (blue) flies. However, both genotypes show impaired locomotion and do not reach group 3 of the CA above the literature value for wt flies [Inagaki *et al.*, 2010]. $\Delta cnir ; appl::Gal4/+$: 90.9 ± 5.5% group 1, 7.6 ± 4.5% group 2, 1.5 ± 1.0% group 3; $\Delta cnir ; UAS::GFP:cnir/+$: 69.8 ± 6.7% group 1, 26.5 ± 5.6% group 2, 3.8 ± 1.9% group 3; bars: mean ± sem; n=5 trials per experimental group; *p ≤ 0.05.

Similar to former experiments, most (90.9 ± 5.5%) of the $\Delta cnir ; appl::Gal4/+$ flies remain in group 1 of the CA. The distribution of $\Delta cnir ; UAS::GFP:cnir/+$ flies in the CA appears similar and 69.8 ± 6.7% remain in group 1. However, the statistical analysis reveals a significant difference (p ≤ 0.05) in the distribution of $\Delta cnir ; appl::Gal4/+$ flies (Cf= 0.07 ± 0.04) and $\Delta cnir ; UAS::GFP:cnir/+$ flies (Cf= 0.21 ± 0.04). Still, both experimental groups do not reach the wt threshold of flies climbing into group 3 of the CA [Inagaki *et al.*, 2010] and show strong impairment in locomotion.

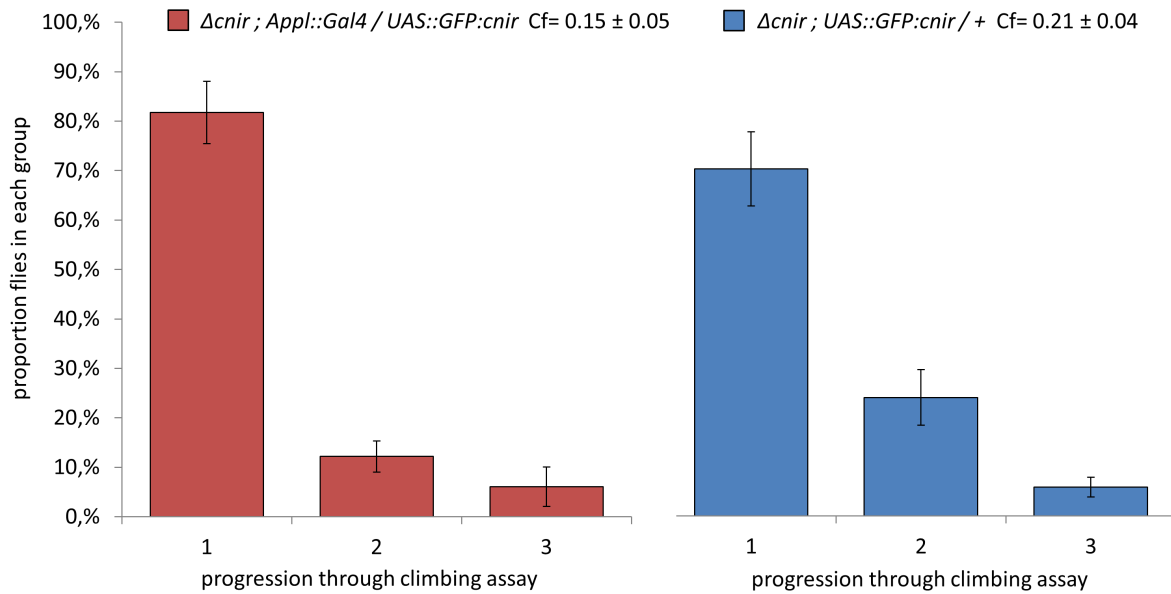


Figure 3.20 | Locomotion of $\Delta cnir ; appl::Gal4/UAS::GFP:cnir$ and $\Delta cnir ; UAS::GFP:cnir/+$ flies

Distribution of flies in groups of the CA after the climbing assay. Analysis of the Cf value reveals no statistically significant difference between $\Delta cnir ; appl::Gal4/UAS::GFP:cnir$ (red) and $\Delta cnir ; UAS::GFP:cnir/+$ (blue) flies. Furthermore, both genotypes show impaired locomotion and do not reach group 3 of the CA above the threshold for wt flies [Inagaki *et al.*, 2010], indicating no successful rescue via neuronal expression of GFP:Cnir. $\Delta cnir ; appl::Gal4/UAS::GFP:cnir$: 81.8 ± 6.3% group 1, 12.2 ± 3.2% group 2, 6.1 ± 4.0% group 3; $\Delta cnir ; UAS::GFP:cnir/+$: 70.2 ± 7.5% group 1, 24.0 ± 5.6% group 2, 5.9 ± 2.0% group 3; bars= mean ± sem; n= 10 trials per experimental group.

The rescue experiment was thus conducted using the $\Delta cnir ; UAS::GFP:cnir/+$ flies as control for the $\Delta cnir ; appl::Gal4/UAS::GFP:cnir$ rescue genotype. Again, this was done because this group showed a higher Cf value in the previous experiment, improving the robustness of a statistically significant rescue. Both experimental groups were tested in 10 trials and the results are shown in fig. 3.20.

However, most flies remained in group 1 of the CA for both tested genotypes and no statistically significant difference was found in the distribution of $\Delta cnir ; appl::Gal4/UAS::GFP:cnir$ (Cf= 0.15 ± 0.05) and $\Delta cnir ; UAS::GFP:cnir/+$ (Cf= 0.21 ± 0.04) flies. Therefore, the neuronal expression of a N-terminally GFP tagged Cnir does not lead to rescue of locomotion defects of $\Delta cnir$ flies.

In order to investigate whether the locomotion impairment in the previous experiment is due to the lack of *cnir* function and not due to dominant effects of the

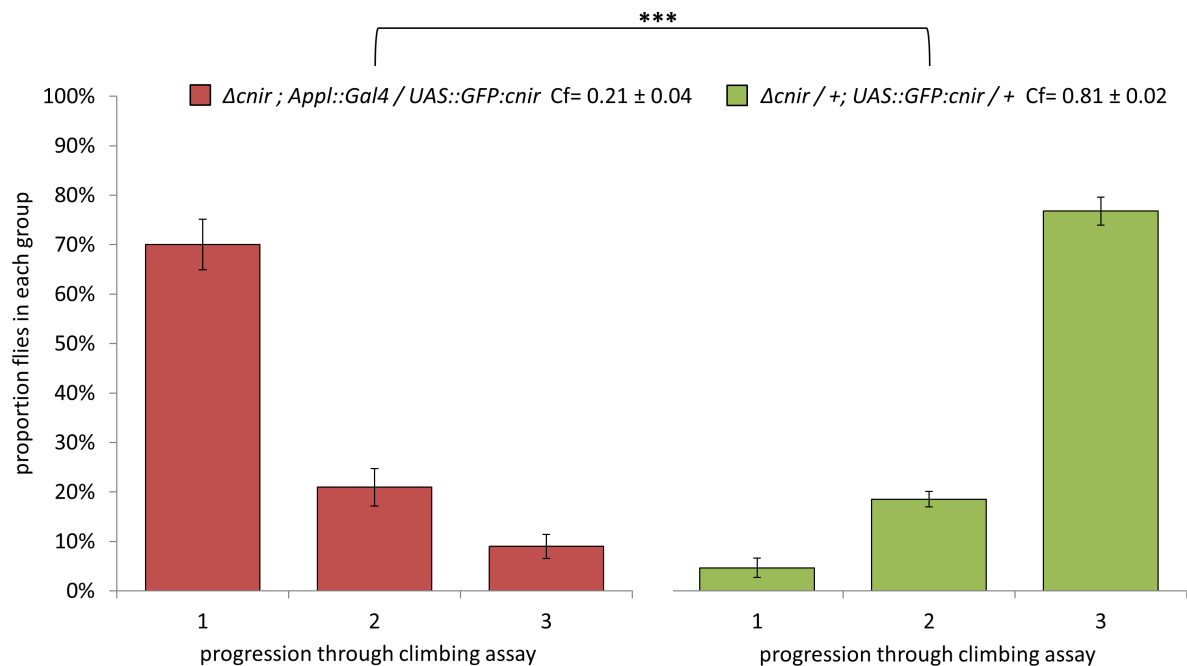


Figure 3.21 | Locomotion of $\Delta cnir ; appl::Gal4/UAS::GFP:cnir$ and $\Delta cnir/+ ; UAS::GFP:cnir/+$ flies

Distribution of flies in groups of the CA after the climbing assay. Analysis of the Cf value reveals a statistically significant difference between $\Delta cnir ; appl::Gal4/UAS::GFP:cnir$ (red) and $\Delta cnir/+ ; UAS::GFP:cnir/+$ (green) flies. In contrast to the control, the rescue genotype shows impaired locomotion and does not reach group 3 of the CA above the literature threshold for wt [Inagaki *et al.*, 2010]. This shows that there is no rescue via neuronal expression of GFP: Cnir in $\Delta cnir$ mutants. $\Delta cnir ; appl::Gal4/UAS::cnir$: 70.0 ± 5.1% group 1, 21.0 ± 3.8%, group 2, 9.0 ± 2.4% group 3; $\Delta cnir/+ ; UAS::GFP:cnir/+$: 4.7 ± 1.9% group 1, 18.5 ± 1.6% group 2 76.8 ± 2.8% group 3; bars= mean ± sem; n= 7 trials per experimental group.

transgenic constructs on the third chromosome, the rescue genotype was compared to $\Delta cnir/+ ; UAS::GFP:cnir/+$ flies, which are heterozygous for the $\Delta cnir$ locus and the $UAS::GFP:cnir$ transgene. Both experimental groups were tested in 7 trials. The results are illustrated in fig. 3.21.

A significant difference ($p \leq 0.001$) in the climbing ability could be observed between the heterozygous control flies (Cf= 0.81 ± 0.02) and the rescue genotype (Cf= 0.21 ± 0.04), which still showed severe locomotor impairment. As expected, the control flies reached group 3 above the literature threshold for wt flies [Inagaki *et al.*, 2010]. Hence, the locomotion defects are caused by the lack of *cnir* function in the rescue genotype and are not restored by expression of a N-terminally GFP tagged

Cnir. Furthermore, the motor impairment is not caused by dominant effects of the transgenic constructs on the third chromosome.

The *UAS::Cnir:GFP* construct was not tested for its ability to rescue locomotor defects of Δ *cnir* mutant flies so far. However, a successful rescue with the epitope tagged Cnir is crucial to support the observed protein localization (fig. 3.18)

3.10 Analysis of a *cnir/cni* double mutant

It was reported that the lack of one *cnir* copy in a *cni*^{AR55} amorphic mutant background leads to synthetic lethality in *Drosophila*. Only in combination with the hypomorphic *cni*^{AA12} allele could some *Df(2L)JS7 cni*^{AR55}/*cni*^{AA12} escapers be observed and these were strongly malformed. Furthermore, it has been shown that expression of *cnir* under the control of a *cni* promoter rescues parts of the synthetic lethality, as well as some somatic phenotypes of *cni* mutant flies [Bökel *et al.*, 2006]. Those experiments indicated a potential functional redundancy of both *cni* genes in *Drosophila*. However, the previous data were generated using the deletion *Df(2L)JS7* [Sekelsky *et al.*, 1995], which removes a 214.5 kb region containing *cnir* and 36 other genes. Therefore, a Δ *cnir/cni*^{AR55} *FRT*_{40A} double mutant was generated to reinvestigate the synthetic lethality crosses from Bökel *et al.* [2006]. Moreover, this double mutant was used for induction of somatic clones to analyze if the lack of both *cni* genes causes cell lethality.

Fig. 3.22 depicts Δ *cnir/cni*^{AR55} mutant clones in the follicular epithelium of a stage 10 egg chamber. The cell shape outlined by DE-Cadherin does not differ between mutant and wt cells. Also, the shape of nuclei of Δ *cnir/cni*^{AR55} mutant cells does not differ from those of wt cells. Most importantly, large clones can be observed, showing that the lack of both *cni* genes does not cause cell lethality in the follicular epithelium of *Drosophila* egg chambers.

To confirm those results, Δ *cnir/cni*^{AR55} clones were induced in a second epithelial tissue, namely in the eye imaginal discs of third instar larvae. Again, the cell shape outlined by the DE-Cadherin does not differ between double mutant and wt cells. Furthermore, the presence of Δ *cnir/cni*^{AR55} clones demonstrates that the lack of both *cni* genes does not cause cell lethality in the eye imaginal disc.

This result was surprising in comparison to the synthetic lethality data from Bökel *et al.* [2006]. Therefore, test crosses with the newly generated Δ *cnir* mutant and the Δ *cnir/cni*^{AR55} double mutant were made to get a better understanding of those former

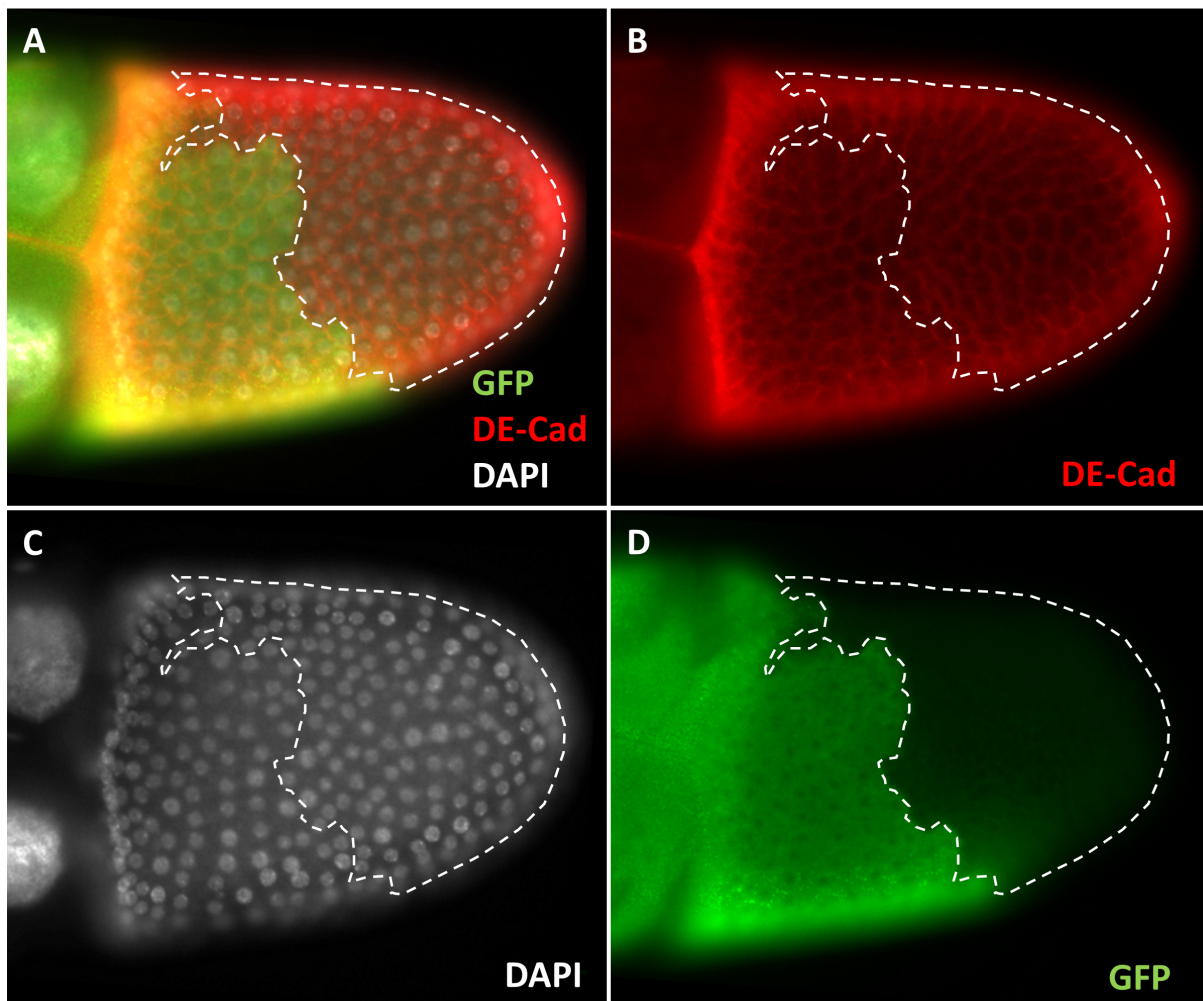


Figure 3.22 | Somatic $\Delta cni/cni^{AR55}$ clones in the follicular epithelium

Follicular epithelium of a stage 10 egg chamber (A-D) oriented with the anterior pole to the left side. Wt cells are marked by the presence of GFP labeled with an anti-GFP antibody (green), while $\Delta cni/cni^{AR55}$ double mutant cells lack GFP expression (encircled by white dashed line). DE-Cad is labeled with the anti-DE-Cad antibody (red) and DNA is stained with DAPI (white). Wt cells, as well as $\Delta cni/cni^{AR55}$ double mutant cells do not differ in shape. Furthermore, the shape of nuclei does not differ between wt and double mutant cells. Large clones can be observed, indicating that the lack of both *cni* genes does not cause cell lethality.

studies. Moreover, some crosses described in that previous study were reproduced. The results are summarized in fig. 3.24.

First, $w^- ; \Delta cni [w^+]/CyO$ flies were crossed to $Df(2l)JS7/SM6a$ flies to see whether the precise *cni* deletion is viable over the large deficiency removing *cni* and 36 adjacent genes. The expected percentage (p exp.) of transheterozygous flies in the progeny (n=152) is 33% and the observed number is 19.7% of $\Delta cni [w^+]/Df(2l)JS7$ flies. Al-

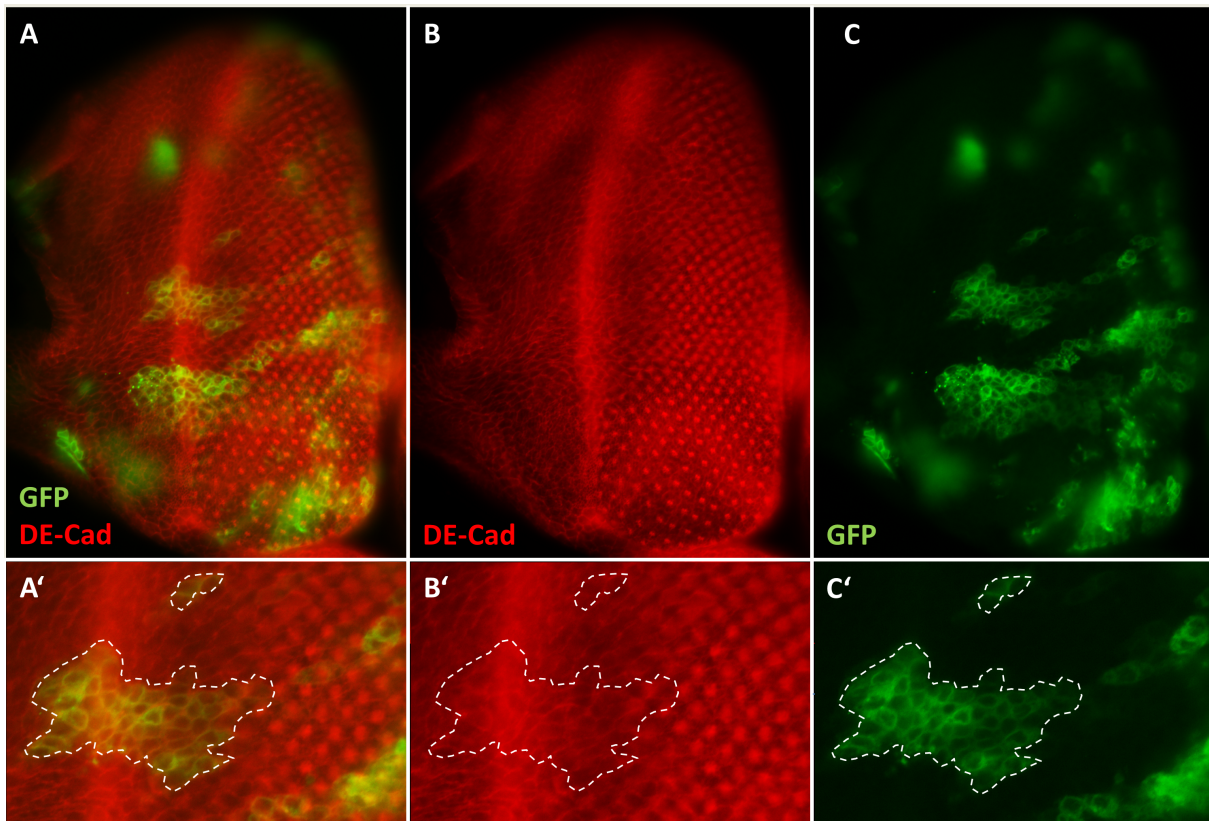


Figure 3.23 | Somatic $\Delta cnir/cni^{AR55}$ clones in third instar larvae eye imaginal discs

Eye imaginal disc of a third instar larva (A-C) and a magnified view of $\Delta cnir/cni^{AR55}$ mutant clones (A'-C'). $\Delta cnir/cni^{AR55}$ cells are marked by the presence of GFP (green) and encircled by a white dashed line in A'-C', while wt cells lack GFP expression. DE-Cad is labeled with the anti-DE-Cad antibody (red). Wt cells and $\Delta cnir/cni^{AR55}$ double mutant cells do not differ in shape. Furthermore, clones can be observed indicating that the lack of both *cni* genes does not cause cell lethality.

though this value is significantly lower ($p \leq 0.001$) than the expected, the result also confirms viability of the homozygous $\Delta cnir$ mutant.

Next, *Df(2l)JS7 b cni^{AR55} pr cn/CyO* flies were crossed to $w^- ; \Delta cnir [w^+]$ flies to test if the lack of one *cni* gene copy (*cni^{AR55}* amorphic allele) in a *cnir* mutant background leads to synthetic lethality as described for the reciprocal state. The p exp. of *Df(2l)JS7 b cni^{AR55} pr cn/ $\Delta cnir [w^+]$* flies in the progeny (n=110) is 50 % and the observed value is 59.1 %. Strikingly, there is no significant difference between p exp. and the observed frequency. Thus, *cnir* mutant flies lacking one copy of *cni* are viable.

Before testing for synthetic lethality as described in the published data [Bökel *et al.*, 2006], a control experiment was set up crossing *b cni^{AR55} FRT40A/CyO ; ry/ry* flies

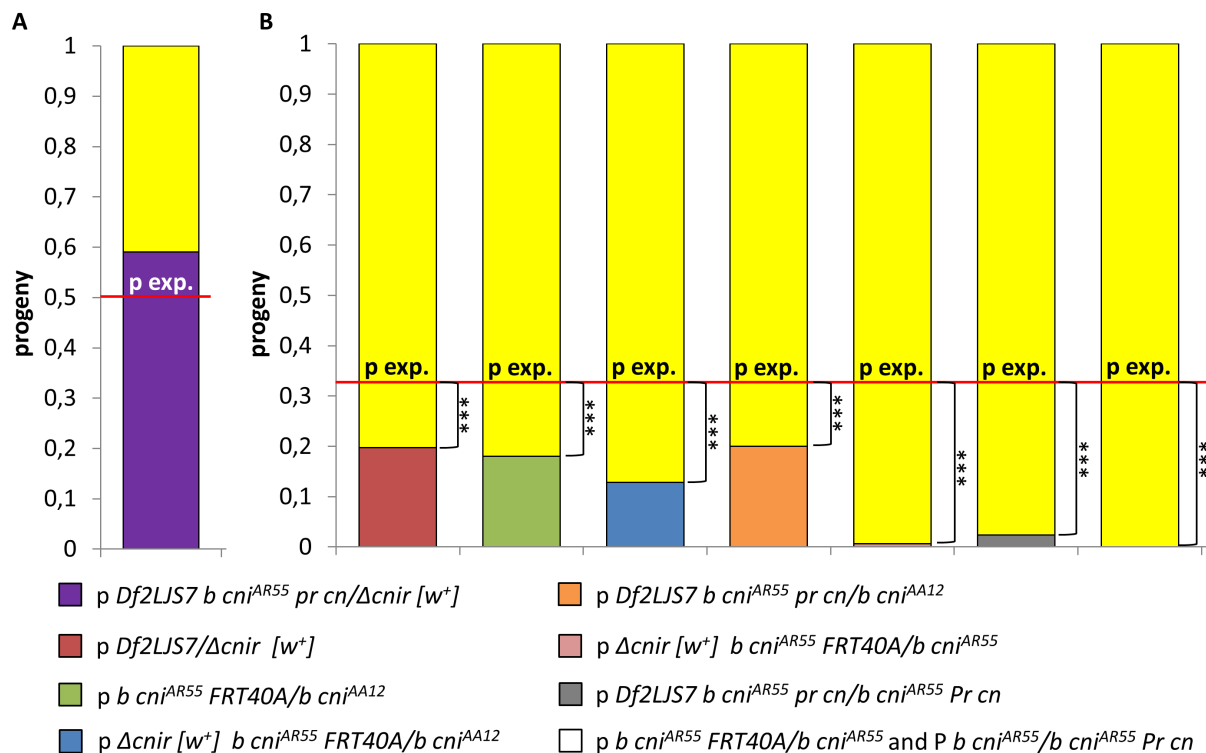


Figure 3.24 | Test crosses for functional redundancy of both *Drosophila cni* genes

Each bar represents the total progeny from a cross. The expected percentage of flies of the genotypes in the figure legend is marked by a red line. The scored percentage of flies of a certain genotype are indicated by the non yellow proportion of the bar. The percentage of flies not corresponding to the monitored genotype is indicated in yellow. Although most observed percentages differ significantly from the expected frequency, no lethality can be seen in *cnir* mutants (red) and *cni^{AR55}/cni^{AR12}* mutants (green). Interestingly, no synthetic lethality can be observed through removal of *cnir* in a *cni^{AR55}/cni^{AA12}* mutant background (blue and orange). Strong lethality can only be observed in *cni^{AR55}/cni^{AR55}* amorphic mutants even without the lack of one *cnir* copy (pink, grey and white). Furthermore, there is no strong lethality in a *cnir* mutant lacking one *cni* copy (purple). *** $p \leq 0.001$ indicates a significant difference between the expected percentage (p exp.) of flies of a scored genotype and the observed percentage.

carrying the *cni* amorphic allele with *b cni^{AA12}/CyO* flies carrying the *cni* hypomorphic allele. The p exp. of *b cni^{AR55} FRT40A/b cni^{AA12}* flies in the progeny (133) is again 33 % and the monitored value 18.0 %. Although p exp. and the observed frequency of transheterozygous flies differs significantly ($p \leq 0.001$), *cni* mutants are viable.

Then, the experimental condition leading to synthetic lethality was reproduced utilizing the newly generated $\Delta cnir/cni^{AR55}$ double mutant instead of the chromosome bearing the *Df(2l)JS7* deletion. $\Delta cnir [w^+] b cni^{AR55} FRT40A/CyO$ flies were crossed to *b cni^{AA12}/CyO* flies. The p exp. of $\Delta cnir [w^+] b cni^{AR55} FRT40A/b cni^{AA12}$ flies in the

progeny (n=203) is 33 % and the observed percentage is 12.8 %. Although the value is significantly lower ($p \leq 0.001$) than the expected, no strong lethality can be seen. Furthermore, *cni* deficient flies from the previous experiment show a similar reduction of the expected genotype.

Because those results were surprising, the experimental conditions leading to synthetic lethality as published by Bökel *et al.* [2006] were repeated. For this purpose, *Df(2l)JS7 b cni^{AR55} pr cn/CyO* flies were crossed to *b cni^{AA12}/CyO* flies. The p exp. for *Df(2l)JS7 b cni^{AR55} pr cn/b cni^{AA12}* flies in the progeny (115) is 33 % and the observed frequency is 20.0 %. Although this value differs significantly ($p \leq 0.001$) from the expected, no synthetic lethality can be seen. Furthermore, Bökel *et al.* [2006] found only very few escapers in this experimental condition (≤ 1 %), which are described as severely malformed. This could not be observed in the crosses performed.

Since neither previous cross shows the reported synthetic lethality, it was tested whether the used stocks carry the mutant *cni* alleles and $\Delta cnir [w^+]$. The $\Delta cnir [w^+]$ deletion can be easily traced by the presence of the *white* gene replacing the *cnir* locus. To confirm that the *cni* alleles are still present in the used stocks, eggs from *b cni^{AR55} FRT40A/b cni^{AA12}* and $\Delta cnir [w^+] b cni^{AR55} FRT40A/b cni^{AA12}$ females were prepared (fig. 3.25). Wt eggs possess two dorsal appendages, an anterior micropyle and a posterior aeropyle. In contrast, *cni^{AR55}/cni^{AA12}* female flies produce ventralized eggs without dorsal appendages and a posterior micropyle due to a failure in Grk signaling [Roth *et al.*, 1995]. Both tested genotypes show ventralized eggs without dorsal appendages and a posterior micropyle. Therefore, the *cni* alleles are still present in the utilized stocks, confirming that no synthetic lethality occurs after removal of one *cnir* copy in a *cni* mutant background.

Next, it was tested whether the stronger *cni^{AR55}* allele in the experimental crosses leads to synthetic lethality. For this purpose, $\Delta cnir [w^+] b cni^{AR55} FRT40A/CyO$ flies were crossed to *b cni^{AR55}/CyO* flies. The p exp. of $\Delta cnir [w^+] b cni^{AR55} FRT40A/b cni^{AR55}$ flies in the progeny (n=148) is 33 % and the observed frequency is 0.7 %. The expected and monitored percentage differs significantly ($p \leq 0.001$). Furthermore, only one fly emerged as adult indicating strong lethality in the *cni* homozygous amorphic mutant lacking one *cnir* copy.

Again, the originally published data were reproduced crossing *Df(2l)JS7 b cni^{AR55} pr cn/CyO* flies to *b cni^{AR55} pr cn/CyO* flies. The p exp. of *Df(2l)JS7 b cni^{AR55} pr cn/b cni^{AR55} pr cn* flies in the progeny (n=127) is 33 % and the monitored percentage 2.4 %.

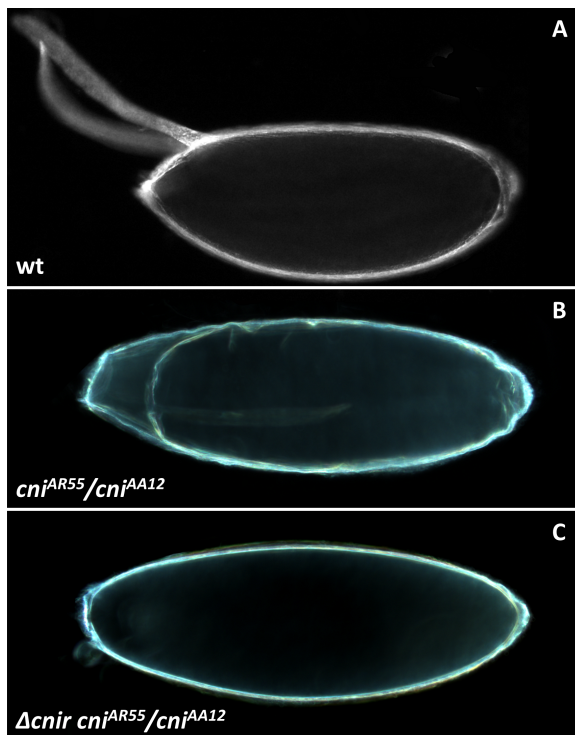


Figure 3.25 | Ventralized eggs from *cni* mutant mothers

Egg shells from wt female flies with two dorsal appendages, an anterior micropyle (left) and a posterior aeropyle (right) (A). Egg shell from a *b cni^{AR55} FRT40A/b cni^{AA12}* mother lacking dorsal appendages and having a posterior micropyle (B). Egg shell from a $\Delta cniir [w^+]$ *b cni^{AR55} FRT40A/b cni^{AA12}* mother without dorsal appendages and also lacking posterior structures, marked by the presence of a posterior micropyle (C).

Even though both values differ significantly ($p \leq 0.001$) and thus reveal a strong lethality, *cni* amorphic mutant flies lacking one *cnir* copy can be seen.

Ultimately, it was tested whether the *cni* amorphic mutant is viable. *b cni^{AR55} FRT40A/CyO ; ry/ry* flies were crossed to *b cni^{AR55}/CyO* flies. The p exp. of *b cni^{AR55} FRT40A/b cni^{AR55}* flies in the progeny (n=73) is 33 % and no fly of that genotype was observed. Another experiment was performed crossing *b cni^{AR55}/CyO* flies to *b cni^{AR55} pr cn/CyO* flies. The p exp. in this setup is the same as in the previous cross but no *b cni^{AR55}/b cni^{AR55} pr cn* flies were seen in the progeny (n= 146). However, in other crosses with an altered third chromosome in comparison to the original amorphic *cni* stocks (supplementary fig. S.1) up to 6.88 % of *b cni^{AR55}/b cni^{AR55} pr cn* flies were observed in the progeny (n= 189) with a p exp. of 11 %. This difference is not statistically significant. Hence, lethality of the *cni* amorphic mutants is most likely caused due to lethal influences in the genetic background.

Since no synthetic lethality can be observed through removal of *cnir* in a *cni^{AR55}/cni^{AA12}* mutant background and there is no lethality in a *cnir* mutant lacking one *cni* copy, both *Drosophila* Cni proteins do not seem to have a functional redundancy in the soma. Furthermore, lethality in *cni^{AR55}* amorphic mutants is most likely caused by influences in the genetic background of the fly stocks.

4 Discussion

4.1 Generation of a mutant for *cnir*: A putative ortholog of human CNIH4

The phylogenetic analysis performed shows that the Cni proteins from yeast and plants do not show clear orthology to Cni proteins from other species. However, insect Cni and nematode CNI-1 are closely related to the vertebrate CNIH1, from which CNIH2 and CNIH3 may have arisen from 2 consecutive gene duplications. *Drosophila* Cni has been shown to play an important role in ER export of the TGF α ligand Grk [Roth *et al.*, 1995; Herpers and Rabouille, 2004; Bökel *et al.*, 2006], which is a function that has been also proposed for the human CNIH1 [Castro *et al.*, 2007]. No such function has been reported for worm CNI-1. Instead, it is involved in regulation of ER export of AMPARs [Herring *et al.*, 2013]. A similar function in trafficking, as well as regulation of AMPAR kinetics has been demonstrated for the vertebrate CNIH2/3 [Schwenk *et al.*, 2009; Kato *et al.*, 2010; Shi *et al.*, 2010; Gill *et al.*, 2011; Coombs *et al.*, 2012; Gill *et al.*, 2012; Harmel *et al.*, 2012; Brockie *et al.*, 2013].

Strikingly, insect Cnir shows highest sequence homology to the vertebrate CNIH4 and is more distantly related to the Cni proteins mentioned above. CNIH4 has been recently shown to be involved in the regulation of ER export of members from the three major GPCR families [Sauvageau *et al.*, 2014]. There appears to be a high functional conservation of Cni proteins in AMPAR regulation and possibly AMPAR and TGF α trafficking. Therefore, it is reasonable to speculate that a functional conservation in GPCR trafficking also applies to Cnir and its human ortholog CNIH4.

There is no published *cnir* mutant *Drosophila* stock. In this thesis a precise deletion of the *cnir* coding sequence and introns was successfully generated using the means of targeted gene knock-out via homologous recombination [Gong and Golic, 2003; Huang *et al.*, 2008]. Furthermore, the efficiency of the knock-out was high and led to generation of multiple $\Delta cnir$ mutant stocks. This facilitates the analysis of *Drosophila* Cnir and may represent the first *in vivo* study of a putative CNIH4 ortholog.

4.2 $\Delta cnir$ is not lethal but has an impact on mortality throughout development and adult life

The generated $\Delta cnir$ flies are homozygously viable and fertile. However, they show an increased mortality in development and adult life.

Although mutants for Cornichon proteins show specific sorting defects, there are only very few *in vivo* studies. Analysis from yeast, *Drosophila* and *C.elegans* show that every mutant analyzed so far is viable [Roth *et al.*, 1995; Powers and Barlowe, 1998, 2002; Bökel *et al.*, 2006; Herring *et al.*, 2013] and in the case of *erv15* does not even show any obvious phenotype [Nakanishi *et al.*, 2007]. As reviewed in Dancourt and Barlowe [2010], it is known from analysis of cargo receptors that their deletion only results in an inefficient ER export of a subset of proteins, while other traffic at normal rates. Furthermore, fully folded cargo of a given receptor still traffics from ER to Golgi in bulk flow rates and is not exposed to ER associated degradation [Belden and Barlowe, 2001b; Bue and Barlowe, 2009]. Therefore, deletion of *cnir* could result in reduced ER exit of its cargoes, but be sufficient for viability of the organism.

Interestingly, it has been demonstrated for the α_{2B} -AR (family A GPCR) that its third intracellular loop interacts directly with the COPII subunits Sec24C/D [Dong *et al.*, 2012]. While it is unclear whether Cnir is involved in trafficking of GPCRs, it could be that the receptors are incorporated into COPII vesicles by diverse mechanisms. It might potentially require a combination of direct COPII recognition and binding by cargo receptors for sufficient concentration of cargo [Sauvageau *et al.*, 2014]. Further evidence for this general mechanistic comes from the yeast transmembrane protein Gap1, which relies on its cargo receptor Erv14p and a diacidic COPII recognition motif for efficient export from the ER [Malkus *et al.*, 2002; Castillon *et al.*, 2009; Sauvageau *et al.*, 2014]. Thus, Cnir cargoes like GPCRs could possibly also traffic from the ER more efficiently than through bulk flow alone. This more efficient ER export could be achieved via direct binding of COPII components and provide an explanation for viability of $\Delta cnir$ mutants.

Nevertheless, the lack of Cnir has a distinct impact on survival of *Drosophila* throughout development and adult life. For example, $\Delta cnir$ flies have a decreased fertilization rate of eggs and a lower hatching rate of embryos from eggs compared to control flies. Although presenting a less consistent view in comparison to the controls, $\Delta cnir$ flies seem to pupate and eclose less successfully. Overall, the survival of $\Delta cnir$ flies into

adulthood is strongly affected by the lack of Cnir protein. Furthermore, the lifespan of adult flies is decreased in comparison to control flies. As mentioned before, even bulk flow rates could potentially suffice for viability of the organism and Cnir cargo might bind to COPII components directly as reported for α_{2B} -AR [Dong *et al.*, 2012]. Therefore, Cargoes could be trafficked at rates which are high enough for survival of the fly. However, the generated data indicate that a lack of Cnir function is disadvantageous and causes increased mortality throughout developmental stages and adult life. If Cnir is involved in trafficking of GPCRs, it is striking that the Δ c*nir* mutant is viable, given the immensely broad range of regulatory functions of GPCRs in almost all physiological and cellular processes in insect life [Bendena *et al.*, 2012; Caers *et al.*, 2012]. Although CNIH4 has been shown to bind to members of the three major families of GPCRs [Sauvageau *et al.*, 2014], only six GPCRs have been tested. Moreover, out of those six only the β_2 -AR was studied intensively for its interaction with CNIH4. Therefore, CNIH4 could bind to only a subset of GPCRs, or at least not influence trafficking of all GPCRs to the same extent. This could possibly depend on the capability of certain GPCRs to bind to COPII subunits, while others might not have this property. The same principles might apply for the CNIH4 ortholog Cnir. However, it is likely that phenotypes associated with *c_{nir}* deletion could be extremely pleiotropic if GPCR trafficking is broadly affected.

4.3 Locomotor behaviour depends on Cnir function in neurons but not in muscles

The lack of Cnir also leads to a severe locomotion defect. The cause of locomotor impairment in *Drosophila* lays in the pathology of muscles, peripheral neurons, or the central nervous system [Slawson *et al.*, 2011]. The generated data indicate that Cnir function in neurons, but not in muscle cells, is crucial for reconstitution of wild type locomotor behavior of Δ c*nir* flies.

As discussed above, *C.elegans* CNI-1 [Herring *et al.*, 2013] and the vertebrate CNIH2/3 are involved in trafficking and regulation of AMPARs. [Schwenk *et al.*, 2009; Kato *et al.*, 2010; Shi *et al.*, 2010; Gill *et al.*, 2011; Coombs *et al.*, 2012; Gill *et al.*, 2012; Harmel *et al.*, 2012; Brockie *et al.*, 2013]. Interestingly, the *Drosophila* NMJ utilizes ionotropic GluRs homologous to AMPARs in the mammalian brain and there is a high degree of conservation of synaptic components between fly and vertebrates [Chen *et al.*, 1986;

Davis *et al.*, 1989; Lahey *et al.*, 1994; Tabuchi and Südhof, 2002; Banovic *et al.*, 2010; Sun *et al.*, 2011; Menon *et al.*, 2013]. Furthermore, the NMJ expresses GluRs postsynaptically in muscle cells [Menon *et al.*, 2013]. Even though unlikely with regard to the phylogenetic data, we hypothesized that Cnir could be the functional ortholog of worm CNI-1 and vertebrate CNIH2/3 and locomotor impairment of Δ c*nir* mutants results from altered synaptic transmission via GluRs. However, the failed rescue in muscle cells provides further evidence for the generated phylogeny and the functional conservation amongst Cornichon proteins. *Drosophila* Cnir is only distantly related to the Cornichon proteins involved in GluR regulation and trafficking in the worm and vertebrates, while fly Cni is more closely related to them. Although not investigated during this thesis, it is an interesting question whether the fly Cni has a distinct function in GluR regulation and trafficking.

As mentioned previously, human CNIH4 has been reported to have an important function in trafficking of the three major families of GPCRs [Sauvageau *et al.*, 2014] and is closely related to *Drosophila* Cnir. Upon activation, GPCRs transduce the extracellular signal into an intracellular response. The conformational change of a GPCR upon ligand binding leads to activation of the G protein. This in turn leads to an exchange of GDP to GTP in the α subunit of the G protein. Subsequently, GTP-bound $G\alpha$ dissociates from the $\beta\gamma$ dimer and both can interact with effector proteins to induce cellular responses. The most frequent α subunits are $G\alpha_q$, $G\alpha_s$ and $G\alpha_{i/o}$. The first two $G\alpha$ subunits are stimulating, while $G\alpha_{i/o}$ acts inhibitory downstream of GPCR signaling [Caers *et al.*, 2012]. GPCRs are involved in a myriad of biological processes, but many of those receptors are activated by neuropeptides [Bendena *et al.*, 2012; Caers *et al.*, 2012]. Strikingly, GPCRs, neuropeptides and GPCR signaling pathways elements are sensitive to minor changes, which are believed to result in behavioral plasticity because of alterations in GPCR controlled pathways [Bendena *et al.*, 2012].

The successful rescue of locomotor impairment via pan neuronal expression of Cnir in Δ c*nir* mutants might indicate restoration of GPCR trafficking in neurons. Thus, Cnir could be a potentially interesting upstream component of GPCR regulation. The G protein coupled dopamine receptors have been directly associated with abnormal locomotor behavior and Parkinson's disease [Missale *et al.*, 1998; Emilien *et al.*, 1999; Vallone *et al.*, 2000; Draper *et al.*, 2007]. Moreover, loss of dopaminergic neurons and therefore loss of signaling via dopamine GPCRs is linked to locomotor dysfunction in *Drosophila*. This motor impairment is marked by a premature loss of climbing ability,

resting tremor and premature death [Feany and Bender, 2000; Haywood and Staveley, 2004; Draper *et al.*, 2007]. In addition, pan neuronal knock-down of the Dopamine D2-like receptor (DD2R; family A GPCR) has been directly associated with low locomotor activity in *Drosophila* [Draper *et al.*, 2007]. Although it was not investigated whether the locomotor dysfunction of $\Delta cnir$ mutants increases with age, a minor resting tremor and premature death can be observed. Furthermore, a rescue of locomotor behavior via *Cnir* expression in neuronal cells, could possibly indicate recovery of trafficking of dopamine activated GPCRs to wild type-like levels. However, the obtained results indicate that the rescue might be only partial. There could be several reasons for an incomplete rescue. It has been shown for the human CNIH4 that both, lack and overexpression of the protein, lead to retention of GPCRs. Since the *UAS/Gal4* technique is a strong overexpression system, it could be that the adequate expression levels are not met in the experimental setup. Moreover, CNIH4 has been shown to interact with members of the three major families of GPCRs [Sauvageau *et al.*, 2014]. Therefore, a multitude of GPCRs might be retained to a certain degree in the ER. Another possibility is that GPCR export levels in other tissues than neurons could also contribute to the locomotor impairment.

4.4 Loss of *Cnir* leads to decreased ethanol sensitivity

Ethanol induces a gradual loss of postural control [Bellen, 1998; Devineni and Heberlein, 2013]. Therefore, we speculated that $\Delta cnir$ flies with an already impaired locomotion, would show an increased sensitivity towards ethanol. However, *cnir* mutant flies exhibit a decreased ethanol sensitivity. Strikingly, signaling downstream of GPCRs has been shown to have a crucial role in ethanol response of *Drosophila* [Moore *et al.*, 1998; Diamond and Gordon, 1997; Bellen, 1998; Ruppert, 2013].

One important downstream effector of GPCR signaling is the adenylyl cyclase (AC) which synthesizes the second messenger cAMP out of ATP [Caers *et al.*, 2012]. In a feedback loop, cAMP can activate the protein kinase A (PKA) which then phosphorylates the cyclic nucleotide phosphodiesterase 4 (PDE4). This leads to hydrolyzation of cAMP and terminates signaling [Conti and Beavo, 2007].

In *Drosophila*, cAMP synthesis is activated as an acute response to ethanol and is reduced through chronic ethanol exposure [Diamond and Gordon, 1997; Bellen, 1998; Ruppert, 2013]. Importantly, alcohol induced behavior is also altered through genetic manipulation of cAMP interacting pathways. Amnesiac is a neuropeptide which acts

as an AC and directly increases cAMP levels [Feany and Quinn, 1995] similarly to Rutabaga, a Ca^{2+} -calmodulin sensitive AC [Livingstone *et al.*, 1984; Levin *et al.*, 1992]. DCo is a major catalytic subunit of the cAMP dependent PKA and thus relies on cAMP for its activity [Lane and Kalderon, 1993]. Mutants for all three cAMP pathway components display an increased ethanol sensitivity [Moore *et al.*, 1998]. Strikingly, Moore *et al.* [1998] did not find any altered ethanol sensitivity in the mutant for the *Drosophila* PDE4 ortholog Dunce (Dnc), which has elevated cAMP levels. However, studies from Ruppert [2013] show a decreased sensitivity towards ethanol in Dnc^{M11} amorphic mutants.

Although speculative, one can reason that the lack of Cnir leads to inefficient trafficking of a GPCR that signals via $G\alpha_{i/o}$. As a consequence, this would lead to elevated cAMP levels and provide an explanation for the reduced ethanol sensitivity of the Δcnir mutant. Even if Cnir is involved in trafficking of a multitude of GPCRs specificity of the phenotype could be mediated via tissue specific expression of the GPCR and $G\alpha_{i/o}$.

4.5 GFP tagged Cnir potentially localizes to the ER but is not functional

Consistent with the conserved role of Cni paralogs as cargo receptors mediating ER export of secretory proteins both, N- and C-terminally GFP tagged Cnir putatively localize to the ER. The Protein Disulfide Isomerase (PDI) is a ER resident protein [Ferrari and Söling, 1999]. Even though no colocalization studies are shown in this thesis, the subcellular distribution of Cnir strongly resembles the localization reported for PDI in the squamous follicular epithelium of *Drosophila* egg chambers [Bökel *et al.*, 2006]. Furthermore, the localization of Cnir is very similar to that reported for its human ortholog CNIH4. In cell culture CNIH4 localizes to a large structure that is dense in the close proximity of the nucleus, but extends throughout the whole cell [Sauvageau *et al.*, 2014].

The expression the N-terminally GFP tagged Cnir in neuronal cells does not restore locomotor behavior in Δcnir flies. This indicates that the protein tag disrupts Cnir function. It could well be that the rather big GFP tag interferes with Cnir binding to the COPII subunits or its cargo. Strikingly, Sauvageau *et al.* [2014] used N-terminal vYFP, CFP, as well as C-terminal eYFP tags of the same size as GFP in their co-

immunoprecipitation experiments with CNIH₄. CFP:CNIH₄ has been shown to bind to the β_2 -AR and CNIH₄:eYFP to the chemokine CCR5 receptor. Therefore, tags on both termini do not seem to interfere with CNIH₄ binding to the GPCR cargo. Furthermore, vYFP:CNIH₄ was demonstrated to bind to Sec23 and Sec24, suggesting that the N-terminal tag does not interfere with binding to COPII subunits. The fact that GFP:Cnir does not rescue locomotor defects of Δ *cnir* flies could indicate that the locomotor impairment is caused by an inefficient ER export of a cargo that is structurally unrelated to the GPCRs tested by Sauvageau *et al.* [2014]. In this scenario the tag could interfere with Cnir binding to this cargo. Another possibility is that the protein tag differentially influences Cnir binding of different GPCRs. In this case, the phenotype could be specifically caused by inefficient trafficking of a subset, or even one GPCR. This in turn could be correlated with the putatively different mechanisms for GPCR concentration into COPII vesicles. While GPCRs that bind COPII subunits directly [Dong *et al.*, 2012] could be more tolerant for reduced affinity to Cnir due to a GFP tag, others that do not bind COPII might be more sensitive for those alterations. Above that, even a slightly reduced affinity of a GPCR cargo to GFP:Cnir could have little influence on an *in vitro* binding assay, while it could have big effects on *in vivo* signaling levels in *Drosophila*. As already mentioned, even slight alterations of GPCR signaling pathways result in behavioral plasticity [Bendena *et al.*, 2012].

It will be interesting to see whether Cnir:GFP can rescue motor impairment of the *cnir* mutant flies. A fully functional tagged Cnir will be crucial for reliable biochemical approaches to identify Cnir cargoes and for Cnir localization studies.

4.6 *Drosophila* Cni and Cnir do not show strong functional redundancy in the soma

It was reported that the lack of one *cnir* copy in an amorphic mutant background leads to synthetic lethality in *Drosophila*. Furthermore, escapers were only observed in combination with the amorphic/hypomorphic *cni* mutant background lacking one *cnir* copy. Moreover, those escapers were strongly malformed. It has also been shown that expression of *cnir* under the control of a *cni* promoter rescues parts of the synthetic lethality, as well as some somatic phenotypes of *cni* mutant flies [Bökel *et al.*, 2006]. The drawback of those experiments is that the data were generated using the deletion

Df(2L)JS7 [Sekelsky *et al.*, 1995]. This deficiency removes a 214.5 kb containing *cnir* and 36 other genes.

Because of those genetic results and the broad range of cargoes transported by Cni paralogs in yeast [Powers and Barlowe, 1998, 2002; Nakanishi *et al.*, 2007; Castillon *et al.*, 2009; Herzig *et al.*, 2012] and vertebrates [Castro *et al.*, 2007; Harmel *et al.*, 2012; Brockie *et al.*, 2013; Sauvageau *et al.*, 2014] we speculated that mutation of both *Drosophila cni* genes could lead to cell lethality. However, no cell lethality can be observed in both somatic tissues tested and large double mutant cell clones can be seen. This could indicate that cargoes of Cni proteins still traffic at sufficient rates for survival of the cell. As discussed above, fully folded cargo of a cargo receptor still traffics from ER to Golgi in bulk flow rates and is not exposed to ERAD [Belden and Barlowe, 2001b; Bue and Barlowe, 2009]. Moreover, a multitude of cargoes of Cni proteins might additionally bind directly to the COPII coat as described for the GPCR α_{2B} -AR [Dong *et al.*, 2012] and the yeast Gap1 [Malkus *et al.*, 2002; Castillon *et al.*, 2009; Sauvageau *et al.*, 2014].

Interestingly, the genetic experiments from Bökel *et al.* [2006] could not be reproduced with the newly generated $\Delta cnir/cni^{AR55}$ double mutant and no synthetic lethality could be observed in *cni* amorphic/hypomorphic mutants hemizygous for $\Delta cnir$. Moreover, reproduction of the experiments with the originally used stock did also not lead to synthetic lethality. A strong lethality could only be detected in *cni* amorphic mutants hemizygous for $\Delta cnir$. However, the lethality is not as strong as described in the published data. Furthermore, the amorphic *cni* mutants used in control crosses also display lethality depending on the chromosomal background. This indicates the presence of lethal factors that might have accumulated in the genetic background of the amorphic stocks. Apart from the somatic phenotypes associated with *cni* mutation, no severely malformed flies could be observed in *cni* mutants hemizygous for $\Delta cnir$. The genetic findings cannot completely rule out a functional redundancy of both *Drosophila* Cni paralogs, but the somatic impact of their mutation is not as strong as initially assumed. Thus, *Drosophila* Cni proteins could have a high selectivity towards a pool of transmembrane cargo as suggested by Sauvageau *et al.* [2014] for human CNIH1-4 proteins.

4.7 Perspectives

There is evidence that human CNIH4 is involved in the regulation of ER export of the three major families of GPCRs [Sauvageau *et al.*, 2014]. Although the investigated effects on survival throughout development, adult lifespan, locomotor function and ethanol sensitivity of $\Delta cnir$ mutants could be reasonably linked to abnormal GPCR signaling, the data in this thesis provide only indirect hints towards a potential role of Cnir in GPCR trafficking. Therefore, the most pressing future experiment is to investigate interaction of Cnir with GPCRs. Although there are only few antibodies available for GPCRs, even those few could suffice to investigate ER exit of the receptors in $\Delta cnir$ mutants, especially if Cnir interacts with a similarly broad range of GPCRs like its ortholog CNIH4. ER exit has been shown to be the bottleneck in maturation and cell surface transport of GPCRs [Petaja-Repo *et al.*, 2000]. Hence, It would be possible to investigate the proportion of different GPCRs reaching the plasma membrane in diverse tissues of *cnir* mutant flies microscopically. Many GPCRs have been shown to undergo consecutive post translational modifications like N- and O-glycosylation after ER exit, which can be used as readouts for their maturation state [Dong *et al.*, 2007; Sauvageau *et al.*, 2014]. Furthermore, Sauvageau *et al.* [2014] demonstrated that the Cnir ortholog CNIH4 interacts with immature β 2-AR and that ER retained cargo undergoes degradation. Therefore, it might be crucial to investigate protein lysates from $\Delta cnir$ mutants via western blots, to find if immature forms of GPCRs are overrepresented due to ER retention. Moreover, one could examine if $\Delta cnir$ mutants possess degradation intermediates of GPCRs, which would indicate retention of receptors in the ER. Furthermore, co-immunoprecipitation of a GPCR with an epitope tagged version of Cnir could provide valuable hints to a putative function of Cnir in trafficking of GPCRs. Although *in vitro* binding assays might not rely on a fully functional epitope tagged Cnir, it would be more reliable to conduct the experiments with a tagged version that is able to rescue the locomotor defects of $\Delta cnir$ mutants. Since a neuronal rescue with a GFP:Cnir was not successful, C-terminally tagged Cnir could provide a tool for those experiments. As previously described, DD2R has been shown to be involved in locomotion of *Drosophila* [Draper *et al.*, 2007]. Therefore, locomotor impairment of $\Delta cnir$ mutants could be directly linked to inefficient ER exit of DD2R. First western blot experiments have already been conducted using an anti-DD2R antibody. However, endogenous expression of DD2R is low. Therefore, it might be necessary to

use overexpression systems in cell culture to see DD2R degradation intermediates, or to perform efficient co-immunoprecipitation experiments with Cnir.

The human CNIH4 localizes to the ER and interacts with the COPII subunits Sec23 and Sec24 [Sauvageau *et al.*, 2014]. Thus, a functional epitope tagged Cnir is also crucial to conduct colocalization studies with COPII components and ER resident proteins like PDI [Ferrari and Söling, 1999] to support its role as cargo receptor. The employed antibodies could then be used for co-immunoprecipitation experiments. An anti-Sec23 antibody has already been tested for staining in ovaries (fig. S.2).

The analysis of Δ *cnir* mutants showed that Cnir function is essential in neurons of *Drosophila* for normal locomotor behavior. However, it would be interesting to know which neuronal circuits depend on Cnir function. Therefore, Cnir expression with different neuronal Gal4 driver lines could provide a better understanding of the affected neuronal circuits. The discovery of those circuits would also narrow down possible GPCR cargoes. Furthermore, it would be essential to investigate whether ethanol sensitivity can be restored to wt levels upon neuronal expression of Cnir.

Finally, it would be of great importance to utilize a functional epitope tagged *cnir* for site specific transgenesis [Bischof *et al.*, 2007] at the Δ *cnir* locus. This would offer the possibility to monitor the subcellular and tissue specific expression of Cnir from its endogenous promoter and could provide valuable insights into neurons relying on Cnir function. Furthermore, this could again help to select for possible GPCR cargoes.

Although initially hypothesized, the results from this thesis do not indicate a strong functional redundancy of *Drosophila* Cni proteins in the soma. As discussed before, *Drosophila* Cni proteins might have a high selectivity towards a pool of transmembrane cargoes. Therefore, an interesting question is whether the apparently conserved function in AMPAR regulation and trafficking that has been proposed for Cornichon proteins in *C.elegans* [Herring *et al.*, 2013] and vertebrates [Schwenk *et al.*, 2009; Kato *et al.*, 2010; Shi *et al.*, 2010; Gill *et al.*, 2011; Coombs *et al.*, 2012; Gill *et al.*, 2012; Harmel *et al.*, 2012; Brockie *et al.*, 2013], also applies to *Drosophila* Cni. To investigate Cni function, it would be crucial to generate a mutant in a cleaner chromosomal background as reported for *cnir* in this thesis. Another option could be to purify the available *cni* amorphic stocks from the seemingly present lethal factors. The larval NMJ expresses GluRs homologous to AMPARs in the mammalian brain postsynaptically in muscle cells [Menon *et al.*, 2013]. Thus, a knock-down of *cni* in muscles cells via RNAi [Dietzl *et al.*, 2007; Ni *et al.*, 2011] might provide evidence for a function of *Drosophila* Cni in

regulation and trafficking of GluRs. The knock-down might cause altered locomotion of flies due to changed synaptic transmission via GluRs. Moreover, a possible change in the proportion of GluRs reaching the cell surface of muscle cells could be monitored microscopically via antibody staining in the larval NMJ.

References

- Adams MD, Celniker SE, Holt RA, Evans CA, Gocayne JD, Amanatides PG, Scherer SE, Li PW, Hoskins RA, Galle RF, George RA, Lewis SE, Richards S, Ashburner M, Henderson SN, Sutton GG, Wortman JR, Yandell MD, Zhang Q, Chen LX, Brandon RC, Rogers YH, Blazej RG, Champe M, Pfeiffer BD, Wan KH, Doyle C, Baxter EG, Helt G, Nelson CR, Gabor GL, Abril JF, Agbayani A, An HJ, Andrews-Pfannkoch C, Baldwin D, Ballew RM, Basu A, Baxendale J, Bayraktaroglu L, Beasley EM, Beeson KY, Benos PV, Berman BP, Bhandari D, Bolshakov S, Borkova D, Botchan MR, Bouck J, Brokstein P, Brottier P, Burtis KC, Busam DA, Butler H, Cadieu E, Center A, Chandra I, Cherry JM, Cawley S, Dahlke C, Davenport LB, Davies P, de Pablos B, Delcher A, Deng Z, Mays AD, Dew I, Dietz SM, Dodson K, Doup LE, Downes M, Dugan-Rocha S, Dunkov BC, Dunn P, Durbin KJ, Evangelista CC, Ferraz C, Ferriera S, Fleischmann W, Fosler C, Gabrielian AE, Garg NS, Gelbart WM, Glasser K, Glodek A, Gong F, Gorrell JH, Gu Z, Guan P, Harris M, Harris NL, Harvey D, Heiman TJ, Hernandez JR, Houck J, Hostin D, Houston KA, Howland TJ, Wei MH, Ibegwam C, Jalali M, Kalush F, Karpen GH, Ke Z, Kennison JA, Ketchum KA, Kimmel BE, Kodira CD, Kraft C, Kravitz S, Kulp D, Lai Z, Lasko P, Lei Y, Levitsky AA, Li J, Li Z, Liang Y, Lin X, Liu X, Mattei B, McIntosh TC, McLeod MP, McPherson D, Merkulov G, Milshina NV, Mobarry C, Morris J, Moshrefi A, Mount SM, Moy M, Murphy B, Murphy L, Muzny DM, Nelson DL, Nelson DR, Nelson KA, Nixon K, Nusskern DR, Pacleb JM, Palazzolo M, Pittman GS, Pan S, Pollard J, Puri V, Reese MG, Reinert K, Remington K, Saunders RD, Scheeler F, Shen H, Shue BC, Sidén-Kiamos I, Simpson M, Skupski MP, Smith T, Spier E, Spradling AC, Stapleton M, Strong R, Sun E, Svirskas R, Tector C, Turner R, Venter E, Wang AH, Wang X, Wang ZY, Wassarman DA, Weinstock GM, Weissenbach J, Williams SM, Woodage T, Worley KC, Wu D, Yang S, Yao QA, Ye J, Yeh RF, Zaveri JS, Zhan M, Zhang G, Zhao Q, Zheng L, Zheng XH, Zhong FN, Zhong W, Zhou X, Zhu S, Zhu X, Smith HO, Gibbs RA, Myers EW, Rubin GM, Venter JC (2000). The genome sequence of *Drosophila melanogaster*. *Science* **287**:2185–2195.
- Allen JA, Roth BL (2011). Strategies to discover unexpected targets for drugs active at G protein-coupled receptors. *Annu Rev Pharmacol Toxicol* **51**:117–144.
- Appenzeller-Herzog C, Nyfeler B, Burkhard P, Santamaria I, Lopez-Otin C, Hauri HP (2005). Carbohydrate- and conformation-dependent cargo capture for ER-exit. *Mol Biol Cell* **16**:1258–1267.
- Aridor M, Weissman J, Bannykh S, Nuoffer C, Balch WE (1998). Cargo selection by the COPII budding machinery during export from the ER. *J Cell Biol* **141**:61–70.
- Ashburner M (1989). *Drosophila: A Laboratory Handbook*. Cold Spring Harbor Laboratory Press, New York.

- Balch WE, McCaffery JM, Plutner H, Farquhar MG (1994). Vesicular stomatitis virus glycoprotein is sorted and concentrated during export from the endoplasmic reticulum. *Cell* **76**:841–852.
- Bannykh SI, Rowe T, Balch WE (1996). The organization of endoplasmic reticulum export complexes. *J Cell Biol* **135**:19–35.
- Banovic D, Khorramshahi O, Oswald D, Wichmann C, Riedt T, Fouquet W, Tian R, Sigrist SJ, Aberle H (2010). *Drosophila* Neuroligin 1 promotes growth and postsynaptic differentiation at glutamatergic neuromuscular junctions. *Neuron* **66**:724–738.
- Barlowe C (2003). Signals for COPII-dependent export from the ER: what's the ticket out? *Trends Cell Biol* **13**:295–300.
- Barlowe C, Orci L, Yeung T, Hosobuchi M, Hamamoto S, Salama N, Rexach MF, Ravazzola M, Amherdt M, Schekman R (1994). COPII: A membrane coat formed by Sec proteins that drive vesicle budding from the endoplasmic reticulum. *Cell* **77**:895–907.
- Bastock R, St Johnston D (2008). *Drosophila* oogenesis. *Curr Biol* **18**:R1082–R1087.
- Beckingham KM, Texada MJ, Baker DA, Munjaal R, Armstrong JD (2005). Genetics of graviperception in animals. *Adv Genet* **55**:105–145.
- Belden WJ, Barlowe C (2001a). Deletion of yeast *p24* genes activates the unfolded protein response. *Mol Biol Cell* **12**:957–969.
- Belden WJ, Barlowe C (2001b). Role of Erv29p in collecting soluble secretory proteins into ER-derived transport vesicles. *Science* **294**:1528–1531.
- Bellen HJ (1998). The fruit fly: A model organism to study the genetics of alcohol abuse and addiction? *Cell* **93**:909–912.
- Bendena WG, Campbell J, Zara L, Tobe SS, Chin-Sang ID (2012). Select Neuropeptides and their G-Protein Coupled Receptors in *Caenorhabditis elegans* and *Drosophila melanogaster*. *Front Endocrinol (Lausanne)* **3**:93.
- Benzer S (1967). BEHAVIORAL MUTANTS OF *Drosophila* ISOLATED BY COUNTER-CURRENT DISTRIBUTION. *Proc Natl Acad Sci U S A* **58**:1112–1119.
- Bischof J, Maeda RK, Hediger M, Karch F, Basler K (2007). An optimized transgenesis system for *Drosophila* using germ-line-specific phiC31 integrases. *Proc Natl Acad Sci U S A* **104**:3312–3317.
- Bland JM, Altman DG (2004). The logrank test. *BMJ* **328**:1073.
- Bonifacino JS, Glick BS (2004). The mechanisms of vesicle budding and fusion. *Cell* **116**:153–166.

- Brand AH, Perrimon N (1993). Targeted gene expression as a means of altering cell fates and generating dominant phenotypes. *Development* **118**:401–415.
- Brockie PJ, Jensen M, Mellem JE, Jensen E, Yamasaki T, Wang R, Maxfield D, Thacker C, Hoerndli F, Dunn PJ, Tomita S, Madsen DM, Maricq AV (2013). Cornichons control ER export of AMPA receptors to regulate synaptic excitability. *Neuron* **80**:129–142.
- Budnik A, Stephens DJ (2009). ER exit sites–localization and control of COPII vesicle formation. *FEBS Lett* **583**:3796–3803.
- Bue CA, Barlowe C (2009). Molecular dissection of Erv26p identifies separable cargo binding and coat protein sorting activities. *J Biol Chem* **284**:24049–24060.
- Bue CA, Bentivoglio CM, Barlowe C (2006). Erv26p directs pro-alkaline phosphatase into endoplasmic reticulum-derived coat protein complex II transport vesicles. *Mol Biol Cell* **17**:4780–4789.
- Bökel C, Dass S, Wilsch-Bräuninger M, Roth S (2006). *Drosophila* Cornichon acts as cargo receptor for ER export of the TGF α -like growth factor Gurken. *Development* **133**:459–470.
- Caers J, Verlinden H, Zels S, Vandersmissen HP, Vuerinckx K, Schoofs L (2012). More than two decades of research on insect neuropeptide GPCRs: An overview. *Front Endocrinol (Lausanne)* **3**:151.
- Castillon GA, Watanabe R, Taylor M, Schwabe TME, Riezman H (2009). Concentration of GPI-anchored proteins upon ER exit in yeast. *Traffic* **10**:186–200.
- Castro CP, Piscopo D, Nakagawa T, Derynck R (2007). Cornichon regulates transport and secretion of TGF α -related proteins in metazoan cells. *J Cell Sci* **120**:2454–2466.
- Chen CN, Denome S, Davis RL (1986). Molecular analysis of cDNA clones and the corresponding genomic coding sequences of the *Drosophila dunce*⁺ gene, the structural gene for cAMP phosphodiesterase. *Proc Natl Acad Sci U S A* **83**:9313–9317.
- Chien S, Reiter LT, Bier E, Gribskov M (2002). Homophila: Human disease gene cognates in *Drosophila*. *Nucleic Acids Res* **30**:149–151.
- Chou TB, Noll E, Perrimon N (1993). Autosomal *P[ovo^{D1}]* dominant female-sterile insertions in *Drosophila* and their use in generating germ-line chimeras. *Development* **119**:1359–1369.
- Chou TB, Perrimon N (1996). The autosomal FLP-DFS technique for generating germline mosaics in *Drosophila melanogaster*. *Genetics* **144**:1673–1679.

- Cohan FM, Graf JD (1985). Latitudinal Cline in *Drosophila melanogaster* for Knockdown Resistance to Ethanol Fumes and for Rates of Response to Selection for Further Resistance. *Evolution* **39**:pp. 278–293.
- Conti M, Beavo J (2007). Biochemistry and physiology of cyclic nucleotide phosphodiesterases: Essential components in cyclic nucleotide signaling. *Annu Rev Biochem* **76**:481–511.
- Coombs ID, Soto D, Zonouzi M, Renzi M, Shelley C, Farrant M, Cull-Candy SG (2012). Cornichons modify channel properties of recombinant and glial AMPA receptors. *J Neurosci* **32**:9796–9804.
- Dancourt J, Barlowe C (2009). Erv26p-dependent export of alkaline phosphatase from the ER requires lumenal domain recognition. *Traffic* **10**:1006–1018.
- Dancourt J, Barlowe C (2010). Protein sorting receptors in the early secretory pathway. *Annu Rev Biochem* **79**:777–802.
- D’Arcangelo JG, Stahmer KR, Miller EA (2013). Vesicle-mediated export from the ER: COPII coat function and regulation. *Biochim Biophys Acta* **1833**:2464–2472.
- Davis RL, Takayasu H, Eberwine M, Myres J (1989). Cloning and characterization of mammalian homologs of the *Drosophila dunce*⁺ gene. *Proc Natl Acad Sci U S A* **86**:3604–3608.
- Dereeper A, Guignon V, Blanc G, Audic S, Buffet S, Chevenet F, Dufayard JF, Guindon S, Lefort V, Lescot M, Claverie JM, Gascuel O (2008). Phylogeny.fr: Robust phylogenetic analysis for the non-specialist. *Nucleic Acids Res* **36**:W465–W469.
- Devineni AV, Heberlein U (2013). The Evolution of *Drosophila melanogaster* as a Model for Alcohol Research. *Annu Rev Neurosci* **36**:121–138.
- Diamond I, Gordon AS (1997). Cellular and molecular neuroscience of alcoholism. *Physiol Rev* **77**:1–20.
- Dietzl G, Chen D, Schnorrer F, Su KC, Barinova Y, Fellner M, Gasser B, Kinsey K, Oepel S, Scheiblauer S, Couto A, Marra V, Keleman K, Dickson BJ (2007). A genome-wide transgenic RNAi library for conditional gene inactivation in *Drosophila*. *Nature* **448**:151–156.
- Dong C, Filipeanu CM, Duvernay MT, Wu G (2007). Regulation of G protein-coupled receptor export trafficking. *Biochim Biophys Acta* **1768**:853–870.
- Dong C, Nichols CD, Guo J, Huang W, Lambert NA, Wu G (2012). A triple arg motif mediates α_{2B} -adrenergic receptor interaction with Sec24C/D and export. *Traffic* **13**:857–868.

- Dong C, Zhou F, Fugetta EK, Filipeanu CM, Wu G (2008). Endoplasmic reticulum export of adrenergic and angiotensin II receptors is differentially regulated by Sar1 GTPase. *Cell Signal* **20**:1035–1043.
- Draper I, Kurshan PT, McBride E, Jackson FR, Kopin AS (2007). Locomotor activity is regulated by D2-like receptors in *Drosophila*: An anatomic and functional analysis. *Dev Neurobiol* **67**:378–393.
- Drummond JB, Simmons M, Haroutunian V, Meador-Woodruff JH (2012). Upregulation of *cornichon* transcripts in the dorsolateral prefrontal cortex in schizophrenia. *Neuroreport* **23**:1031–1034.
- Dupré DJ, Robitaille M, Ethier N, Villeneuve LR, Mamarbachi AM, Hébert TE (2006). Seven transmembrane receptor core signaling complexes are assembled prior to plasma membrane trafficking. *J Biol Chem* **281**:34561–34573.
- Emilien G, Maloteaux JM, Geurts M, Hoogenberg K, Cragg S (1999). Dopamine receptors—physiological understanding to therapeutic intervention potential. *Pharmacol Ther* **84**:133–156.
- Feany MB, Bender WW (2000). A *Drosophila* model of Parkinson's disease. *Nature* **404**:394–398.
- Feany MB, Quinn WG (1995). A neuropeptide gene defined by the *Drosophila* memory mutant *amnesiac*. *Science* **268**:869–873.
- Ferrari DM, Söling HD (1999). The Protein Disulphide-Isomerase family: Unravelling a string of folds. *Biochem J* **339** (Pt 1):1–10.
- Floor K, Barøy T, Misceo D, Kanavin OJ, Fannemel M, Frengen E (2012). A 1 Mb *de novo* deletion within 11q13.1q13.2 in a boy with mild intellectual disability and minor dysmorphic features. *Eur J Med Genet* **55**:695–699.
- Gargano JW, Martin I, Bhandari P, Grotewiel MS (2005). Rapid iterative negative geotaxis (RING): A new method for assessing age-related locomotor decline in *Drosophila*. *Exp Gerontol* **40**:386–395.
- Gill MB, Kato AS, Roberts MF, Yu H, Wang H, Tomita S, Brecht DS (2011). Cornichon-2 modulates AMPA receptor-transmembrane AMPA receptor regulatory protein assembly to dictate gating and pharmacology. *J Neurosci* **31**:6928–6938.
- Gill MB, Kato AS, Wang H, Brecht DS (2012). AMPA receptor modulation by Cornichon-2 dictated by transmembrane AMPA receptor regulatory protein isoform. *Eur J Neurosci* **35**:182–194.
- Gong WJ, Golic KG (2003). Ends-out, or replacement, gene targeting in *Drosophila*. *Proc Natl Acad Sci U S A* **100**:2556–2561.

- Harmel N, Cokic B, Zolles G, Berkefeld H, Mauric V, Fakler B, Stein V, Klöcker N (2012). AMPA receptors commandeered an ancient cargo exporter for use as an auxiliary subunit for signaling. *PLoS One* 7:e30681.
- Haywood AFM, Staveley BE (2004). Parkin counteracts symptoms in a *Drosophila* model of Parkinson's disease. *BMC Neurosci* 5:14.
- Herpers B, Rabouille C (2004). mRNA localization and ER-based protein sorting mechanisms dictate the use of transitional endoplasmic reticulum-golgi units involved in Gurken transport in *Drosophila* oocytes. *Mol Biol Cell* 15:5306–5317.
- Herring BE, Shi Y, Suh YH, Zheng CY, Blankenship SM, Roche KW, Nicoll RA (2013). Cornichon proteins determine the subunit composition of synaptic AMPA receptors. *Neuron* 77:1083–1096.
- Herzig Y, Sharpe HJ, Elbaz Y, Munro S, Schuldiner M (2012). A systematic approach to pair secretory cargo receptors with their cargo suggests a mechanism for cargo selection by Erv14. *PLoS Biol* 10:e1001329.
- Huang J, Zhou W, Watson AM, Jan YN, Hong Y (2008). Efficient ends-out gene targeting in *Drosophila*. *Genetics* 180:703–707.
- Inagaki HK, Kamikouchi A, Ito K (2010). Methods for quantifying simple gravity sensing in *Drosophila melanogaster*. *Nat Protoc* 5:20–25.
- Jonikas MC, Collins SR, Denic V, Oh E, Quan EM, Schmid V, Weibezahn J, Schwappach B, Walter P, Weissman JS, Schuldiner M (2009). Comprehensive characterization of genes required for protein folding in the endoplasmic reticulum. *Science* 323:1693–1697.
- Kamikouchi A, Inagaki HK, Effertz T, Hendrich O, Fiala A, Göpfert MC, Ito K (2009). The neural basis of *Drosophila* gravity-sensing and hearing. *Nature* 458:165–171.
- Kappeler F, Klopfenstein DR, Foguet M, Paccaud JP, Hauri HP (1997). The recycling of ERGIC-53 in the early secretory pathway. ERGIC-53 carries a cytosolic endoplasmic reticulum-exit determinant interacting with COPII. *J Biol Chem* 272:31801–31808.
- Kato AS, Gill MB, Ho MT, Yu H, Tu Y, Siuda ER, Wang H, Qian YW, Nisenbaum ES, Tomita S, Brecht DS (2010). Hippocampal AMPA receptor gating controlled by both TARP and Cornichon proteins. *Neuron* 68:1082–1096.
- Kincaid MM, Cooper AA (2007). Misfolded proteins traffic from the endoplasmic reticulum (ER) due to ER export signals. *Mol Biol Cell* 18:455–463.
- Kuehn MJ, Herrmann JM, Schekman R (1998). COPII-cargo interactions direct protein sorting into ER-derived transport vesicles. *Nature* 391:187–190.

- Lahey T, Gorczyca M, Jia XX, Budnik V (1994). The *Drosophila* tumor suppressor gene *dlg* is required for normal synaptic bouton structure. *Neuron* **13**:823–835.
- Lane ME, Kalderon D (1993). Genetic investigation of cAMP-dependent protein kinase function in *Drosophila* development. *Genes Dev* **7**:1229–1243.
- Lee MCS, Miller EA, Goldberg J, Orci L, Schekman R (2004). Bi-directional protein transport between the ER and Golgi. *Annu Rev Cell Dev Biol* **20**:87–123.
- Lee MCS, Orci L, Hamamoto S, Futai E, Ravazzola M, Schekman R (2005). Sar1p N-terminal helix initiates membrane curvature and completes the fission of a COPII vesicle. *Cell* **122**:605–617.
- Levin LR, Han PL, Hwang PM, Feinstein PG, Davis RL, Reed RR (1992). The *Drosophila* learning and memory gene *rutabaga* encodes a Ca²⁺/Calmodulin-responsive adenylyl cyclase. *Cell* **68**:479–489.
- Livingstone MS, Sziber PP, Quinn WG (1984). Loss of calcium/calmodulin responsiveness in adenylate cyclase of *rutabaga*, a *Drosophila* learning mutant. *Cell* **37**:205–215.
- Losev E, Reinke CA, Jellen J, Strongin DE, Bevis BJ, Glick BS (2006). Golgi maturation visualized in living yeast. *Nature* **441**:1002–1006.
- Lu W, Shi Y, Jackson AC, Bjorgan K, During MJ, Sprengel R, Seeburg PH, Nicoll RA (2009). Subunit composition of synaptic AMPA receptors revealed by a single-cell genetic approach. *Neuron* **62**:254–268.
- Malkus P, Jiang F, Schekman R (2002). Concentrative sorting of secretory cargo proteins into COPII-coated vesicles. *J Cell Biol* **159**:915–921.
- Martínez-Menárguez JA, Geuze HJ, Slot JW, Klumperman J (1999). Vesicular tubular clusters between the ER and Golgi mediate concentration of soluble secretory proteins by exclusion from COPI-coated vesicles. *Cell* **98**:81–90.
- Matsuoka K, Orci L, Amherdt M, Bednarek SY, Hamamoto S, Schekman R, Yeung T (1998). COPII-coated vesicle formation reconstituted with purified coat proteins and chemically defined liposomes. *Cell* **93**:263–275.
- McClure KD, Schubiger G (2005). Developmental analysis and squamous morphogenesis of the peripodial epithelium in *Drosophila* imaginal discs. *Development* **132**:5033–5042.
- Menon KP, Carrillo RA, Zinn K (2013). Development and plasticity of the *Drosophila* larval neuromuscular junction. *Wiley Interdiscip Rev Dev Biol* **2**:647–670.
- Miller E, Antonny B, Hamamoto S, Schekman R (2002). Cargo selection into COPII vesicles is driven by the Sec24p subunit. *EMBO J* **21**:6105–6113.

- Miller EA, Beilharz TH, Malkus PN, Lee MCS, Hamamoto S, Orci L, Schekman R (2003). Multiple cargo binding sites on the COPII subunit Sec24p ensure capture of diverse membrane proteins into transport vesicles. *Cell* **114**:497–509.
- Missale C, Nash SR, Robinson SW, Jaber M, Caron MG (1998). Dopamine receptors: From structure to function. *Physiol Rev* **78**:189–225.
- Mizuno M, Singer SJ (1993). A soluble secretory protein is first concentrated in the endoplasmic reticulum before transfer to the Golgi apparatus. *Proc Natl Acad Sci U S A* **90**:5732–5736.
- Moore MS, DeZazzo J, Luk AY, Tully T, Singh CM, Heberlein U (1998). Ethanol intoxication in *Drosophila*: Genetic and pharmacological evidence for regulation by the cAMP signaling pathway. *Cell* **93**:997–1007.
- Mossessova E, Bickford LC, Goldberg J (2003). SNARE selectivity of the COPII coat. *Cell* **114**:483–495.
- Mullis K, Faloona F, Scharf S, Saiki R, Horn G, Erlich H (1986). Specific enzymatic amplification of DNA *in vitro*: The polymerase chain reaction. *Cold Spring Harb Symp Quant Biol* **51 Pt 1**:263–273.
- Mullis KB, Faloona FA (1987). Specific synthesis of DNA *in vitro* via a polymerase-catalyzed chain reaction. *Methods Enzymol* **155**:335–350.
- Nakanishi H, Suda Y, Neiman AM (2007). Erv14 family cargo receptors are necessary for ER exit during sporulation in *Saccharomyces cerevisiae*. *J Cell Sci* **120**:908–916.
- Ni JQ, Zhou R, Czech B, Liu LP, Holderbaum L, Yang-Zhou D, Shim HS, Tao R, Handler D, Karpowicz P, Binari R, Booker M, Brennecke J, Perkins LA, Hannon GJ, Perrimon N (2011). A genome-scale shRNA resource for transgenic RNAi in *Drosophila*. *Nat Methods* **8**:405–407.
- Nishimura N, Balch WE (1997). A di-acidic signal required for selective export from the endoplasmic reticulum. *Science* **277**:556–558.
- Orci L, Ravazzola M, Meda P, Holcomb C, Moore HP, Hicke L, Schekman R (1991). Mammalian Sec23p homologue is restricted to the endoplasmic reticulum transitional cytoplasm. *Proc Natl Acad Sci U S A* **88**:8611–8615.
- Otte S, Barlowe C (2004). Sorting signals can direct receptor-mediated export of soluble proteins into COPII vesicles. *Nat Cell Biol* **6**:1189–1194.
- Partridge L, Alic N, Bjedov I, Piper MDW (2011). Ageing in *Drosophila*: The role of the insulin/Igf and TOR signalling network. *Exp Gerontol* **46**:376–381.

- Petaja-Repo UE, Hogue M, Laperriere A, Walker P, Bouvier M (2000). Export from the endoplasmic reticulum represents the limiting step in the maturation and cell surface expression of the human δ opioid receptor. *J Biol Chem* **275**:13727–13736.
- Powers J, Barlowe C (1998). Transport of Axl2p depends on Erv14p, an ER-vesicle protein related to the *Drosophila cornichon* gene product. *J Cell Biol* **142**:1209–1222.
- Powers J, Barlowe C (2002). Erv14p directs a transmembrane secretory protein into COPII-coated transport vesicles. *Mol Biol Cell* **13**:880–891.
- Quinn P, Griffiths G, Warren G (1984). Density of newly synthesized plasma membrane proteins in intracellular membranes II. Biochemical studies. *J Cell Biol* **98**:2142–2147.
- Rexach MF, Latterich M, Schekman RW (1994). Characteristics of endoplasmic reticulum-derived transport vesicles. *J Cell Biol* **126**:1133–1148.
- Rossanese OW, Soderholm J, Bevis BJ, Sears IB, O'Connor J, Williamson EK, Glick BS (1999). Golgi structure correlates with transitional endoplasmic reticulum organization in *Pichia pastoris* and *Saccharomyces cerevisiae*. *J Cell Biol* **145**:69–81.
- Roth S, Neuman-Silberberg FS, Barcelo G, Schüpbach T (1995). *cornichon* and the EGF receptor signaling process are necessary for both anterior-posterior and dorsal-ventral pattern formation in *Drosophila*. *Cell* **81**:967–978.
- Rubin GM, Spradling AC (1983). Vectors for P element-mediated gene transfer in *Drosophila*. *Nucleic Acids Res* **11**:6341–6351.
- Ruppert MB (2013). *Dissecting Tbh and Hangover function in ethanol tolerance in Drosophila melanogaster*. PhD thesis, University of Cologne.
- Saiki RK, Gelfand DH, Stoffel S, Scharf SJ, Higuchi R, Horn GT, Mullis KB, Erlich HA (1988). Primer-directed enzymatic amplification of DNA with a thermostable DNA polymerase. *Science* **239**:487–491.
- Salama NR, Yeung T, Schekman RW (1993). The Sec13p complex and reconstitution of vesicle budding from the ER with purified cytosolic proteins. *EMBO J* **12**:4073–4082.
- Sanger F, Nicklen S, Coulson AR (1977). DNA sequencing with chain-terminating inhibitors. *Proc Natl Acad Sci U S A* **74**:5463–5467.
- Sauvageau E, Rochdi DM, Oueslati M, Hamdan FF, Percherancier Y, Simpson JC, Pepperkok R, Bouvier M (2014). CNIH4 interacts with newly synthesized GPCR and control their export from the endoplasmic reticulum. *Traffic* .
- Schuster CM, Davis GW, Fetter RD, Goodman CS (1996). Genetic dissection of structural and functional components of synaptic plasticity. I. Fasciclin II controls synaptic stabilization and growth. *Neuron* **17**:641–654.

- Schwenk J, Harmel N, Zolles G, Bildl W, Kulik A, Heimrich B, Chisaka O, Jonas P, Schulte U, Fakler B, Klöcker N (2009). Functional proteomics identify Cornichon proteins as auxiliary subunits of AMPA receptors. *Science* **323**:1313–1319.
- Sciaky N, Presley J, Smith C, Zaal KJ, Cole N, Moreira JE, Terasaki M, Siggia E, Lippincott-Schwartz J (1997). Golgi tubule traffic and the effects of brefeldin A visualized in living cells. *J Cell Biol* **139**:1137–1155.
- Sekelsky JJ, Newfeld SJ, Raftery LA, Chartoff EH, Gelbart WM (1995). Genetic characterization and cloning of *mothers against dpp*, a gene required for *decapentaplegic* function in *Drosophila melanogaster*. *Genetics* **139**:1347–1358.
- Sharpe HJ, Stevens TJ, Munro S (2010). A comprehensive comparison of transmembrane domains reveals organelle-specific properties. *Cell* **142**:158–169.
- Shi Y, Suh YH, Milstein AD, Isozaki K, Schmid SM, Roche KW, Nicoll RA (2010). Functional comparison of the effects of TARPs and Cornichons on AMPA receptor trafficking and gating. *Proc Natl Acad Sci U S A* **107**:16315–16319.
- Sinadinos C, Cowan CM, Wyttenbach A, Mudher A (2012). Increased throughput assays of locomotor dysfunction in *Drosophila* larvae. *J Neurosci Methods* **203**:325–334.
- Slawson JB, Kuklin EA, Ejima A, Mukherjee K, Ostrovsky L, Griffith LC (2011). Central regulation of locomotor behavior of *Drosophila melanogaster* depends on a CASK isoform containing CaMK-like and L27 domains. *Genetics* **187**:171–184.
- Stagg SM, Gürkan C, Fowler DM, LaPointe P, Foss TR, Potter CS, Carragher B, Balch WE (2006). Structure of the Sec13/31 COPII coat cage. *Nature* **439**:234–238.
- Sun M, Xing G, Yuan L, Gan G, Knight D, With SI, He C, Han J, Zeng X, Fang M, Boulianne GL, Xie W (2011). Neuroligin 2 is required for synapse development and function at the *Drosophila* neuromuscular junction. *J Neurosci* **31**:687–699.
- Tabuchi K, Südhof TC (2002). Structure and evolution of *neurexin* genes: Insight into the mechanism of alternative splicing. *Genomics* **79**:849–859.
- Torroja L, Chu H, Kotovsky I, White K (1999). Neuronal overexpression of APPL, the *Drosophila* homologue of the amyloid precursor protein (APP), disrupts axonal transport. *Curr Biol* **9**:489–492.
- Vallone D, Picetti R, Borrelli E (2000). Structure and function of dopamine receptors. *Neurosci Biobehav Rev* **24**:125–132.
- Vembar SS, Brodsky JL (2008). One step at a time: Endoplasmic reticulum-associated degradation. *Nat Rev Mol Cell Biol* **9**:944–957.

- Wang X, Shaw WR, Tsang HTH, Reid E, O’Kane CJ (2007). *Drosophila* spichthyn inhibits BMP signaling and regulates synaptic growth and axonal microtubules. *Nat Neurosci* **10**:177–185.
- Ward TH, Polishchuk RS, Caplan S, Hirschberg K, Lippincott-Schwartz J (2001). Maintenance of Golgi structure and function depends on the integrity of ER export. *J Cell Biol* **155**:557–570.
- Wendeler MW, Paccaud JP, Hauri HP (2007). Role of Sec24 isoforms in selective export of membrane proteins from the endoplasmic reticulum. *EMBO Rep* **8**:258–264.
- Xu T, Rubin GM (1993). Analysis of genetic mosaics in developing and adult *Drosophila* tissues. *Development* **117**:1223–1237.
- Yasuyama K, Salvaterra PM (1999). Localization of choline acetyltransferase-expressing neurons in *Drosophila* nervous system. *Microsc Res Tech* **45**:65–79.
- Ziegler A, Lange S, Bender R (2007). Survival analysis: Log rank test. *Dtsch Med Wochenschr* **132 Suppl 1**:e39–e41.

Supplement

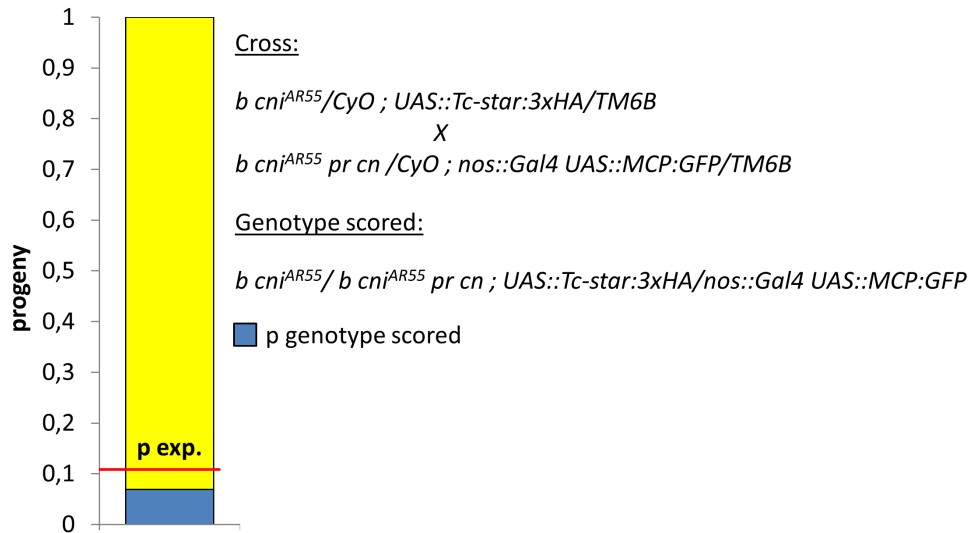


Figure S.1 | The *cni^{AR55}* amorphic mutation is not lethal in an altered chromosomal background

The *cni^{AR55}* amorphic mutant progeny with an altered third chromosome (scored genotype) is viable. Furthermore, there is no statistically significant difference between the p.exp and the observed frequency of the scored genotype. The percentage of the scored genotype is indicated (blue) and the expected percentage of this genotype is marked by a red line. The yellow proportion of the bar represents all non scored genotypes in the total progeny (n= 189) from the cross.

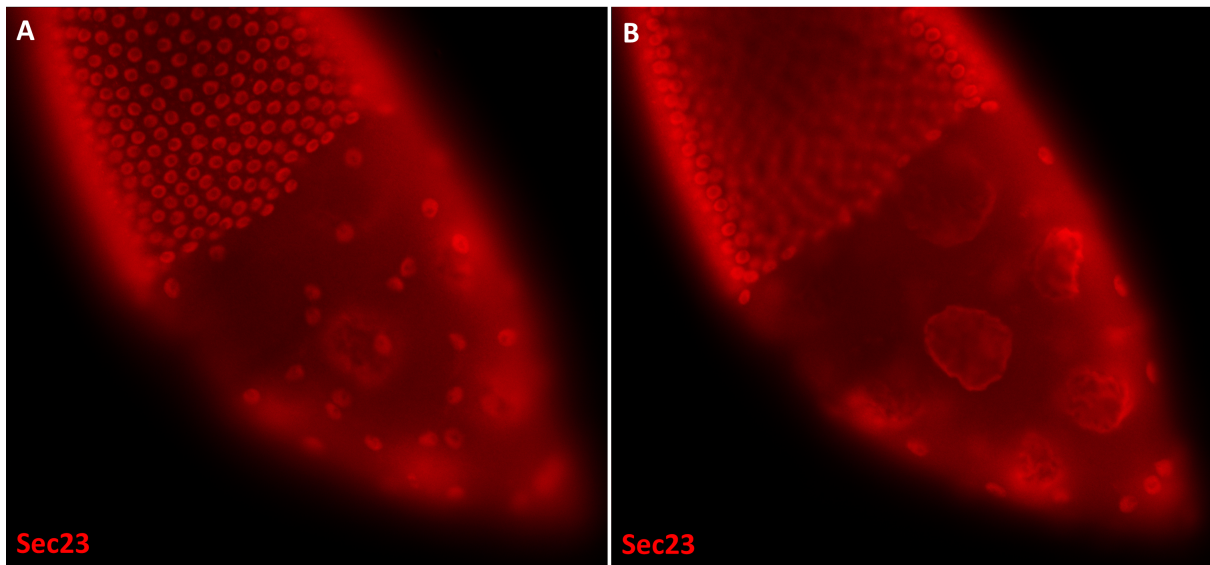


Figure S.2 | Localization of the COPII subunit Sec23 in a stage 10 egg chamber

Stage 10 egg chamber with the anterior pole to the top left. Sec23 is labeled with an anti-Sec23 antibody (red). A. Sec23 signal can be seen in a crescent shape at nuclei of the follicular epithelium. B. Image from A with an altered microscopical focus. Sec23 localization can be observed around the nurse cell nuclei.

List of figures

1.1	Bidirectional transport between ER and Golgi	3
1.2	COPII vesicle formation and cargo selection	5
1.3	Model of Erv14p	9
2.1	Scheme of the countercurrent apparatus	23
2.2	Scheme of the inebriometer	26
3.1	Phylogenetic Analysis of Cni Proteins	37
3.2	Predicted Cnr membrane topology	38
3.3	The <i>cnir</i> genomic locus	39
3.4	Targeting of <i>cnir</i>	40
3.5	Test for <i>cnir</i> knock-out and removal of the <i>white</i> marker	41
3.6	Analysis of survival rates throughout development	43
3.7	Survivorship until adulthood	44
3.8	Survivorship of adult <i>Drosophila</i>	46
3.9	Locomotion of <i>w</i> ¹¹¹⁸ and Δ <i>cnir</i> /+ flies	47
3.10	Locomotion of Δ <i>cnir</i> /+ and Δ <i>cnir</i> flies	48
3.11	Ethanol sensitivity of <i>w</i> ¹¹¹⁸ , Δ <i>cnir</i> /+ and Δ <i>cnir</i> flies	49
3.12	Locomotion of Δ <i>cnir</i> ; <i>mhc::Gal4</i> /+ and Δ <i>cnir</i> ; UAS:: <i>cnir</i> /+ flies	50
3.13	Locomotion of Δ <i>cnir</i> ; <i>mhc::Gal4</i> /UAS:: <i>cnir</i> and Δ <i>cnir</i> ; UAS:: <i>cnir</i> /+ flies	51
3.14	Locomotion of Δ <i>cnir</i> ; <i>mhc::Gal4</i> /UAS:: <i>cnir</i> and Δ <i>cnir</i> /+ ; UAS:: <i>cnir</i> /+ flies	52
3.15	Locomotion of Δ <i>cnir</i> ; <i>appl::Gal4</i> /+ and Δ <i>cnir</i> ; UAS:: <i>cnir</i> /+ flies	54
3.16	Locomotion of Δ <i>cnir</i> ; <i>appl::Gal4</i> /UAS:: <i>cnir</i> and Δ <i>cnir</i> ; UAS:: <i>cnir</i> /+ flies	55
3.17	Locomotion of Δ <i>cnir</i> ; <i>appl::Gal4</i> /UAS:: <i>cnir</i> and Δ <i>cnir</i> /+ ; UAS:: <i>cnir</i> /+ flies	56
3.18	Subcellular localization of GFP tagged Cnr	57
3.19	Locomotion of Δ <i>cnir</i> ; <i>appl::Gal4</i> /+ and Δ <i>cnir</i> ; UAS:: <i>GFP:cnir</i> /+ flies	58
3.20	Locomotion of Δ <i>cnir</i> ; <i>appl::Gal4</i> /UAS:: <i>GFP:cnir</i> and Δ <i>cnir</i> ; UAS:: <i>GFP:cnir</i> /+ flies	59
3.21	Locomotion of Δ <i>cnir</i> ; <i>appl::Gal4</i> /UAS:: <i>GFP:cnir</i> and Δ <i>cnir</i> /+ ; UAS:: <i>GFP:cnir</i> /+ flies	60
3.22	Somatic Δ <i>cnir</i> / <i>cnir</i> ^{AR55} clones in the follicular epithelium	62
3.23	Somatic Δ <i>cnir</i> / <i>cnir</i> ^{AR55} clones in third instar larvae eye imaginal discs	63
3.24	Test crosses for functional redundancy of both <i>Drosophila cni</i> genes	64
3.25	Ventralized eggs from <i>cni</i> mutant mothers	66
S.1	The <i>cnir</i> ^{AR55} amorphic mutation is not lethal in an altered chromosomal background	89
S.2	Localization of the COPII subunit Sec23 in a stage 10 egg chamber	90

List of tables

2.1	Reaction Kits	14
2.2	Restriction enzymes	15
2.3	Solutions and media	15
2.4	Fly stocks	17
2.5	Oligonucleotides	19
2.6	Vectors and plasmids	20
2.7	Primary antibodies	21
2.8	Secondary antibodies	21
2.9	Fluorescent dyes	21
2.10	Computer software	22

Zusammenfassung

Cornichon-Proteine bilden eine hochkonservierte Proteinfamilie von Cargorezeptoren, die den effizienten Export von Transmembranproteinen aus dem endoplasmatischen Retikulum (ER) aller bis jetzt untersuchter Eukaryoten gewährleisten. *Drosophila* besitzt zwei *cornichon*-Gene: *cornichon* und *cornichon-related* (*cnir*). Ersteres ist bekannt für seine Funktion bei der Festlegung der dorsoventralen Polarität in der Oozyte. Dieser Prozess benötigt den ER-Export und die Prozessierung des TGF α -Liganden Gurken, sowie dessen Transport zur Oozytenoberfläche. Die Funktion von *Cnir* wurde bisher nicht untersucht und ist Gegenstand dieser Arbeit. Die phylogentische Analyse zeigte, dass *Cnir* das mutmaßliche Otholog des menschlichen Cornichon homolog 4 (CNIH4) ist. Eine präzise Deletion des *cni*-Gens wurde mittels ends-out targeting durch homologe Rekombination erzeugt. Die *cnir*-Mutanten sind lebensfähig, zeigen jedoch eine erhöhte Mortalität in ihrer Entwicklung und im adulten Alter. Des Weiteren haben *cnir*-Mutanten starke Lokomotionsdefekte und eine reduzierte Sensitivität für Ethanol. Rettungsexperimente zeigten, dass die *Cnir*-Funktion in Neuronen zur Wiederherstellung des Lokomotionsverhaltens nötig ist. Durch GFP-Fusionsproteine wurde gezeigt, dass *Cnir* mutmaßlich im ER lokalisiert ist, was mit einer konservierten Rolle als Cargorezeptor im Einklang ist. Eine Doppelmutante beider *Drosophila* Cornichon-Proteine wurde hergestellt, jedoch gaben die klonale Analyse und Kreuzungsgenetik keine Hinweise auf funktionale Redundanz im Soma. Dies deutet auf eine Selektivität beider Cornichon-Proteine für Gruppen von Cargoproteinen hin. Für das mutmaßliche *Cnir* Otholog CNIH4 wurde gezeigt, dass es mit den drei Hauptfamilien G-Protein-gekoppelter Rezeptoren (GPCR) interagiert und an deren Transport beteiligt ist. GPCRs bilden die größte Überfamilie von Zelloberflächenrezeptoren und regulieren nahezu jeden physiologischen und zellulären Prozess. Dies macht ihren Transport zu einem wichtigen Forschungsfeld. Lokomotionsdefekte und die Parkinson-Krankheit werden in der Fliege und Vertebraten mit dopaminergen Signalwegen in Verbindung gebracht. Darüber hinaus wird Ethanolensitivität mit verändertem cAMP-Spiegel nach einem GPCR-Signal assoziiert. Daher könnte die niedrigere Ethanolensitivität von *cnir*-Mutanten mit ineffizientem Transport und somit mit verringertem GPCR-Signal in Verbindung stehen.

Abstract

Cornichon proteins represent a highly conserved protein family of cargo receptors mediating efficient endoplasmic reticulum (ER) export of numerous transmembrane proteins in all eukaryotes analyzed so far. *Drosophila* possesses two *cornichon* genes: *cornichon* and *cornichon-related (cnir)*. The former is well known for its function in establishment of dorsoventral polarity in the oocyte. This process relies on ER export and processing of the TGF α ligand Gurken and its transport to the oocyte surface. The function of Cnir has not been studied so far and is the subject of this thesis. Phylogenetic analysis showed that Cnir represents a putative ortholog of the human Cornichon homolog 4 (CNIH4). A precise deletion of the *cnir* gene was generated through ends-out targeting via homologous recombination. The *cnir* mutants are viable but have an increased mortality throughout development and adult life. Furthermore *cnir* mutant flies display a strong locomotor defect, as well as a reduced sensitivity towards ethanol. Analysis via rescue experiments demonstrated that Cnir function is required in neurons for restoration of locomotor behavior. Using GFP tagged proteins, Cnir was found to putatively localize to the endoplasmic reticulum, supporting a conserved role as cargo receptor. A double mutant for both *Drosophila* Cornichon proteins was generated and its clonal analysis, as well as crossing genetics, indicate no functional redundancy in the soma. This suggests a selectivity of Cornichon proteins towards specific cargo pools. The putative Cnir ortholog CNIH4 has been shown to interact with the three major families of G protein coupled receptors (GPCRs) and is involved in their trafficking. GPCRs represent the largest superfamily of cell surface receptors and regulate almost every physiological and cellular process, making their trafficking an important field of study. Locomotor impairment and Parkinson's disease have been linked to perturbation of dopaminergic pathways in fly and vertebrates. Furthermore, ethanol sensitivity is associated with altered cAMP levels downstream of GPCR signaling. Therefore, locomotor impairment and reduced ethanol sensitivity of *cnir* mutants might be linked to inefficient GPCR trafficking and thus reduced signaling levels.

Danksagungen

Zuerst möchte ich Herrn Prof. Dr. Siegfried Roth für die Möglichkeit danken diese Arbeit in seinem Labor bearbeiten zu dürfen. Des Weiteren gilt ihm großer Dank für die Betreuung dieser Arbeit und für die anregenden Hilfestellungen.

Frau Prof. Dr. Henrike Scholz danke ich für das Erstellen des Zweitgutachtens und zudem für die Einführung in *Drosophila* Verhaltensexperimente und deren Diskussion.

Des Weiteren gebührt Dr. Sebastian Grönke großer Dank für die Bereitstellung der Materialien zum Gen-Knock-Out durch homologe Rekombination und für das Teilen seiner Erfahrungen auf diesem Gebiet.

Ich möchte mich auch bei Jan Losse bedanken, der während seiner Masterarbeit "MS2-MCP-GFP screen for identification of new asymmetrically localized mRNA in *Drosophila* ovaries" eine große Hilfe beim Bearbeiten des in dieser Arbeit unbehandelten Themas war. Zudem hat er technisch großen Anteil an der Generierung transgener Fliegen gehabt.

Ich möchte Frau Dr. Kristen Panfilio für das Korrekturlesen dieser Arbeit und die Diskussionen danken. Dank gilt auch allen anderen Korrekturlesern dieser Arbeit.

Oliver Karst und Stefan Kölzer sei an dieser Stelle auch für sämtliche technische Hilfestellung gedankt. Insbesondere gilt dies für die Generierung transgener Fliegen.

Besonderer Dank gilt natürlich auch allen früheren und jetzigen Mitgliedern der Arbeitsgruppen Roth und Scholz. Dies gilt sowohl für die hilfreichen Diskussionen, als auch für die überaus freundschaftliche Atmosphäre während und auch abseits der Arbeitszeiten.

Ich danke natürlich auch meiner gesamten Familie in Deutschland und Kolumbien, die mich im Verlaufe dieser Arbeit bedingungslos unterstützt hat, vor allem wenn es mal nicht so gut lief. Gleiches gilt auch für alle meine Freunde.

Erklärung

Ich versichere, dass ich die von mir vorgelegte Dissertation selbständig angefertigt, die benutzten Quellen und Hilfsmittel vollständig angegeben und die Stellen der Arbeit - einschließlich Tabellen, Karten und Abbildungen -, die anderen Werken im Wortlaut oder dem Sinn nach entnommen sind, in jedem Einzelfall als Entlehnung kenntlich gemacht habe; dass diese Dissertation noch keiner anderen Fakultät oder Universität zur Prüfung vorgelegen hat; dass sie - abgesehen von unten angegebenen Teilpublikationen - noch nicht veröffentlicht worden ist sowie, dass ich eine solche Veröffentlichung vor Abschluss des Promotionsverfahrens nicht vornehmen werde. Die Bestimmungen der Promotionsordnung sind mir bekannt. Die von mir vorgelegte Dissertation ist von Prof. Dr. Siegfried Roth betreut worden.

.....
(Ort, Datum)

.....
(Waldemar Wojciech)

Lebenslauf

Persönliche Daten

Name Waldemar Miroslaw Wojciech
Anschrift Marie-Juchacz Straße 17 50129 Bergheim
Geburtsdatum und -ort 12.03.1982 in Laurahütte
Staatsangehörigkeit deutsch

Schulische Ausbildung

1989-1993 Fortunaschule in Oberaußem/Niederaußem
1993-2002 Erftgymnasium in Bergheim

Zivildienst

2002-2003 Zivildienst an der Paul-Kraemer-Schule in Frechen

Studium

10/2003-11/2009 Biologiestudium and der Universität zu Köln
Diplomsprüfungsfächer: Genetik, Entwicklungsbiologie, Biochemie

Diplomarbeit bei Prof. Dr. Siegfried Roth am Institut für Entwicklungsbiologie der Universität zu Köln

Titel: Genetic and Molecular Analysis of a new Component of the Oocyte Polarity in *Drosophila*

Seit 2010

Doktorarbeit bei Prof Dr. Siegfried Roth am Institut für Entwicklungsbiologie der Universität zu Köln
Titel: Analysis of a second *Drosophila* Cornichon Protein
